The Dissertation Committee for Aditya Chopra
certifies that this is the approved version of the following dissertation:

Modeling and Mitigation of Interference in Wireless Receivers with Multiple Antennae

Committee:

Brian L. Evans, Supervisor

Jeffrey G. Andrews

Robert W. Heath, Jr.

Elmira Popova

Haris Vikalo

Modeling and Mitigation of Interference in Wireless Receivers with Multiple Antennae

by

Aditya Chopra, B.Tech.; M.S.E.

DISSERTATION

Presented to the Faculty of the Graduate School of

The University of Texas at Austin

in Partial Fulfillment

of the Requirements

for the Degree of

DOCTOR OF PHILOSOPHY

THE UNIVERSITY OF TEXAS AT AUSTIN

December 2011

To Bauji, Mumma, Papa, Shachi, Ginni,

and my mouseketeers: Arya, Akshit, and Sana.

Acknowledgments

There is a singular dichotomy to writing a dissertation: it is an isolated endeavor, yet impossible without the support of family, friends, and colleagues. First of all, I would like to thank my family, for their unconditional love, support, and sacrifices. I would like to thank my father for teaching me the value of patience (with mild success), my mother for teaching me the value of spontaneity (with great success), and my sisters Shachi and Shruti for showering me with love, affection, and attention. They made me the person I am today.

I would like to express my deepest gratitude towards my advisor Prof. Brian L. Evans. Prof. Evans has been a constant source of support and ideas; someone to talk to, rather than report to; guiding me to find my path, rather than directing me towards one. His intelligence, breadth of experience, and organizational ability are attributes that I can only hope to duplicate.

I would like to thank my committee members Prof. Jeff Andrews, Prof. Robert Heath, Prof. Elmira Popova, and Prof. Haris Vikalo for their prying questions and invaluable comments. I would especially like to thank Prof. Andrews and Prof. Heath, whose classes have been a most enriching experience. I would also like to thank Prof. Surendra Prasad and Prof. Shiv Joshi for inspiring me to pursue signal processing and communications.

I would like to thank my best friends from high school: Mayank Sharma,

ADITYA CHOPRA

The University of Texas at Austin
December 2011

Modeling and Mitigation of Interference in Wireless Receivers with Multiple Antennae

Publication No. _____

Aditya Chopra, Ph.D.
The University of Texas at Austin, 2011

Supervisor: Brian L. Evans

Recent wireless communication research faces the challenge of meeting a predicted 1000× increase in demand for wireless Internet data over the next decade. Among the key reasons for such explosive increase in demand include the evolution of Internet as a provider of high-definition video entertainment and two-way video communication, accessed via mobile wireless devices.

One way to meet some of this demand is by using multiple antennae at the transmitter and receiver in a wireless device. For example, a system with 4 transmit and 4 receive antennae can provide up to a 4× increase in data throughput. Another key aspect of the overall solution would require sharing radio frequency spectral resources among users, causing severe amounts of interference to wireless systems. Consequently, wireless receivers with multiple antennae would be deployed in network environments that are rife with interference primarily due to wireless resource sharing among users. Other significant sources

of interference include computational platform subsystems, signal leakage, and external electronics. Interference causes severe degradation in communication performance of wireless receivers.

Having accurate statistical models of interference is a key requirement to designing, and analyzing the communication performance of, multi-antenna wireless receivers in the presence of interference. Prior work on statistical modeling of interference in multi-antenna receivers utilizes either the Gaussian distribution, or non-Gaussian distributions exhibiting either statistical independence or spherical isotropy. This dissertation proposes a framework, based on underlying statistical-physical mechanism of interference generation and propagation, for modeling multi-antenna interference in various network topologies. This framework can model interference which is spherically isotropic, or statistically independent, or somewhere on a continuum between these two extremes.

The dissertation then utilizes the derived statistical models to analyze communication performance of multi-antenna receivers in interference-limited wireless networks. Accurate communication performance analysis can highlight the tradeoffs between communication performance and computational complexity of various multi-antenna receiver designs.

Finally, using interference statistics, this dissertation proposes receiver algorithms that best mitigate the impact of interference on communication performance. The proposed algorithms include multi-antenna combining strategies, as well as, antenna selection algorithms for cooperative communications.

Table of Contents

List of Tables

List of Figures

Chapter 1

Introduction

This chapter begins with a description of wireless communications in Section 1.1, with an emphasis on wireless systems utilizing multiple antennae. In Section 1.2, I introduce the notion of interference in wireless systems, and its impact on communication performance. Due to the ever increasing demand for higher wireless data rates, interference mitigation is a crucial challenge that must be overcome. Section 1.3 summarizes this dissertation, presenting the thesis statement, providing a synopsis of the key contributions, and discussing the overall organization of this dissertation. I conclude this chapter with Section 1.4 providing the mathematical notation used throughout the dissertation, along with a list of commonly used mathematical symbols and acronyms.

1.1 Wireless Communications

In this decade, wireless technologies have defined the way we communicate, gather, and disseminate information. Wireless mobile devices are constantly finding new and innovative uses of high-speed 'always connected' wireless Internet, to the point that they are becoming victims of their own success. Current and next-generation of wireless communication research and standards

face the challenge of meeting a predicted 1000× increase in demand for wireless Internet data over the next decade[13]. Much of this explosive increase in demand can be attributed to the ubiquity of small form factor devices accessing high-definition video entertainment and two-way video communication, to such an extent that video traffic is expected to account for two-thirds of all mobile Internet traffic by 2015[1].

Wireless communications is made possible via transmission of electromagnetic (EM) waves over the air. The magnitude of the electro-magnetic field generated by EM waves is sinusoidal in nature, and the frequency of an EM wave is defined as the number of sinusoidal cycles per second, or hertz (Hz). In all long range wireless communications, the frequency of EM waves is usually within 3kHz to 30GHz. This block of frequencies, also known as the Radio frequency (RF) spectrum, is managed by the Federal Communications Commission (FCC) for commercial and other non-federal uses, and by the National Telecommunications and Information Administration (NTIA) for federal government use within the United States[53].

A mobile wireless device, also known as user equipment (UE) uses the RF spectrum to transfer data to a base-station. The base-station acts as hub for wireless networking within a small area around it. The base-station is also a gateway between the wireless network, and a wired network connected to other base-stations and the Internet. Mobile UEs can connect to other mobile UEs, or access Internet data via the link to their base-stations. Thus, base-stations can be considered as a tool used by Internet service providers (ISP) to deliver wireless
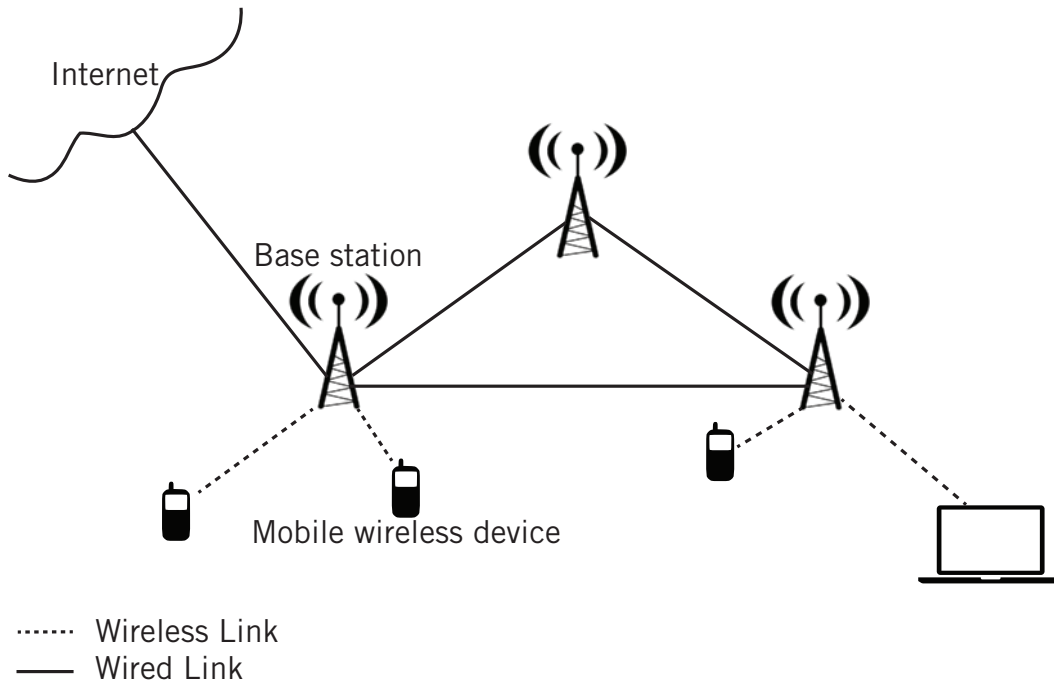
Figure 1.1: A typical wireless data network.

Internet services to their subscribers. In this model, each wireless connection between the UE and the base-station is called a 'link'; data transfer from the base station to UE is termed 'downlink', whereas data transfer from UE to base station is termed 'uplink'. The wireless 'network' comprises of many links transferring data simultaneously. Figure 1.1 describes this model of wireless Internet access.

To ensure wireless communications on a global scale, and to guarantee compatibility among wireless devices, standardization in the methods of wireless communications is needed. Wireless standards cover a large swath of wireless communication applications, ranging from personal area networks such as Bluetooth[24] and ZigBee[185], to local area networks such as WiFi[85], and city-

wide metropolitan area networks such as the 3rd generation partnership program (3GPP) long term evolution (LTE)[2, 120]. These standards specify the subset of the RF spectrum used for communication, the communication techniques used by devices to transfer data over the air, and the protocols through which multiple users simultaneously transfer data. Base-station and UE manufacturers build wireless communication systems and devices that adhere to these standards.

ISPs, mobile wireless system manufacturers, and wireless standards bodies have to work in concord, in order to ensure that mobile wireless systems of the future are able to reliably accommodate an ever increasing number of users, simultaneously accessing the Internet with ever higher data rates. Proffered solutions to support this growth in demand must address the inherent difficulties in wireless communications.

At the link level, wireless transmissions suffer from path loss[65], whereby the EM signal strength decays according to an inverse power-law function of the distance traveled. Objects between the source and destination absorb and reflect EM transmissions. The motion of the source, destination, or these objects causes the received signal strength at the destination to vary in a random fashion, sometimes dropping precipitously, a phenomenon also known as fading[23]. Wireless receivers also pick up unwanted signals along with the desired signal. These unwanted signals may arise from the receiver circuitry, or from other transmitting users. These are interchangeably referred to as either noise, or interference.

At the network level, the simultaneous operation of many links causes interference. Further compounding the problem of interference is that ISPs are

allowing base stations to share spectral resources in order to increase the number of supported users. Increased spectrum sharing in one area of coverage causes interference in nearby areas of coverage[109]. In addition, interference may also come from emissions from computational platform subsystems and external electronics and from leakage in wireless services in nearby frequency bands[147]. The data rate available to wireless mobile users is increasingly limited by interference.

1.1.1 Wireless Communications using Multiple Antennae

Wireless communications research over the past decade has increasingly focused on the use of multiple antennas at the transmitter and receiver to improve data rate and enhance communication reliability in wireless networks[23]. Standards such as 3GPP-LTE also support multi-antenna wireless communications[120]. Multi-input multi-output (MIMO) communication involves the use of multiple transmit and receive antennas to communicate information over a single link. While conventional single-antenna wireless systems exploit the time and frequency dimensions of the communication link, MIMO wireless systems can realize further gains in communication performance by leveraging the additional spatial dimension. Communication performance of wireless systems can be improved by the use of multiple antennae via the following avenues:

- *Multiplexing:* Multiplexing simply denotes the notion of transmitting multiple independent streams of data via multiple transmit antennae, and subsequently receiving these streams at multiple receive antennae. Under

ideal channel conditions, and if the number of receive antennae equals the number of transmit antennae, the communication system can be considered to comprise of multiple independent wireless links. For example, a wireless system with 4 transmit and 4 receive antennae may ideally be considered as 4 independent wireless links with 1 transmit and 1 receive antenna each. In such a scenario, it is fairly straightforward to see that the MIMO wireless system can communicate data 4 times as fast as the single-antenna wireless system.

- *Spatial diversity:* A wireless receiver with multiple antennae receives multiple copies of the same transmitted signal, increasing the chances that atleast one of these copies is relatively impairment-free, a phenomenon known as *spatial diversity*. Spatial diversity can be obtained from antenna arrays at the transmitter, receiver, or both. Diversity can be used to improve wireless communication performance via various transmit and receive strategies depending on the available computational complexity and the level of wireless channel information available to the transmitter or receiver.

- *Interference mitigation:* A common method of interference mitigation in MIMO systems is to use either *transmit beamforming* or *receive beamforming*. In transmit beamforming, multiple transmit antennae direct signal energy at the intended receiver and minimize interference to other users. In receive beamforming, multiple receive antennae capture signal energy

only from the direction of the transmitter and minimize interference received from other users.

Each of the benefits described above exploit the spatial degrees of freedom afforded by the wireless channel between the multiple transmit and receive antennae. Consequently, it follows that all of these benefits may not be realized simultaneously, indeed, typical MIMO system design uses a combination of some or all of these techniques to increase data rate and improve communication reliability.

1.1.2 Wireless Communications using Distributed Antennae

A special case of multiple antenna communication involves using distributed antennae for transmission, reception, or both. In distributed antennae systems (DAS), antenna modules are geographically distributed and each antenna is connected to a centralizing node via a wired, or wireless link[10]. While conventional multi-antenna systems also comprise of physically separate antennae, they are present on the same device; in DAS, however, the antenna separation is orders of magnitude larger than that of conventional multi-antennae devices. The distributed antenna modules and the base-station together can be construed as a macroscopic multiple-antenna system.

It has been shown that using DAS at the transmitter can reduce transmission power, and combat wireless channel fading via spatial separation to improve the signal-to-interference-plus-noise ratio (SINR) at the receiver[39, 45, 128, 180]. Based on these advantages, many cellular service providers or system

7

manufacturers are seriously considering replacing legacy cellular systems with distributed antenna systems or adopting the distributed antenna architecture in the future.

1.2   Interference

Wireless transceivers suffer degradation in communication performance due to radio frequency interference (RFI) generated by both human-made and natural sources. Human-made sources of interference include uncoordinated wireless devices operating within the same frequency band (co-channel interference), devices communicating in adjacent frequency bands (adjacent channel interference), computational platform subsystems radiating clock frequencies and their harmonics, and power lines. Interference is also generated from environmental sources such as atmospheric noise and electrical discharge. Based on the nature of its sources, interference can be classified into the following categories[42].

1.2.1   Circuit Noise

Circuit noise is unavoidable noise which arises from electronic circuitry present at a wireless receiver. Walter Schottky classified circuit noise as either thermal noise, or shot noise[142]. Thermal noise occurs due to random motion of electrons in a conductor, caused by thermal agitation at any temperature above absolute zero. The rate of such motion is independent to the voltage applied across the conductor, subsequently the level of thermal noise in a circuit

depends only on the ambient temperature. Shot noise, on the other hand, occurs due to the quantized nature of current flow. In reality, current flowing through a conductor is a quantized stream of electrons. When current is high, electrons flow through a conductor in such large quantities that they can be well approximated as a continuous stream. However, when current is low and electrons are flowing through the conductor in small quantities, the quantized nature of the flow cannot be ignored. Statistical variations in electrical current occur when electrons arrive in 'bursts' from time to time. Thus, the level of shot noise in a conductor is highly dependent on the voltage applied across the conductor. Schottky's study on the electromagnetic generation mechanisms of circuit noise showed that fluctuations caused by thermal noise and shot noise follow a Gaussian distributed statistics. In this dissertation, the term circuit noise refers to thermal noise and is assumed to be Gaussian distributed.

1.2.2 Interference from Extraneous Sources

There are several ways to classify interference caused by sources external to a receiver. Interference can arise due to conductive contact between a receiver and an interferer, and is known as Electromagnetic Interference (EMI). Interference can also arise when a receiver radio picks up a radiated emission from an interfering source, also known as Radio Frequency Interference (RFI). In this dissertation, I study the impact of RFI on communication systems, thus the term interference denotes RFI unless explicitly stated. Figure 1.2 illustrates the typical sources of interference in a wireless receive antenna embedded on a mobile

platform, which are classified into the following categories:

1.2.2.1 Interference from Intelligent Sources

Intelligent sources of interference are typically communication devices emitting radiation that carries some information content within it. Intelligent sources cause most severe interference when the interfering emission from the source is radiated across the same frequencies that the receiver is tuned to observe. This phenomenon is also known as co-channel interference. Co-channel interference usually arises when users in a dense wireless network environment are forced to share the same frequency spectrum to communicate[44, 109]. Co-channel interference is also caused when the same frequency spectrum is home to many co-existing wireless standards. This is especially true in the unlicensed 2.4 GHz Industrial, Scientific and Medical (ISM) band[38]. This band is used by a multitude of wireless communication standards such as IEEE 802.16 (Wi-Fi)[85], IEEE 801.2 (Bluetooth)[24], and IEEE 802.15.4 (ZigBee)[185]. Co-channel interference can be severe in environments with a large density of computing devices such as universities, business and apartment complexes, and entertainment hotspots[131]. Such locations contain a large number of devices using the same communication standards, as well as devices using co-existing technologies, such as a Bluetooth mouse, that interfere with wireless communications[38].

Another weaker, but significant, form of intelligent interference is caused by source radiations that lie outside the frequency band used by the victim re-

ceiver. While the intention of using non-overlapping frequency bands is primarily to ensure that devices do not cause interference to each other, the non-ideal nature of transmitter circuitry may cause some of the transmitted energy to leak outside the desired transmission frequency band. Such interference is commonly referred to as adjacent channel interference (ACI). This can be a severe problem in wireless standards such as Wi-Fi, which divides the frequency spectrum into discrete smaller blocks of spectrum, also known as channels. Power leakage from a transmitter into neighboring channels is a very common occurrence in Wi-Fi based communications. The level of power leakage into adjacent channels is controlled by strict regulations by the FCC in United States[53]. Yet, adjacent channel interference is may aggregate from multiple nearby users and is a significant impairment to unencumbered high speed wireless communications.

1.2.2.2 Interference from Non-Intelligent Sources

Non-intelligent sources of interference emit radiation that does not bear any information, and is usually an unintended consequence of their primary operation. Commercial electronic devices, such as microwave ovens, emit electromagnetic radiations as a integral aspect of their operation. However, due to lack of adequate shielding, some radiation may leak into the environment outside the device and cause interference to wireless receivers. Other devices, such as powerlines, radiate interference emissions due to the electronic circuitry present in them. Commercial electronic devices are required to abide by regulations (from

11

regulatory organizations such as the FCC in United States) that limit the electromagnetic interference that they can produce with regards to human health and safety, and devices operating within these limits may still cause significant degradation to other communicating devices. For example, microwave ovens may radiate as high as 50 dBm power at a distance of 15m in the 2.4 GHz ISM band, which is comparable to the transmit power of an access point of a Wi-Fi network[94]. Thus, interference from microwave interference is a cause for concern for 802.11b/g networks working in the 2.4GHz ISM band.

With ever-increasing complexity and computational density of electronic devices, coupled with their ever shrinking size, sometimes the most significant source of interference to a wireless receiver is the platform on which the receiver is deployed. In-platform sources of interference include clocks and busses in the computational platform on which the wireless transceiver is embedded[147]. Because of their close proximity, in-platform sources do not need to emit high-levels of radiation to cause interference in the wireless devices operating on the platform; even regulatory organizations do not regulate emitted power as such close distances around an electronic device.

1.2.3 Self Interference

In wireless telecommunications, multipath is the term given to the propagation phenomenon that results in radio signals reaching the receiving antenna by two or more paths. Causes of multipath include atmospheric ducting, ionospheric reflection and refraction, and reflection from water bodies and terrestrial
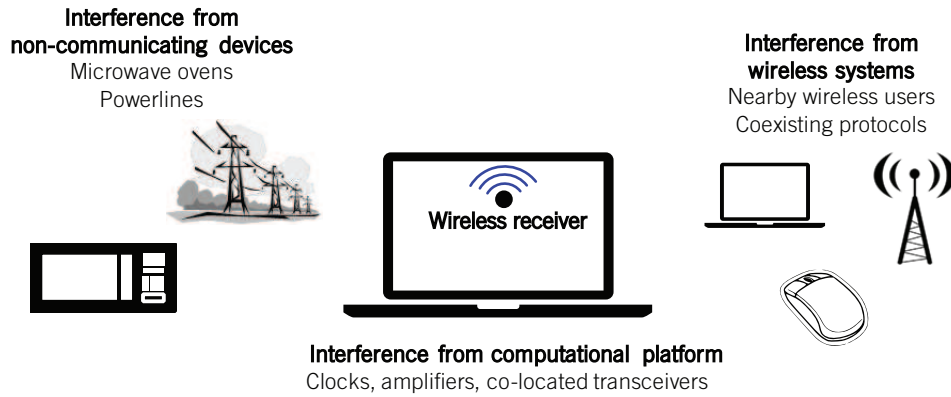
Figure 1.2: Typical sources of interference in wireless communication systems.

objects such as mountains and buildings[65]. Self-interference arises when a receiver observes delayed replicas of the transmitted signal due to multipath[23]. Such delays can cause interference as the received signal may be contaminated by replicas of earlier transmissions. Self-interference is particularly destructive to single carrier communication techniques such as CDMA. Other communication techniques allow for guard intervals in time (TDMA), or actually exploit multipath to improve communication performance (FDMA)[65]. In this dissertation, the problem of self-interference and wireless channel multipath is ignored, as techniques to mitigate self-interference work in complement with our techniques to mitigate extraneous interference.

1.3   Dissertation Summary

In this dissertation, I defend the following thesis statement:

Accurate statistical modeling of interference observed by multi-antenna

13

wireless receivers facilitates design of multi-antenna wireless systems with significant improvement in communication performance in interference-limited networks.

1.3.1   Contributions

1. *Statistical modeling:* I formulate a statistical-physical network model with a multi-antenna wireless receiver surrounded by interfering sources distributed randomly as a Poisson point process. The Poisson point process is typically used to model interferer locations in wireless networks. Based on this formulation, I derive the joint statistics of resultant interference. The interference statistics follow the symmetric alpha stable distribution in decentralized wireless networks such as *ad hoc* and sensor networks. I show that the joint statistics of interference in decentralized networks are well approximated by the symmetric alpha stable distribution even when the multiple receiver antennae are geographically disparate. In centralized wireless networks that can enforce a interferer-free *guard zone* around the receiver, I show that the interference statistics follow the Middleton Class A distribution.

2. *Communication performance analysis:* Using the system model of interference generation in decentralized wireless networks, I analyze the communication performance of typical multi-antenna receive algorithms in such networks. A key aspect of my system model is that interference statistics are modeled to exist within a continuum between spatial isotropy and

spatial independence, in other words, joint statistics of interference exhibit partial spatial dependence. I study the impact of spatial dependence on communication performance, in this case interpreted as probability that a receiver experiences communication outage. Results show that the derived outage probability expressions closely match a simulated multi-antenna receiver in the presence of interferers.

3. *Receiver Design:* A key motivation of deriving interference statistics is to use these statistics to design wireless systems with improved communication performance in the presence of interference. I develop non-linear receiver algorithms that are able to outperform conventional multi-antenna receivers in the presence of impulsive interference. I also use knowledge of interference statistics in geographically distributed receivers to develop antenna selection strategies for cooperative MIMO systems.

1.3.2 Organization

This dissertation is organized as follows. Chapter 2 presents a thorough survey of prior research on statistical modeling of interference in multi-antenna wireless receivers, communication performance analysis of conventional multi-antenna wireless receivers in interference-limited wireless networks, and design of novel reception strategies with improved performance in interference-limited wireless networks. The relative merits and weakness of prior literature in each of these topics are discussed in great detail.

Chapter 3 derives the joint interference statistics in wireless networks

with interferer-free regions, also known as *guard zones*. I refer to such networks as centralized networks, as these networks usually require a central authority to enforce guard zones around an active receiver.

Chapter 4 derives the joint statistics of interference in networks without guard zones. I denote these networks to be decentralized; i.e., any device can choose to transmit or receive at any time as there is no central coordinating authority.

Chapter 5 derives the probability of outage for different multi-antenna receiver algorithms in interference-limited wireless networks without guard zones. Outage is defined as an event where the wireless receiver is unable to correctly receive transmitted data due to overwhelming corruption by interference. The outage probability expressions provide insight into the impact of interference on different types of multi-antenna reception schemes, and can inform design of receivers that are more robust to interference.

Chapter 6 proposes novel multi-antenna receiver algorithms for receivers with co-located or geographically distributed antennae. Proposed receiver designs include multi-antenna signal combining algorithms, and antenna selection algorithms for receivers with distributed antennae.

1.4   Nomenclature

1.4.1   General Mathematical Notation

The following general mathematical notation is used throughout this dissertation:

Z	Scalar
$\mathbf{z}$	Column vector
$\mathbf{Z}$	Matrix
$\mathbb{E}_{\mathbf{X}}\{f(\mathbf{X})\}$	Expected value of the $f(\mathbf{X})$ w.r.t. the random variable $\mathbf{X}$
$\mathbb{P}(E)$	Probability of a random event E
$|Z|$	Absolute value of Z
$\|\mathbf{z}\|_p$	$p-$norm of vector $\mathbf{z}$
$\|\mathbf{z}\|$	$2-$norm of vector $\mathbf{z}$
$\mathbb{R}$	Set of real numbers
$\mathbb{R}^k$	Set of real vectors with dimension k

1.4.2   List of Abbreviations

3GPP Third Generation Partnership Project

3GPP2 Third Generation Partnership Project 2

ACI Adjacent Channel Interference

AF Amplify and Forward

AWGN Additive White Gaussian noise

BER Bit-error-rate

BPSK Binary Phase-Shift Keying

CCI Co-channel Interference

CDMA Code Division Multiple Access

CSMA Carrier Sense Multiple Access

DAS Distributed Antenna Systems

DF Decode and Forward

EGC Equal Gain Combining

EMI Electromagnetic Interference

FWC Fixed Weight Combining

FDMA Frequency Division Multiple Access

GMM Gaussian mixture model

i.i.d. independent and identically distributed

LCD Liquid Crystal Display

LTE Long Term Evolution

MAC Medium Access Control

MCA Middleton Class A

MRC Maximum Ratio Combining

MSE Mean squared error

MUD Multi-User Detection

NTIA National Telecommunications and Information Administration

OFDM Orthogonal Frequency Division Multiplexing

OFDMA Orthogonal Frequency Division Multiple Access

PDC Post Detection Combining

PGFL Probability Generating Functional

PHY Physical

PPP Poisson Point Process

QAM Quadrature Amplitude Modulation

RAS Random Antenna Selection

RF Radio Frequency

RFI Radio Frequency Interference

SAS Symmetric Alpha Stable

SC Selection Combining

SIC Successive Interference Cancellation

SINR Signal-to-interference-plus-noise ratio

SIR Signal-to-interference ratio

SNR Signal-to-noise ratio

TDMA Time Division Multiple Access

UE User Equipment

Wi-Fi Wireless Fidelity (WLAN)

WiMAX Worldwide Interoperability for Microwave Access

WLAN Wireless Local Area Networks

w.r.t. with respect to

Chapter 2

Background

2.1 Introduction

In Chapter 1, I briefly discussed how the demand for wireless Internet data is exponentially increasing, and interference is the key bottleneck preventing service providers from meeting this demand. This has motivated active research into mitigating the harmful impact of interference on wireless communication performance. In this dissertation, I propose to develop statistical models of interference, and use them to analyze communication performance of conventional wireless receivers and design novel algorithms better suited to data reception in the presence of interference.

In this chapter, I begin by reviewing the vast variety of techniques used to mitigate interference in wireless communications. Section 2.2 categorizes and discusses common interference mitigation strategies. I review recent and seminal prior work on statistical modeling of interference in wireless networks in Section 2.3. Next, I review prior literature on communication performance analysis of interference-limited wireless receivers in Section 2.4 . Finally in Section 2.5, I present a survey of prior research on design of single-antenna, multi-antenna, and distributed-antenna receivers in interference-limited networks.

2.2 Interference Mitigation in Multi-Antenna Wireless Communications

Interference mitigation methods can be classified as either static methods that avoid interference through device design or network planning, or as active methods that estimate and cancel interference during data transmission. Following is a discussion on key interference mitigation strategies from both categories.

2.2.1 Static Methods

- *Receiver shielding:* Shielding at the wireless receiver is typically used to prevent the receiver from observing platform noise generated from other subsystems from the wireless device such as a laptop or mobile phone. While shielding can reduce interference from non-communicating platform sources, it incurs a cost of materials and weight on mobile devices, and cannot prevent co-channel interference from other communicating devices[147].

- *Spectrum allocation:* The frequency spectrum can be considered a finite resource pool in wireless communications. Devices communicating across a non-intersecting subset within this spectrum generally do not cause co-channel interference to each other, as shown in Figure 2.1. Through spectrum sharing, adjacent cells on the network can transmit and receive data without causing interference to each other.

  The key disadvantage of this approach is that it severely reduces the peak
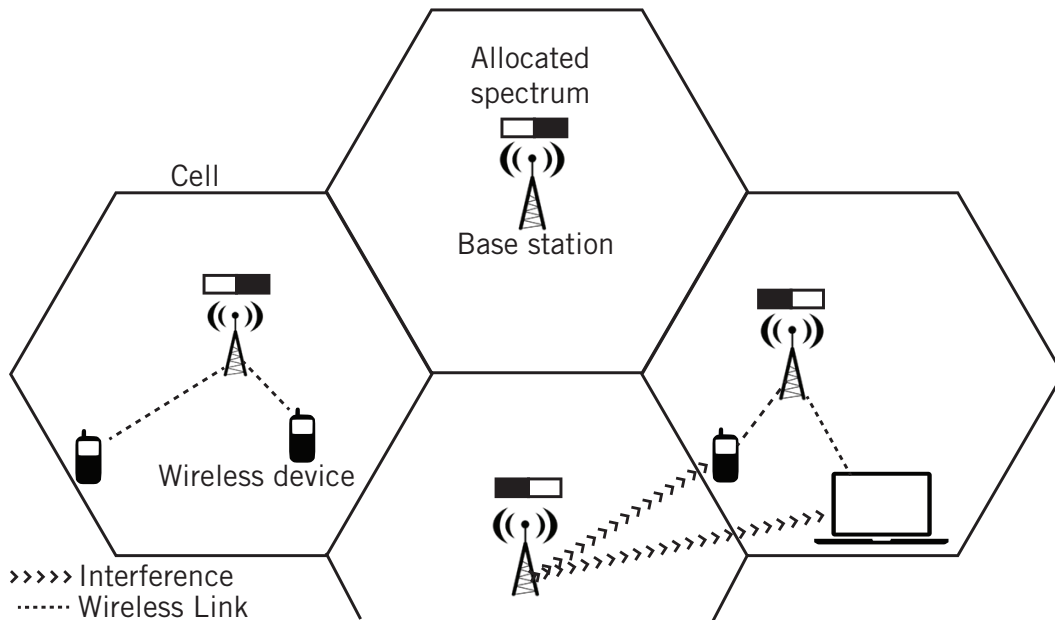
Figure 2.1: Out-of-cell interference caused by resource allocation.

available data rates as each cell can only use a small amount of spectral resource. Furthermore, devices communicating in neighboring blocks of frequency spectrum can still interfere with each other, also known as adjacent channel interference[141]. Due to a high demand in wireless data rates, network providers are increasingly using overlapping segments of the frequency spectrum in adjacent cells (frequency reuse), and deploying interference mitigation strategies on base-stations and mobile devices[44, 89, 109].

23

2.2.2 Dynamic Methods

- *Multiple access protocols:* In wireless communications, data transmission uses a chunk of resource in the time, frequency or code dimension. If two users transmit in different subspaces in this resource space, they generally do not cause interference to each other. For example, two users transmitting during different time periods do not interfere with each other even if they transmit over the same chunk of frequency, just as two users transmitting in different chunks frequency spectrum do not interfere with each other even if they transmit at the same time.

  Multiple access protocols allow many users to transmit in non-intersecting subsets of either the time, frequency, or code dimension. The corresponding orthogonal multiple access schemes are referred to as time division multiple access (TDMA), frequency division multiple access (FDMA), and code division multiple access (CDMA). Current and future wireless standards employ one or many of such schemes in order to accommodate the increasing density of wireless devices. Multiple access schemes can be understood as algorithms that distribute a finite number of resource blocks among users based on resource availability and user demand, trying to prevent interference by ensuring that two users do not use the same resource.

  There is significant prior research on multiple access algorithms[18, 166, 176]. Schemes such as ALOHA and time/frequency hopping attempt to reduce simultaneous user transmissions over the same frequency spec-

trum[18], and carrier sense multiple access (CSMA) involves listening to the wireless medium and schedule a user transmission only if no ongoing transmissions are observed[97]. Dynamic spectrum allocation in networks is also a well researched method for allowing multiple access while minimizing interference[32, 33]. While multiple access protocols are a requirement for any wireless network, they alone are unable to eliminate interference because of the following key reasons:

1. Multiple access schemes require user coordination in order to work. Users from adjacent cells, or co-existing networks may not be coordinated to each other, thereby causing interference.

2. As the number of wireless users grow, there may not be enough resources to satisfy user demand, inevitably causing interference between nearby users sharing the same resource.

- *Interference cancellation:* Interference cancellation denotes the class of receiver algorithms which attempt to estimate, and subsequently subtract the interference component within the received signal. Typical interference cancellation algorithms include multi-user detection (MUD), successive interference cancellation (SIC), and multi-antenna beamforming[14, 80]. Interference cancellation has been well studied in literature, with a multitude of receiver-side algorithms[12, 58], theoretical bounds on communication performance [80, 133, 173, 174], and reduced computational complexity implementations[5, 52, 104, 108, 110]. It requires high compu-

tational resources from wireless devices and generally cancels dominant interferers, leaving residual interference from uncoordinated users.

- *Interference alignment:* While interference cancellation is a receiver side technique that removes interference, interference alignment is a transmit side technique where a transmitter manipulates the signal in such a manner that the interference caused to other wireless device is orthogonal to its signal[31]. Interference alignment has shown great promise, however, in order to achieve proposed gains, each transmitter and receiver must have a global knowledge of all interfering links in the network, and the transmitter must have a large number of antennae depending upon the number of interferers to be canceled. This requires a high amount of channel state feedback between receivers and transmitters, and the residual interference from uncoordinated devices cannot be canceled. Methods for interference alignment in cellular networks[31, 150], wireless ad hoc networks[121, 153], cognitive networks[183], and MIMO wireless networks[28, 49, 99, 154] have been studied in recent past. The feasibility of interference alignment techniques in practice, due to limited capacity, accuracy and delay in the feedback channels, has also been studied extensively[6, 21, 31, 81, 87, 164, 181, 182].

- *Statistical mitigation:* In this category, interference is treated as random noise at the receiver and special receiver blocks are designed to improve communication performance. Thus, while interference is strictly not canceled at the receiver, the goal of these algorithms is to improve data rates

or reduce bit errors. These methods require an accurate knowledge of the statistical properties of interference. This dissertation focuses on this approach of statistical modeling and receiver design around statistical models of interference. The following sections present a detailed survey of prior work on statistical modeling of interference, and receiver design to mitigate interference.

2.3   Statistical Modeling of Interference

In typical communication receiver design, interference is usually modeled as a Gaussian distributed random variable[23]. While the Gaussian distribution is a good model for thermal noise at the receiver[65], interference has predominantly non-Gaussian statistics[50, 115, 130] and is well modeled using impulsive distributions such as symmetric alpha stable[140] and Middleton Class A distributions[114]. The impulsive nature of interference may cause significant degradation in communication performance of wireless receivers designed under the assumption of additive Gaussian noise[118].

The statistical techniques used in modeling interference can be divided into two categories: (1) empirical methods and (2) statistical-physical methods. Empirical approaches fit a mathematical model to interference signal measurements, without regard to the physical generation mechanisms behind the interference. Statistical-physical models, on the other hand, model interference based on the physical principles that govern the generation and propagation of interference-causing emissions. Statistical-physical models can therefore be

more useful than empirical models in designing robust receivers in the presence of interference[115]. The following sub-sections discuss key prior results in statistical modeling of interference in single- and multi-antenna receivers.

2.3.1 Prior Work in Single-Antenna Interference Models

In [149], it was shown that interference from a homogeneous Poisson field of interferers distributed over the entire plane can be modeled using the symmetric alpha stable distribution[140]. This result was later extended to include channel randomness in [86]. In [115], it was shown that the Middleton Class A distribution well models the statistics of sum interference from a Poisson field of interferers distributed within a circular annular region around the receiver. Their results were generalized in [70], by using the Gaussian mixture distributions to model interference statistics in network environments with clustered interferers. Recent work on statistical modeling of interference, and network capacity evaluations also assumes a homogeneous Poisson Point Process distribution of interferers[16, 17, 19, 74, 131, 139, 175].

The Middleton Class A and the Gaussian mixture distributions can also incorporate thermal noise present at the receiver without changing the nature of the distribution, unlike the symmetric alpha stable distribution. The Middleton Class A models are also canonical, i.e, no knowledge of the physical environment is needed to estimate the model parameters[179]. The symmetric alpha stable and Middleton Class A distribution functions are listed in Table 2.1.

Table 2.1: Key statistical models of interference observed by single-antenna receiver systems

Model Name	Statistical Model
Symmetric alpha stable	Characteristic Function $\Phi_{\mathbf{Y}}(\omega) = e^{-\sigma|\omega|^{\alpha}}$ α : Characteristic exponent. Range: $(0,2]$ σ : Dispersion parameter. Range: $(0,\infty)$ Wireless Network Decentralized (e.g. *ad hoc* and femtocells)
Middleton Class A	Amplitude Distribution $f_{\mathbf{Y}}(y) = \sum_{k=0}^{\infty} \frac{e^{-A}A^k}{k!\sqrt{2\pi\frac{k/A+\Gamma}{1+\Gamma}\sigma^2}} e^{-\frac{y^2}{2\frac{k/A+\Gamma}{1+\Gamma}\sigma^2}}$ A : Overlap index. Range: $(0,\infty)$ Γ : Ratio of Gaussian to non-Gaussian variance. Range: $(0,\infty)$ σ^2 : Noise power. Range: $(0,\infty)$ Wireless Network Centralized (e.g. LTE, Wimax, and WiFi)

2.3.2   Prior Work in Multi-Antenna Interference Models

Prior work on statistical modeling of interference in multi-antenna wireless systems has typically focused on using multi-variate extensions of single-antenna interference statistical models. As described in Section 2.3.1, key statistical models of single antenna interference include the Middleton Class A and symmetric alpha stable models. The two common approaches of generating multi-variate extensions of uni-variate distributions assume that either (a) interference is independent across the receive antennae, or (b) the multi-variate interference model is isotropic.

In [86], the authors apply the spherically isotropic symmetric alpha stable distribution [125] to model interference generated from a Poisson distributed

29

field of interferers. The authors assume that each receiver is surrounded by the same set of active interferers, and receiver separation is ignored. The spherically isotropic alpha stable model is derived under both homogeneous and non-homogeneous distribution of interferers, with the signal propagation model incorporating pathloss, lognormal shadowing and Rayleigh fading. The study is limited to baseband signaling and neglects any correlation in the interferer to receive antenna channel model or correlation in the interference signal generation model.

In [47], the author proposes three possible extensions to the univariate Class A model. The three multidimensional extensions, whose distribution functions are listed in Table 2.2, are as follows:

1. Model I - Each receive antenna experiences additive uni-variate Class A noise with the identical parameters. interference is spatially and temporally independent and identically distributed. Model I cannot capture spatial dependence or sample correlation of interference across receive antennae.

2. Model II - interference is assumed to be spatially dependent and correlated across receive antennae. Model II can represent correlated or uncorrelated random variables; however, it cannot represent independent Class-A random variables.

3. Model III - This model incorporates spatial dependence in multi-antenna interference, but does not support spatial correlation across antenna sam-

ples. Model III can represent uncorrelated and spatially dependent Class A random variables but it cannot represent independent or correlated random variables.

These models are multivariate extensions of the Class A distribution and are not derived from physical mechanisms that govern interference generation. While these models have been very useful in analyzing MIMO receiver performance under interference [62] and designing receiver algorithms to improve communication performance in presence of interference[113], a statistical-physical basis for these models would further enhance their appeal[112] in linking wireless network performance with environmental factors such as interferer density, fading parameters, etc.

In [112], the authors attempt to derive interference statistics for a two antenna receiver based on the statistical-physical mechanisms that produce the interference. The authors use a physical generation model for the received interference at each of the two antennae that is the sum of interference from stochastically placed interferers which include interferers observed by both antennae as well as interferers observed exclusively by a single antenna. Their resulting model is canonical in form and also incorporates an additive Gaussian background noise component. However, it is incomplete as it enforces statistical dependence among receive antennae similar to Model II. In other words, either both receive antennae observe an impulsive event or no antenna observes an impulsive event. This is contrary to their statistical-physical generation mecha-

Table 2.2: Key statistical models of interference observed by multi-antenna receivers.

Model Name	Statistical Model
Isotropic symmetric alpha stable	Characteristic Function: $\Phi_{\mathbf{Y}}(\mathbf{w}) = e^{-\sigma\|\mathbf{w}\|^{\alpha}}$ α : Characteristic exponent σ : Dispersion parameter
Multidimensional Class A – Model I	Amplitude Distribution: $f_{\mathbf{Y}}(\mathbf{y}) = \sum_{k=0}^{\infty} \dfrac{e^{-A}A^k}{k!} \dfrac{1}{\sqrt{2\pi\frac{k/A+\Gamma}{1+\Gamma}|\boldsymbol{\Sigma}|}} e^{-\frac{\mathbf{y}^T\boldsymbol{\Sigma}^{-1}\mathbf{y}}{2\frac{k/A+\Gamma}{1+\Gamma}}}$ A : Overlap index Γ : Ratio of Gaussian to non-Gaussian variance $\boldsymbol{\Sigma}$: Noise covariance matrix
Multidimensional Class A – Model II	Amplitude Distribution: $f_{\mathbf{Y}}(\mathbf{y}) = \prod_{n=1}^{N_R}\sum_{k=0}^{\infty} \dfrac{e^{-A_n}A_n{}^k}{k!\sqrt{2\pi\frac{k/A_n+\Gamma_n}{1+\Gamma_n}\sigma_n^2}} e^{-\frac{y_n^2}{2\frac{k/A_n+\Gamma_n}{1+\Gamma_n}\sigma_n^2}}$ For each antenna n, A_n : Overlap index Γ_n : Ratio of Gaussian to non-Gaussian noise power σ_n^2 : Noise power
Multidimensional Class A – Model III	Amplitude Distribution: $f_{\mathbf{Y}}(\mathbf{y}) = \sum_{k=0}^{\infty} \dfrac{e^{-A}A^k}{k!} \dfrac{1}{\sqrt{2\pi|\boldsymbol{\Sigma}_k|}} e^{-\frac{\mathbf{y}^T\boldsymbol{\Sigma}_k^{-1}\mathbf{y}}{2}}$ $\boldsymbol{\Sigma}_k = (\mathbf{I}+\boldsymbol{\Gamma})^{-1}\left(\frac{k}{A}\mathbf{I}+\boldsymbol{\Gamma}\right)$ A : Overlap index $\boldsymbol{\Gamma}$: Diagonal matrix of Gaussian to non-Gaussian variance ratios
Bivariate Class A	Amplitude Distribution: $f_{\mathbf{n}}(n_1,n_2) = \dfrac{e^{-A}}{2\pi|\mathbf{K}_0|^{\frac{1}{2}}} e^{\frac{-\mathbf{n}^T\mathbf{K}_0^{-1}\mathbf{n}}{2}} + \dfrac{\left(1-e^{-A}\right)}{2\pi|\mathbf{K}_1|^{\frac{1}{2}}} e^{\frac{-\mathbf{n}^T\mathbf{K}_1^{-1}\mathbf{n}}{2}}$ $\mathbf{K}_m = \begin{bmatrix} c_m^2 & \kappa c_m\hat{c}_m \\ \kappa c_m\hat{c}_m & \hat{c}_m^2 \end{bmatrix}, c_m^2 = \dfrac{\frac{m}{A}+\Gamma_1}{1+\Gamma_1}, \hat{c}_m^2 = \dfrac{\frac{m}{A}+\Gamma_2}{1+\Gamma_2}$ A : Overlap index Γ_n : Ratio of Gaussian to non-Gaussian variance at antenna n κ : Correlation coefficient

nism which assumes that each receive antenna has a subset of surrounding interferers that are observed exclusively by that antenna alone. For example, their interference model cannot accommodate a scenario in which each of the two receivers observe interference distributed as independent univariate Class A density functions, a scenario entirely possible within the framework of their system model. While their model is strictly limited to two antenna receivers[112], it has found application in receiver design[37] and efficient parameter estimation algorithms for this distribution are also available[69, 90]. This dissertation extends their work by using a similar interference generation and propagation framework to develop statistical-physical interference distributions for any number of receive antenna. Table 2.2 lists the different joint statistical models of interference that have been proposed in prior work.

Models of interference in multi-antenna receivers are multidimensional since the random interference is observed at multiple spatial coordinates. In a similar vein, multidimensional models of interference are also developed to represent random interference observed at multiple temporal coordinates, to study the joint temporal characteristics of interference. The physical generation mechanism of temporally separate interference observations can be similar to that of spatially separated interference observations[178]. In [178], the authors study second-order statistics and temporal correlation in interference, and establish a link between the hold times of the interfering sources and the long-range dependence of resulting sum interference.

The multivariate extensions to the Middleton Class A model and the sym-

33

metric alpha stable model are not based on derivation of sum interference statistics from stochastic placement of interferers around the receiver. The extension to the Class A distribution based on an underlying statistical-physical generation model is limited to receivers with two antennas and does not translate spatial correlation of the active interferer location distribution into spatial dependence of the interference distribution. These are serious limitations in prior work on multi-antenna interference modeling as these models are subsequently used to analyze MIMO receiver performance under interference and design receiver algorithms to improve communication performance in presence of interference. Thus, derivation of multi-antenna interference statistical models would provide a clear link between interferer distribution parameters and communication performance. To the best of my knowledge, such a link does not exist right now due to the paucity of statistical-physical models of multi-antenna interference. The motivation of deriving accurate multidimensional statistical-physical interference models is evidenced by the use of the multivariate Class A and alpha stable distributions in literature, even though these models have not been justified by an underlying stochastic interference generation mechanism.

2.4 Communication Performance of Wireless Recievers

Multiple antenna communication systems have been extensively studied with regard their communication performance, under the assumption of Gaussian distributed additive noise[23]. Such analysis showed increased throughput and reliability as the key benefits of using MIMO communications, consequently,

most of the current and future standards, such as LTE, support multiple antennae at transmitter and receiver. With increasing deployment of multi antenna wireless systems, it is imperative to study the impact of interference on conventional MIMO communication techniques.

For uncoded communication systems, bit-error rate (BER) is a fundamental metric of communication performance. Prior work on BER analysis of receiver diversity algorithms under interference has usually focused on analysis of various single antenna reception schemes in the presence of additive impulsive noise[123, 130, 156]. BER analysis is highly dependent on the assumption regarding interference statistics. Thus, it is important that interference models based on statistical physical generation mechanisms be used for accurate analysis. For multi-antenna communication systems, typical statistical distributions that have been used to model interference are the spherically invariant symmetric alpha-stable distribution[86], spherically invariant Middleton Class A distribution[47], and multi-dimensional independent Middleton Class A noise model[47]. These statistical distributions model two extreme cases of interference statistics; i.e, interference is either statistically isotropic across antennae or statistically independent across receive antennae.

In [88], the isotropic symmetric alpha-stable noise model was used to evaluate BER of the optimal detector by assuming that the alpha stable noise follows the Cauchy distribution. This work was extended in [134] to more reception techniques, but only considered Binary Phase Shift Keying (BPSK) modulation. In [152], the authors investigated the performance of different diversity

combining techniques over fading channels with impulsive noise modeled using either isotropic or independent multi-dimensional Middleton Class A distribution. In [77], the authors analyze performance bounds for optimum and sub-optimum receivers in the presence of Middleton Class A impulsive noise over non-fading channels. In [41], the authors evaluate performance bounds of 2×2 MIMO communication with Alamouti codes using a generalized statistical-physical interference model from [113]. In [102] the performance of maximum ratio combining techniques was investigated in multi-user environments and in presence of receiver channel estimation error. While the authors did use the notion of statistical-physical interference propagation mechanisms, they assumed a fixed number and locations of the interference generating sources. In [7], a statistical-physical model similar to ours was used to study performance of optimum diversity combining. However, this model also assumed that interference was isotropic and the optimum receiver was impractical to implement as it required information about interferer locations at each sampling instant. Simulation based results have also been used in lieu of closed form expressions to show the impact of interference on multi antenna receivers[34, 135]. By using impulsive statistical distributions to model interference, communication performance analysis can provide a link between communication performance and noise parameters. On the other hand, starting from a statistical-physical noise generation mechanism, performance analysis can provide a link between communication performance and network parameters such as user density and user distribution. Table 2.3 provides a summary of the interference models and receiver algorithms

studied in prior literature and proposed in this dissertation.

While evaluating the performance of a point-to-point wireless link is important, another aspect of performance analysis lies in accurately characterizing the network performance. Network performance takes into account the point-to-point link performance, access control protocols, and user demand and traffic patterns, among others. Capacity analysis has been performed on networks of randomly distributed nodes[56, 72, 119], showing that the link throughput decays as $\mathcal{O}\left(\frac{1}{\sqrt{n}}\right)$ for n nodes per unit area in the network. An alternative and widely used method of evaluating physical layer techniques with regard to network performance is the framework of *transmission capacity*, defined in [174]. Transmission capacity evaluates the number of successful transmissions per unit area within the network, subject to an outage probability constraint. The Poisson Point Process distribution of user nodes has enabled much of the network performance analysis[172], however, there also exist results on network performance with non-Poisson distribution of user nodes[60]. In *ad hoc* networks, transmission capacity analysis can accommodate both PHY layer techniques such as interference cancellation[173], and MAC layer scheduling[172]. Transmission capacity has also been evaluated for networks with multiple antennae[83, 164].

2.5   Prior Work on Receiver Design in Interference

As interference has rapidly become a bottleneck to the performance of wireless communication systems, many receiver structures have been proposed to combat interference. With MIMO communications being the key focus of

Table 2.3: Prior work on analysis of receive diversity performance in a Poisson field of interferers. (SAS: Symmetric alpha stable, MCA: Middleton Class A, 'Iso.': Isotropic, 'Ind.': Independent, 'Cont.': Continuum)

Paper	Interference Model				Diversity Combiner					
	Type	Iso.	Ind.	Cont.	FWC	EGC	MRC	SC	PDC	MMSE
[134]	SAS		✓			✓	✓		✓	
[152]	MCA	✓	✓			✓	✓	✓	✓	
[102]	SAS	✓					✓			
[7]	SAS	✓								✓
this	SAS	✓	✓	✓	✓	✓	✓	✓	✓	

the past decade, many studies have been performed on MIMO communications in interference-limited networks[29, 95, 96]. The subject of interference cancellation in multi-antenna receivers has also been well studied in literature[12], with results on time-, frequency-, and code-domain cancellation algorithms[159, 171], and transmitter side algorithms (interference alignment)[28]. Proposed receiver structures usually remove a few dominant interfering sources[46], whose channel state information must be known to the receiver[46].

Wireless systems utilizing interference cancellation or interference alignment may not be able to remove all co-channel interference from devices within and outside the cellular coverage boundary. Residual interference may still be present, arising from other uncoordinated wireless users, devices that are using co-existing wireless protocols, and other non-communication devices. To mitigate such interference, receivers are designed to contain filtering and detection algorithms using accurate statistical models of interference.

2.5.1 Single-Antenna Receiver Design

The key statistical models of additive interference are the symmetric alpha stable[86] and the Middleton Class A distributions[115]. A major hindrance to developing optimal hypothesis tests in the presence of additive symmetric alpha stable noise, is that no closed-form probability density function exists for most values of the parameter α. Thus, optimum detection structures exists only for scenarios when closed-form distributions are known, such as the Gaussian distribution ($\alpha = 2$), and the Cauchy distribution ($\alpha = 1$)[155].

In [100], Kuruoglu proposed a non-linear Volterra type filtering approach to mitigate interference, showing improved performance over linear signal estimation structures. Other non-linear filtering structures include the myriad filter, shown to be optimal for signal estimation in alpha stable noise[68], and subsequently used for receiver design in alpha stable noise[66, 67, 118]. Prior work also includes non-linear receiver structures to estimate signals in a mixture of alpha stable and Gaussian noise[127].

Middleton Class A noise is a special case of the Gaussian mixture distribution. Consequently, the multitude of estimation and filtering structures designed for Gaussian mixture distributions[9, 51, 148] can be applied to MCA noise as well[55]. In particular, code division multiple access (CDMA) network interference has been widely modeled as Gaussian mixture impulsive interference and CDMA receivers need to compensate for multipath fading. Detection and pre-filtering based CDMA receiver algorithms in impulsive environments are thus common in literature [98, 111, 138, 159, 170, 171].

Finally, non-parametric approaches do not assume knowledge of noise distribution parameters, and involve using median filters, or removing signal samples thought to be corrupted by an impulsive noise event[27, 75]. Some non-parametric approaches do not assume any density distribution model for noise, and only regard noise as "impulsive"[15, 82, 167]; i.e., extreme values of noise occur more commonly than they would if noise followed the Gaussian distribution. The parametric and non-parametric approaches lie on different points of design tradeoff curve between robustness and estimation performance.

2.5.2 Multi-Antenna Receiver Design

The applicability MIMO receiver design in prior work is limited due to lack of accurate statistical models of interference[69, 106, 116]. In [37], the authors investigate sequence detection algorithms, such as the Viterbi decoder in impulsive noise modeled using the Gaussian mixture distribution model. The Gaussian mixture noise model used in the study is not linked to any statistical physical noise model and furthermore the noise is assumed to be independent across receiver antennas. Thus the receiver design may not be optimal in environments where interference is expected to show spatial dependence across receiver antennas. In [22], the authors propose decision feedback equalizer receivers to improve communication performance in symmetric alpha stable noise. As is usually the case in the presence of symmetric alpha stable noise, much of the receiver performance can be attributed to non-linear blanking, or clipping filters in the receive chain.

Prior work typically assumes statistically independent impulsive noise across receive antennae[11, 25, 127, 136, 177]. The filter structures proposed in prior work are limited in applicability to multi-antenna wireless receivers due to lack of statistical-physical generation based interference models. In particular, there is little prior work that considers spatial dependence in interference across receive antennas, which is a key factor in multi-antenna interference. Analyzing the effect of such spatial dependence on typical receiver algorithms is relevant to improving the communication performance of wireless receivers in frequency selective fading.

2.5.3 Distributed-Antenna Receiver Design

A recently proposed extension to MIMO systems utilizes distributed antennae to obtain capacity gain and diversity gain associated with MIMO communications. Cooperative reception in two distributed antennae can be considered analogous to the two-hop relay problem. There exists a bevy of prior research on two-hop relay communications: from information-theoretic performance analysis[40, 54, 144, 169], to signal design[145], to practical receiver implementations[59, 107].

Prior work in cooperative reception focuses primarily on improve transmission capacity by mitigating the impact of deep channel fades between the source and the destination[36, 64, 76, 165]. There exists a significant body of research on evaluating the tradeoffs between different relay signaling and relay selection techniques[117, 161–163]. Other research focuses on selecting the best

relays[93], using relays to improve channel diversity[160], or suppress interference[63, 117, 151, 160] via receive side cancellation[20], or transmit side alignment[151]. Usually, inteference cancellation removes a few dominant interferers, and residual interference is assumed to be Gaussian distributed.

In [35], the authors consider a symmetric alpha stable model of interference in a two-hop amplify and forward cooperative reception scheme. However, only the marginal distribution at the relay and the destination is modeled as symmetric alpha stable, while the joint statistics of interference are completely ignored.

2.6   Conclusions

In this chapter, I have summarized recent and seminal prior work on statistical modeling of interference in multi-antenna receivers, communication performance analysis of multi-antenna receivers in the presence of interference, and design of multi-antenna receivers to mitigate the impact of interference on data rates. Typical non-Gaussian statistical models of interference are not derived from a statistical-physical mechanism of interference generation. This limits the usefulness of subsequent communication performance analysis or receiver design performed using such statistical models. In Chapter 3 and 4, I derive interference statistics using a statistical-physical model of interference generation and propagation.

Chapter 3

Statistical Modeling of Interference in Centralized Networks

3.1 Introduction

In Chapter 2, I motivated the need for accurate statistical modeling of multi-antenna interference and subsequent receiver, or network, design based on the resultant models. Robust and accurate statistical models of wireless network interference can be derived using stochastic-physical models of interferer distribution, interference generation, and signal propagation. Prior work on statistical models of interference observed by multi-antenna receivers lacks such a statistical-physical derivation.

In this chapter, I derive statistical models of interference observed by multi-antenna receivers, in wireless networks in which a central authority has the ability to create an interferer-free *guard zone* around the receiver. In such centralized networks, interferers are located only outside of this guard zone. As many wireless networks employ contention-based MAC protocols (e.g. CSMA and multiple access with collision avoidance) or other local coordination techniques to limit the interference, they create a guard zone around the receiver (e.g. in wireless *ad hoc* networks [79] and in dense Wi-Fi networks [17, 85]). Guard

zones around the receiver can also occur due to scheduling-based MAC protocols, such as in cellular networks in which the users in the same cell site are orthogonal to each other and all interfering users are outside the cell site in which the receiver is located[139].

3.2   Organization and Notation

Section 3.3 presents a brief survey of multi-dimensional statistical models of interference. Section 3.4 discusses the system model of interference generation and propagation. Section 3.5 derives the joint interference statistics. Section 3.6 discusses the impact of removing certain system model assumptions on interference statistics. Section 3.7 presents numerical simulations to corroborate the validity of the derived statistical distributions. Section 3.8 provides a summary of key insights and concludes this chapter. Table 3.1 provides a summary of the key symbols used in this chapter.

3.3   Prior Work

Prior work on statistical modeling of interference in multi-antenna wireless systems has typically focused on using multi-variate extensions of single-antenna interference statistical models. The two common approaches of generating multi-variate extensions of uni-variate distributions assume that either (1) interference is independent across the receive antennae, or (2) the multi-variate interference model is isotropic.

Table 3.1: Summary of key symbols used in this chapter

Symbol	Description
Indexing Variables	
i	Interferer index in a set of interferers
n	Antenna index in a multi-antenna receiver
Sets	
$\mathbb{S}_0$	Set of interferers observed by all receive antennae
$\mathbb{S}_n$	Set of interferers observed by n^{th} receive antenna
Constants	
γ	Power pathloss exponent
λ_0, λ_n	Intensity of the Poisson interferer fields Π_0, Π_n
$\delta_\downarrow, \delta_\uparrow$	Inner, outer radii of annular interferer region
Random Variables	
B, χ	Amplitude and phase of interferer emissions
H, Θ	Amplitude and phase of fast fading channel
$\mathbf{Z} = \mathbf{Z}_I + j\mathbf{Z}_Q$	(Complex) Vector sum interference at receiver
$\Phi_{\overline{\mathbf{Z}}}(\mathbf{w})$	Joint characteristic function of $\overline{\mathbf{Z}}$
$\Psi_{\overline{\mathbf{Z}}}(\mathbf{w})$	Joint log-characteristic function of $\overline{\mathbf{Z}}$
$\omega_{n,I}, \omega_{n,Q}$	Frequency variables for $\Phi_{\overline{\mathbf{Z}}}(\mathbf{w})(n = 1, \ldots, N)$
$\mathbf{w}$	$[\omega_{1,I}, \omega_{1,Q}, \omega_{2,I} \ldots \omega_{N,Q}]$

In [47], the author proposes three possible multi-variate extensions to the uni-variate Middelton Class A distribution. The three multidimensional extensions, whose distribution functions are listed in Table 3.2, are as follows:

1. Model I - Each receive antenna experiences additive uni-variate Class A noise with the identical parameters. interference is spatially and temporally independent and identically distributed. Model I cannot capture spatial dependence or sample correlation of interference across receive antennae.

2. Model II - interference is assumed to be spatially dependent and correlated across receive antennae. Model II can represent correlated or uncorrelated random variables; however, it cannot represent independent Class-A random variables.

3. Model III - This model incorporates spatial dependence in multi-antenna interference, but does not support spatial correlation across antenna samples. Model III can represent uncorrelated and spatially dependent Class A random variables but it cannot represent independent or correlated random variables.

These models are multivariate extensions of the Class A distribution and are not derived from physical mechanisms that govern interference generation. While these models have been very useful in analyzing MIMO receiver performance under interference [62] and designing receiver algorithms to improve communication performance in presence of interference, a statistical-physical basis for

these models would further enhance their appeal[112] in linking wireless network performance with environmental factors such as interferer density, fading parameters, etc.

In [112], the authors attempt to derive interference statistics for a two antenna receiver based on the statistical-physical mechanisms that produce the interference. The authors use a physical generation model for the received interference at each of the two antennae that is the sum of interference from stochastically placed interferers which include interferers observed by both antennae as well as interferers observed exclusively by a single antenna. Yet, their resulting model enforces statistical dependence among receive antennae similar to Model II. In other words, either both receive antennae observe an impulsive event or no antenna observes an impulsive event. This is contrary to their statistical-physical generation mechanism, as their resultant model cannot accommodate a scenario in which each of the two receivers observe interference distributed as independent univariate Class A density functions.While the model proposed in [112] is strictly limited to two antenna receivers, it has found application in receiver design[37] and efficient parameter estimation algorithms for this distribution are also available[69, 90]. This dissertation extends the results in [112] by using a similar interference generation and propagation framework to develop statistical-physical interference distributions for any number of receive antenna.

Table 3.2: Key statistical models of interference observed by multi-antenna receivers in interference-limited networks with guard zones.

Model Name	Statistical Model
Multidimensional Class A – Model I	Amplitude Distribution: $$f_{\mathbf{Z}}(\mathbf{z}) = \sum_{k=0}^{\infty} \frac{e^{-A}A^k}{k!} \frac{1}{\sqrt{2\pi \frac{k/A+\Gamma}{1+\Gamma}|\boldsymbol{\Sigma}|}} e^{-\frac{\mathbf{z}^T\boldsymbol{\Sigma}^{-1}\mathbf{z}}{2\frac{k/A+\Gamma}{1+\Gamma}}}$$ A : Overlap index Γ : Ratio of Gaussian to non-Gaussian variance $\boldsymbol{\Sigma}$: Noise covariance matrix
Multidimensional Class A – Model II	Amplitude Distribution: $$f_{\mathbf{Z}}(\mathbf{z}) = \prod_{n=1}^{N_R} \sum_{k=0}^{\infty} \frac{e^{-A_n}A_n{}^k}{k!\sqrt{2\pi\frac{k/A_n+\Gamma_n}{1+\Gamma_n}\sigma_n^2}} e^{-\frac{z_n^2}{2\frac{k/A_n+\Gamma_n}{1+\Gamma_n}\sigma_n^2}}$$ For each antenna n, A_n : Overlap index Γ_n : Ratio of Gaussian to non-Gaussian noise power σ_n^2 : Noise power
Multidimensional Class A – Model III	Amplitude Distribution: $$f_{\mathbf{Z}}(\mathbf{Z}) = \sum_{k=0}^{\infty} \frac{e^{-A}A^k}{k!} \frac{1}{\sqrt{2\pi|\boldsymbol{\Sigma}_k|}} e^{-\frac{\mathbf{z}^T\boldsymbol{\Sigma}_k^{-1}\mathbf{z}}{2}}$$ $\boldsymbol{\Sigma}_k = (\mathbf{I}+\boldsymbol{\Gamma})^{-1}\left(\frac{k}{A}\mathbf{I}+\boldsymbol{\Gamma}\right)$ A : Overlap index $\boldsymbol{\Gamma}$: Diagonal matrix of Gaussian to non-Gaussian variance ratios
Bivariate Class A	Amplitude Distribution: $$f_{\mathbf{Z}}(z_1,z_2) = \frac{e^{-A}}{2\pi|\mathbf{K}_0|^{\frac{1}{2}}} e^{\frac{-\mathbf{z}^T\mathbf{K}_0^{-1}\mathbf{z}}{2}} + \frac{\left(1-e^{-A}\right)}{2\pi|\mathbf{K}_1|^{\frac{1}{2}}} e^{\frac{-\mathbf{z}^T\mathbf{K}_1^{-1}\mathbf{z}}{2}}$$ $\mathbf{K}_m = \begin{bmatrix} c_m^2 & \kappa c_m \hat{c}_m \\ \kappa c_m \hat{c}_m & \hat{c}_m^2 \end{bmatrix}, c_m^2 = \frac{\frac{m}{A}+\Gamma_1}{1+\Gamma_1}, \hat{c}_m^2 = \frac{\frac{m}{A}+\Gamma_2}{1+\Gamma_2}$ A : Overlap index Γ_n : Ratio of Gaussian to non-Gaussian variance at antenna n κ : Correlation coefficient
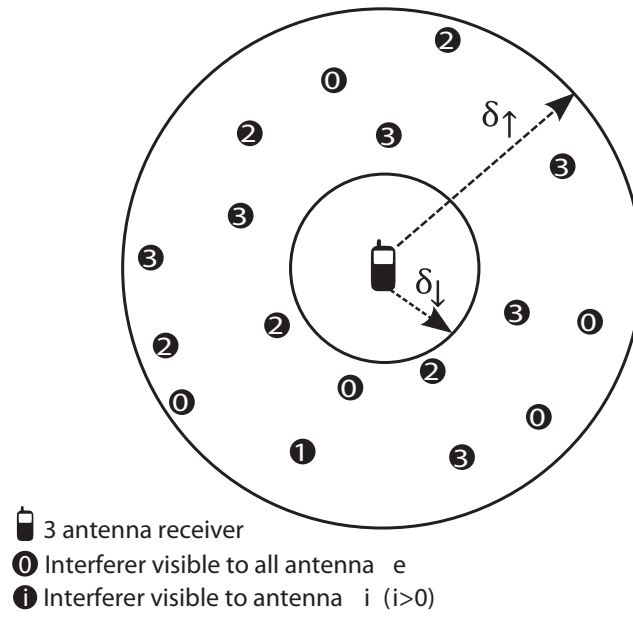
Figure 3.1: Illustration of interferer placement around a 3-antenna receiver at a sampling time instant.

3.4 System model and list of assumptions

I describe a multi-antenna receiver within an interference-limited network via the following assumptions:

Assumption 3.1. *A receiver with N antennae is located at the origin.*

Assumption 3.2. *Interferers are located in a two-dimensional plane around the receiver.*

This assumption is used only for ease of analysis. Distributing interferers in a three-dimensional volume does not alter the nature of any results, other than certain parameter values.

Assumption 3.3. *Interferers are distributed as a spatial Poisson Point Process.*

At each sampling time instant, the locations of the active interferers in $\mathcal{S}_n$ $\forall\ n = 0, \cdots, N$ are distributed according to a homogeneous spatial Poisson Point Process in the two-dimensional plane around the receiver. The intensity of set $\mathcal{S}_n$ is denoted by $\lambda_n\ \forall\ n = 0, \ldots, N$. The Poisson Point Process distribution is usually applied to modeling the statistical distribution of interfering sources in wireless communication systems[12]. A spatial Poisson point process distribution of interferers allows each interferer set $\mathcal{S}_n$ to have potentially infinite number of interferers. The distance of each interferer from the origin provides an ordering function, ensuring that the interferers in each set are countable. In other words, the ith interferer in $\mathcal{S}_n$, located at coordinates $\mathbf{R}_{n,i}$, is defined by implicitly assuming $\|\mathbf{R}_{n,1}\|_2 < \|\mathbf{R}_{n,2}\|_2 < \|\mathbf{R}_{n,3}\|_2 < \cdots$.

Assumption 3.4. *The interferers are located within a annulus with inner and outer radii $\delta_\downarrow$ and $\delta_\uparrow$, respectively.*

By allowing $\delta_\downarrow > 0$, I constrain the active interferers to be located outside of a finite disk around the multi-antenna wireless receiver. This models a wireless network where interferers are placed such that there exists a guard zone around the receiver in which no interferer is present. n many centralized communication systems, a central authority such as a base station may limit transmissions within a radius around an active receiver. Many medium access control protocols can also enforce such a *guard-zone* around the receiver[17, 79]. Such a model can be applied to cellular and *ad-hoc* networks with contention-based or

scheduling-based MAC protocols which have the effect of creating a guard zone around the receiver [79].

Assumption 3.5. *Inter-antenna separation at the receiver is insignificant compared to the distance between interferers and the receiver.*

This is a reasonable assumption, given the rise of small form-factor mobile devices utilizing multiple antennae. Inter-antenna separation gains import when modeling interference generated from the receiver platform itself[147], or in cooperative networks where the distance between two nodes is comparable to their distance from other interference causing users. Incorporating antenna separation into joint statistical models of interference is beyond the scope of this paper and a very interesting topic of future research.

Assumption 3.6. *Inteferers are either observed by all antennae, or by only one antenna.*

At each time snapshot, the active interfering sources are classified into $N+1$ independent sets $\mathcal{S}_0, \mathcal{S}_1, \cdots, \mathcal{S}_N$. $\mathcal{S}_0$ denotes the set of interferers that cause interference to every receive antenna. $\mathcal{S}_n \ \forall \ n = 1, \cdots, N$ denotes the set of interferers that are observed by antenna n alone. This is the key assumption in the proposed framework for modeling spatial dependence in interference observed by a multi-antenna receiver. In prior work, interference is typically modeled as one of two extremes, either all interferers are observed by every receive antenna, or different receivers observe independent sets of interferers. My pro-

posed model generalizes this notion, ensuring that the results are not only applicable to these two extreme scenarios, but also to a continuum between these two extremes.

A common scenario in which such an interferer environment may arise is with the use of sectorized antennae with full frequency reuse, which are co-located wireless directional antennae with radiation patterns shaped as partially overlapping sectors that combine to cover the entire space around the receiver [48]. Combining the signals received by sectorized antennae can be useful as it can provides the advantages of spatial diversity and mitigates the harm from multipath delay[105]. Interference signals common to all antennae may arise in the overlapping sections, i.e., where the antenna gain for all antennae is similar, and individual antennae may still see independent interference in sectors where one antenna exhibits high gain while others exhibit a null. While antenna radiation patterns are not accounted for in my analysis, they can easily be combined with the fading channel and my results would be applicable.

To simplify the derivation of the multi-antenna interference model, the notion of interferers observed only by one antenna and interferers observed by all receive antennas can be applied to the system model. This results in $N_R + 1$ sets of active interferers that include N_R sets of interferers observed by one of the N_R receive antennas and one set of interferers observed by all of the receive antennas. Each receive antenna now observes interference from two sets of active interferers, similar to the two antenna interference model. This greatly simplifies the system model, yet it still maintains the key aspect of modeling correlation be-

52

tween the set of active interferers across antennas. This model can be applied to scenarios where each antenna observes interference generated from independent interferers as well as scenarios where each receiver observes interference generated from the same set of interferers.

Case I - Interferer set $\mathcal{S}_0$ is empty, i.e., $\lambda_n > 0$ and $\lambda_0 = 0$. In this scenario, each receiver is under the influence of an independent set of interferers. It is trivial to see that the resulting interference would also exhibit independence across the receive antennae, i.e., Case I results in interference that has characteristics of Model I in Table 2.2.

Case II - Interferer sets $\mathcal{S}_n \ \forall \ n = 1, \cdots, N$ are empty sets, i.e., $\lambda_n = 0$ and $\lambda_0 > 0$. Both receivers observe the same set of interferers, thereby causing the resulting interference to have spatial dependence across receive antennae. Model II and III in [47], also shown in Table 2.2, have the same characteristic in spatial statistics but there is no statistical physical derivation linking these models to any interference generation mechanism, such as one described in my system model.

Case III - All interferer sets are non-empty, i.e., $\lambda_n > 0$ and $\lambda_0 > 0$. This models partial correlation in the interferer field observed by each of the receive antennae. The common set of interferers in $\mathcal{S}_0$ models correlation between the interferer fields of two antennae. The level of correlation can be tuned by changing the intensity of the Poisson point process representing each set in the interferer field. This model is quite commonly used in multi-dimensional temporal[178] and spatial interference modeling[25]. The resulting interference is spatially de-

53

pendent across receive antennae and neither of Models I, II, or III appropriately capture the joint spatial statistics of interference generated in such an environment. A statistical model that represents the amplitude distribution of interference resulting from interferer fields in Case III would unify the disparate Models I, II and III.

Assumption 3.7. *The wireless signal energy decays according to the power-law path-loss model with coefficient γ.*

Assumption 3.8. *There is fast fading between the interferer and receiver.*

The fast-fading channel between the interfering sources and the receiver is modeled using the Rayleigh distribution[65].

Assumption 3.9. *Additive thermal noise is ignored at the receiver.*

With high user density and frequency reuse, many communication systems are interference-limited; i.e., interference at the receiver is much stronger than the thermal noise component. Consequently, the resulting statistical model is applicable to interference-limited communication scenarios.

Assumption 3.10. *The receiver is placed at the origin of the two-dimensional plane.*

Without loss of generality, the receiver is placed at the origin of the two-dimensional plane. Since the spatial Poisson Point Process is invariant to translation, any derived results remain unchanged by the choice of origin.

Figure 3.1 illustrates the interferer distribution model for a three antenna receiver.

3.5 Joint Statistics of Interference across Multiple Antennae

In this section, I derive joint interference statistics under the assumption that the antenna are co-located. This is a reasonable assumption in many mobile devices where the distance between other interfering users and the device is much larger than the distance between the antennae on the device. At each receive antenna n, the baseband sum interference signal at any sampling time instant can be expressed as the sum total of the interference signal observed from common interferers and the interference signal from interferers visible only to antenna n. I can express the interference signal at the nth antenna as

$$Z_n = Z'_{\mathcal{S}_0,n} + Z'_{\mathcal{S}_n} \tag{3.1}$$

where $Z'_{\mathcal{S}_n}$, $Z'_{\mathcal{S}_0,n}$ represent the sum interference signal from interfering sources in $\mathcal{S}_n$ (visible only to antenna n), and interfering sources in $\mathcal{S}_0$ (visible to all antennae), respectively. The sum interference signal $Z'_{\mathcal{S}_n}$ from interferers in $\mathcal{S}_n$ can be written as [114]

$$Z'_{\mathcal{S}_n} = \sum_{i \in \mathcal{S}_n} B_i^n e^{j\chi_i^n} (D_{n,i})^{-\frac{\gamma}{2}} H_i^n e^{j\Theta_i^n}. \tag{3.2}$$

$Z'_{\mathcal{S}_n}$ is the sum of interfering signals $B_i^n e^{j\chi_i^n} (D_{n,i})^{-\frac{\gamma}{2}} H_i^n e^{j\Theta_i^n}$ emitted by each interferer $i \in \mathcal{S}_n$ located at $\mathbf{R}_{n,i}$. $B_i^n e^{j\chi_i^n}$ denotes interferer emissions from interfering source i where B_i^n is the emission signal envelope and χ_i^n is the phase of the emission. I assume that the signal envelope B_i^n is constant. $D_{n,i} = \|\mathbf{R}_{n,i}\|$

denotes the distance between the receiver n (located at origin) and the interferer, and γ is the power pathloss coefficient ($\gamma > 2$), consequently, $(D_{n,i})^{-\frac{\gamma}{2}}$ indicates the reduction in interfering signal energy during propagation through the wireless medium. $H_i^n e^{j\Theta_i^n}$ denotes the complex fast-fading channel between the interferer and receiver n. For the fast fading channel model, I assume that the channel amplitude H_i^n follows the Rayleigh distribution, and that the channel phase Θ_i^n is uniformly distributed on $[0, 2\pi]$. H_i^n, Θ_i^n, B_i^n, and χ_i^n are assumed to be *i.i.d.* across all interfering sources $i \in \mathcal{S}_n$. In Sections 3.6.1 and 3.6.3, I study the impact of removing many of these assumptions on the statistics of interference. The signal from the common set of interferers $\mathcal{S}_0$ is expressed as

$$Z'_{\mathcal{S}_0,n} = \sum_{i^0 \in \mathcal{S}_0} B_i^0 e^{j\chi_i^0}(D_{0,i})^{-\frac{\gamma}{2}} H_{n,i}^0 e^{j\Theta_{n,i}^0}. \tag{3.3}$$

Note that the difference between (3.2) and (3.3) is that the interferer emission signal $B_i^0 e^{j\chi_i^0}$ and the distance D_i^0 between interferer i and the receive antenna n (placed at origin), is independent of the antenna under observation (n). This is because I ignore inter-antenna spacing and assume all antennae are located at the origin. The channel between the interferer and n^{th} receiver, denoted by $H_{n,i}^0 e^{j\theta_{n,i}^0}$, is also assumed *i.i.d.* across n and i. In Section 3.6.3, I will discuss the impact of spatial correlation of the channel model on interference statistics. Combining (3.1), (3.2), and (3.3) I can write the resultant interference signal at the nth receive antenna as

$$Z_n = \sum_{i_0 \in \mathcal{S}_0} B_{i_0}^0 D_{0,i_0}^{-\frac{\gamma}{2}} H_{n,i_0}^0 e^{j(\chi_{i_0}^0 + \Theta_{n,i_0}^0)} + \sum_{i \in \mathcal{S}_n} B_i^n D_{n,i}^{-\frac{\gamma}{2}} H_i^n e^{j(\chi_i^n + \Theta_i^n)}. \tag{3.4}$$

The complex baseband interference at each receive antenna can then be decomposed into its in-phase and quadrature components $Z_n = Z_{n,I} + j Z_{n,Q}$, where

$$Z_{n,I} = \sum_{i_0 \in \mathcal{S}_0} B_{i_0}^0 D_{0,i_0}^{-\frac{\gamma}{2}} H_{n,i_0}^0 \cos(\chi_{i_0}^0 + \Theta_{n,i_0}^0) + \sum_{i \in \mathcal{S}_n} B_i^n D_{n,i}^{-\frac{\gamma}{2}} H_i^n \cos(\chi_i^n + \Theta_i^n), \qquad (3.5)$$

and

$$Z_{n,Q} = \sum_{i_0 \in \mathcal{S}_0} B_{i_0}^0 D_{0,i_0}^{-\frac{\gamma}{2}} H_{n,i_0}^0 \sin(\chi_{i_0}^0 + \Theta_{n,i_0}^0) + \sum_{i \in \mathcal{S}_n} B_i^n D_{n,i}^{-\frac{\gamma}{2}} H_i^n \sin(\chi_i^n + \Theta_i^n). \qquad (3.6)$$

In order to study the spatial statistics of interference across multiple receive antennae, I will derive the joint characteristic function of the in-phase and quadrature components of interference. Using (3.1), (3.5) and (3.6), the joint characteristic function $\Phi_\mathbf{Z}$ can be written as

$$\Phi_\mathbf{Z}(\mathbf{w}) = \mathbb{E}\left\{ e^{\sum_{n=1}^N j \omega_{n,I} \mathbf{Z}_{n,I} + j \omega_{n,Q} \mathbf{Z}_{n,Q}} \right\} \qquad (3.7)$$

where $\mathbf{w} = \begin{bmatrix} \omega_{1,I} & \omega_{1,Q} & \omega_{2,I} & \omega_{2,Q} & \cdots & \omega_{N,I} & \omega_{N,Q} \end{bmatrix}$. Note that the expectation is evaluated over the random variables $|\mathcal{S}_0|$, $|\mathcal{S}_n|$, $D_{0,i}$, $D_{n,i}$, $H_{n,i}^0$, H_i^n, B_i^0, B_i^n, χ_i^0, χ_i^n, $\Theta_{n,i}^0$ and $\Theta_i^n \ \forall \ n = 1,\dots,N$. For the sake of brevity and readability, I refrain from listing all of these random variables in the subscript of the expectation operator. I can separate the independent terms in the expectation by noting that the interferers in the different sets $\mathcal{S}_n$ are distributed in space as independent homogeneous processes, and their emissions and channel realizations are also independent as well. Substituting (3.4) in (3.7) and separating independent

57

terms in the expectation, I get

$$\Phi_{\mathbf{Z}}(\mathbf{w}) = \prod_{n=1}^{N} \mathbb{E}\left\{ e^{j\sum_{i=1}^{|S_n|} D_{n,i}^{-\frac{\gamma}{2}} H_i^n B_i^n \left(\omega_{n,I}\cos(\chi_i^n+\Theta_i^n)+\omega_{n,Q}\sin(\chi_i^n+\Theta_i^n)\right)} \right\}$$
$$\times \mathbb{E}\left\{ e^{j\sum_{n=1}^{N}\sum_{i_0=1}^{|S_0|} D_{i_0}^{-\frac{\gamma}{2}} H_{n,i_0}^0 B_{i_0}^0 \left(\omega_{n,I}\cos(\chi_{i_0}^0+\Theta_{n,i_0}^0)+\omega_{n,Q}\sin(\chi_{i_0}^0+\Theta_{n,i_0}^0)\right)} \right\}. \qquad (3.8)$$

To simplify notation, (3.8) is decomposed into the product form

$$\Phi_{\mathbf{Z}}(\mathbf{w}) = \Phi_{S_0}(\mathbf{w})\prod_{n=1}^{N}\Phi_{S_n}(\mathbf{w}) \qquad (3.9)$$

where,

$$\Phi_{S_0}(\mathbf{w}) = \mathbb{E}\left\{ e^{j\sum_{n=1}^{N}\sum_{i_0=1}^{|S_0|} D_{i_0}^{-\frac{\gamma}{2}} H_{n,i_0}^0 B_{i_0}^0 \left(\omega_{n,I}\cos(\chi_{i_0}^0+\Theta_{n,i_0}^0)+\omega_{n,Q}\sin(\chi_{i_0}^0+\Theta_{n,i_0}^0)\right)} \right\} \qquad (3.10)$$

$$\Phi_{S_n}(\mathbf{w}) = \mathbb{E}\left\{ e^{j\sum_{i=1}^{|S_n|} D_{n,i}^{-\frac{\gamma}{2}} H_i^n B_i^n \left(\omega_{n,I}\cos(\chi_i^n+\Theta_i^n)+\omega_{n,Q}\sin(\chi_i^n+\Theta_i^n)\right)} \right\}. \qquad (3.11)$$

Each component term in (3.9) is the characteristic function of the interference contribution by one of each interferer sets $\{S_0, S_1, \ldots, S_n\}$. I can rewrite (3.10) and (3.11) in their polar forms as

$$\Phi_{S_0}(\mathbf{w}) = \mathbb{E}\left\{ e^{j\sum_{n=1}^{N}|\overline{\omega}_n|\sum_{i=1}^{|S_0|} D_{0,i}^{-\frac{\gamma}{2}} H_{n,i}^0 B_i^0 \cos(\chi_i^0+\Theta_{n,i}^0+\xi_{\omega,n})} \right\} \qquad (3.12)$$

$$\Phi_{S_n}(\mathbf{w}) = \mathbb{E}\left\{ e^{j|\overline{\omega}_n|\sum_{i=1}^{|S_n|} D_i^{-\frac{\gamma}{2}} H_i^n B_i^n \cos(\chi_i^n+\Theta_i^n+\xi_{\omega,n})} \right\} \qquad (3.13)$$

where $|\overline{\omega}_n| = \sqrt{\omega_{n,I}^2 + \omega_{n,Q}^2}$ and $\xi_{\omega,n} = \tan^{-1}\left(\frac{\omega_{n,I}}{\omega_{n,Q}}\right)$. I will now evaluate each component term in (3.9) for interferer environments with and without *guard zones*, as described in Section 5.4.

3.5.1 Evaluation of $\Phi_{S_0}(\mathbf{w})$ (Interference Contribution from S_0)

In this section, I evaluate the contribution of the interferers in set S_0 to the joint spatial statistics of interference, denoted by the term $\Phi_{S_0}(\mathbf{w})$ in (3.7).

58

In the constrained interferer placement system model, the interferers within $\mathcal{S}_0$ are distributed according to a homogeneous spatial Poisson Point Process inside an annulus with finite inner and outer radii $\delta_\downarrow$ and $\delta_\uparrow$, respectively. Consequently, the number of interferers $|\mathcal{S}_0|$ is a Poisson random variable with parameter $\lambda\pi(\delta_\uparrow^2 - \delta_\downarrow^2)$. Conditioned on $|\mathcal{S}_0|$, (3.12) can be expressed as

$$\Phi_{\mathcal{S}_0}(\mathbf{w}) = \mathbb{E}\left\{e^{j\sum_{n=1}^{N}|\overline{\omega}_n|\sum_{i=1}^{|\mathcal{S}_0|}D_{0,i}^{-\frac{\gamma}{2}}H_{n,i}^0 B_i^0 \cos(\chi_i^0 + \Theta_{n,i}^0 + \xi_{\omega,n})}\right\} \tag{3.14}$$

$$= \sum_{k=0}^{\infty}\mathbb{E}\left\{e^{j\sum_{n=1}^{N}|\overline{\omega}_n|\sum_{i=1}^{k}D_{0,i}^{-\frac{\gamma}{2}}H_{n,i}^0 B_i^0 \cos(\chi_i^0 + \Theta_{n,i}^0 + \xi_{\omega,n})}\,\Big|\,|\mathcal{S}_0| = k\right\}\mathbb{P}(|\mathcal{S}_0| = k) \tag{3.15}$$

$$= \sum_{k=0}^{\infty}\mathbb{E}\left\{e^{j\sum_{n=1}^{N}|\overline{\omega}_n|D_0^{-\frac{\gamma}{2}}H_n^0 B^0 \cos(\chi^0 + \Theta_n^0 + \xi_{\omega,n})}\right\}^k \mathbb{P}(|\mathcal{S}_0| = k) \tag{3.16}$$

Once conditioned on a fixed number of total points, the points in a Poisson Point Process are distributed independently and uniformly across the region in consideration. This allows us to remove the interferer index i and treat the contribution to interference from each interferer as an independent random variable. $H_{n,i}^0$, $B_{n,i}^0$, $\chi_{n,i}^0$ and $\Theta_{n,i}^0$ are all $i.i.d$ and can be replaced in (3.16) by H_n^0, B_n^0, χ_n^0 and Θ_n^0, respectively. $D_{0,i}$ is assumed to be increasing with the index i, since I assumed that the interferers are ordered according to how close they are located to the origin. However, by virtue of a property of Poisson Point Processes, the points are uniformly distributed within the region of the Point Process when conditioned on the total number of points k. Thus, I replace $D_{0,i}$ by the random variable D_0, that follows the distribution

$$f_{D_0|k}(D_0|k) = \begin{cases} \frac{2D_0}{\delta_\uparrow^2 - \delta_\downarrow^2} & \text{if } \delta_\downarrow \leq D_0 \leq \delta_\uparrow, \\ 0 & \text{otherwise.} \end{cases}$$

59

This distribution arises when I consider the annular disc with inner and outer radius of $\delta_\downarrow$ and $\delta_\uparrow$, and k points distributed uniformly in this region. The number of interferers k within the annular region is a Poisson random variable with mean $\lambda_0 \pi(\delta_\uparrow^2 - \delta_\downarrow^2)$. Combining this notion with (3.16) I get

$$\Phi_{\mathcal{S}_0}(\mathbf{w}) = \sum_{k=0}^{\infty} \mathbb{E}\left\{ e^{j \sum_{n=1}^{N} |\overline{\omega}_n| D_0^{-\frac{\gamma}{2}} H_n^0 B^0 \cos(\chi^0 + \Theta_n^0 + \xi_{\omega,n})} \right\}^k e^{-\lambda_0 \pi(\delta_\uparrow^2 - \delta_\downarrow^2)} \frac{\left(\lambda_0 \pi(\delta_\uparrow^2 - \delta_\downarrow^2)\right)^k}{k!}$$

$$\tag{3.17}$$

$$= e^{-\lambda_0 \pi(\delta_\uparrow^2 - \delta_\downarrow^2)} \sum_{k=0}^{\infty} \frac{\left[\left(\lambda_0 \pi(\delta_\uparrow^2 - \delta_\downarrow^2)\right) \mathbb{E}\left\{ e^{j \sum_{n=1}^{N} |\overline{\omega}_n| D_0^{-\frac{\gamma}{2}} H_n^0 B^0 \cos(\chi^0 + \Theta_n^0 + \xi_{\omega,n})} \right\}\right]^k}{k!}$$

$$\tag{3.18}$$

$$= e^{-\lambda_0 \pi(\delta_\uparrow^2 - \delta_\downarrow^2)} e^{\mathbb{E}\left\{ e^{j \sum_{n=1}^{N} |\overline{\omega}_n| D_0^{-\frac{\gamma}{2}} H_n^0 B^0 \cos(\chi^0 + \Theta_n^0 + \xi_{\omega,n})} \right\} \lambda_0 \pi(\delta_\uparrow^2 - \delta_\downarrow^2)}$$

$$\tag{3.19}$$

$$= e^{\left[\mathbb{E}\left\{ e^{j \sum_{n=1}^{N} |\overline{\omega}_n| D_0^{-\frac{\gamma}{2}} H_n^0 B^0 \cos(\chi^0 + \Theta_n^0 + \xi_{\omega,n})} \right\} - 1\right] \lambda_0 \pi(\delta_\uparrow^2 - \delta_\downarrow^2)}$$

$$\tag{3.20}$$

By taking the logarithm of $\Phi_{\mathbf{Z}, \mathcal{S}_0}(\mathbf{w})$ in (3.20), the log-characteristic function is

$$\Psi_{\mathcal{S}_0}(\mathbf{w}) \triangleq \log \Phi_{\mathbf{Z}, \mathcal{S}_0}(\mathbf{w}) \tag{3.21}$$

$$= \lambda_0 \pi(\delta_\uparrow^2 - \delta_\downarrow^2) \left(\mathbb{E}\left\{ e^{j \sum_{n=1}^{N} |\overline{\omega}_n| D_0^{-\frac{\gamma}{2}} H_n^0 B^0 \cos(\chi^0 + \Theta_n^0 + \xi_{\omega,n})} \right\} - 1 \right) \tag{3.22}$$

$$= \overline{K} \left(\mathbb{E}\left\{ \prod_{n=1}^{N} e^{j |\overline{\omega}_n| D_0^{-\frac{\gamma}{2}} H_n^0 B^0 \cos(\chi^0 + \Theta_n^0 + \xi_{\omega,n})} \right\} - 1 \right) \tag{3.23}$$

where $\overline{K} = \lambda_0 \pi(\delta_\uparrow^2 - \delta_\downarrow^2)$. Next I use the identity

$$e^{j a \cos(b)} = \sum_{m=0}^{\infty} j^m \epsilon_m J_m(a) \cos(mb) \tag{3.24}$$

where $\epsilon_0 = 1$, $\epsilon_m = 2$ for $m \geq 1$, and $J_m(\cdot)$ denotes the Bessel function of order m. Combining (3.24) and (3.23), the log-characteristic function $\Psi_{\mathbf{Z},\mathcal{S}_0}(\mathbf{w})$ can be expressed as

$$\Psi_{\mathcal{S}_0}(\mathbf{w})$$
$$= \overline{K}\left(\mathbb{E}\left\{ \prod_{n=1}^{N} \sum_{m_n=0}^{\infty} j^{m_n} \epsilon_{m_n} J_{m_n}\left(|\overline{\omega}_n| D_0^{-\frac{\gamma}{2}} H_n^0 B^0 \cos\left(m_n\left(\chi^0 + \Theta_n^0 + \xi_{\omega,n} \right) \right) \right) \right\} - 1 \right).$$
(3.25)

Since χ^0 and Θ_n^0 are uniform random variables within $[0, 2\pi]$, for any value of $\xi_{\omega,n}$ and m_n, $m_n\left(\chi^0 + \Theta_n^0 + \xi_{\omega,n} \right)$ modulo 2π is also uniformly distributed over $[0, 2\pi]$. Thus, all terms in (3.25) with $m_n > 0 \ \forall \ n = 1 \to N$ reduce to zero after taking expectation with respect to Θ_n^0, and (3.25) reduces to

$$\Psi_{\mathcal{S}_0}(\mathbf{w}) = \overline{K}\left(\mathbb{E}\left\{ \prod_{n=1}^{N} J_0\left(|\overline{\omega}_n| D_0^{-\frac{\gamma}{2}} H_n^0 B^0 \right) \right\} - 1 \right).$$
(3.26)

Note that the expectation is now with respect to the remaining random variables in (3.26). To evaluate the expectation in (3.26), I re-write it as

$$\Psi_{\mathcal{S}_0}(\mathbf{w}) = \overline{K}\left(\mathbb{E}\left\{ \prod_{n=1}^{N} \mathbb{E}_{H_n^0}\left\{ J_0\left(|\overline{\omega}_n| D_0^{-\frac{\gamma}{2}} H_n^0 B^0 \right) \right\} \right\} - 1 \right).$$
(3.27)

Note that I used the assumption that the fast-fading channel between interferer and receive antennae are spatially independent across the antenna index n. Using the series expansion of the zero-order Bessel function,

$$J_0(x) = \sum_{m=0}^{\infty} \frac{(-1)^m x^{2m}}{2^{2m} m! \Gamma(m+1)}$$
(3.28)

I can rewrite (3.27) as

$$\Psi_{\mathcal{S}_0}(\mathbf{w}) = \overline{K}\left(\mathbb{E}\left\{\prod_{n=1}^{N}\mathbb{E}_{H_n^0}\left\{\sum_{m=0}^{\infty}\frac{(-1)^m\left(|\overline{\omega}_n|D_0^{-\frac{\gamma}{2}}H_n^0 B^0\right)^{2m}}{2^{2m}m!\Gamma(m+1)}\right\}\right\} - 1\right) \qquad (3.29)$$

$$= \overline{K}\left(\mathbb{E}\left\{\prod_{n=1}^{N}\sum_{m=0}^{\infty}\frac{(-1)^m\left(|\overline{\omega}_n|D_0^{-\frac{\gamma}{2}}B^0\right)^{2m}\mathbb{E}_{H_n^0}\left\{(H_n^0)^{2m}\right\}}{2^{2m}m!\Gamma(m+1)}\right\} - 1\right) \qquad (3.30)$$

Under the assumption that the fading channel is Rayleigh distributed, the $2m^{\text{th}}$ moment of H_n^0 is $\left(\mathbb{E}\left\{H^{0^2}\right\}\right)^m\Gamma(1+m)$. Applying to (3.30), I get

$$\Psi_{\mathcal{S}_0}(\mathbf{w}) = \overline{K}\left(\mathbb{E}\left\{\prod_{n=1}^{N}\sum_{m=0}^{\infty}\frac{(-1)^m\left(|\overline{\omega}_n|D_0^{-\frac{\gamma}{2}}B^0\right)^{2m}\left(\mathbb{E}\left\{H^{0^2}\right\}\right)^m\Gamma(1+m)}{2^{2m}m!\Gamma(m+1)}\right\} - 1\right)$$

$$\qquad (3.31)$$

$$= \overline{K}\left(\mathbb{E}\left\{\prod_{n=1}^{N}\sum_{m=0}^{\infty}\frac{(-1)^m\left(|\overline{\omega}_n|D_0^{-\frac{\gamma}{2}}B^0\sqrt{\left(\mathbb{E}\left\{H^{0^2}\right\}\right)}\right)^{2m}}{2^{2m}m!}\right\} - 1\right) \qquad (3.32)$$

$$= \overline{K}\left(\mathbb{E}\left\{\prod_{n=1}^{N}e^{-\frac{\left(|\overline{\omega}_n|D_0^{-\frac{\gamma}{2}}B^0\sqrt{\left(\mathbb{E}\left\{H^{0^2}\right\}\right)}\right)^2}{4}}\right\} - 1\right) \qquad (3.33)$$

$$= \overline{K}\left(\mathbb{E}\left\{e^{-\frac{\left(D_0^{-\frac{\gamma}{2}}B^0\right)^2\mathbb{E}\left\{H^{0^2}\right\}}{4}\sum_{n=1}^{N}(|\overline{\omega}_n|)^2}\right\} - 1\right) \qquad (3.34)$$

$$= \overline{K}\left(\mathbb{E}\left\{e^{-\frac{\left(D_0^{-\frac{\gamma}{2}}B^0\right)^2\mathbb{E}\left\{H^{0^2}\right\}\|\mathbf{w}\|^2}{4}}\right\} - 1\right). \qquad (3.35)$$

Expanding the expectation in (3.35) with respect to the random variable D_0, I have

$$\Psi_{S_0}(\mathbf{w}) = \lim_{\delta_\uparrow \to \infty} \overline{K} \left(\mathbb{E}\left\{ \int_0^{\delta_\uparrow} e^{-\|\mathbf{w}\|^2 \left(D_0^{-\frac{\gamma}{2}} B^0 \right)^2 \mathbb{E}\{H^{0^2}\}} \frac{2 D_0}{\delta_\uparrow^2 - \delta_\downarrow^2} d D_0 \right\} - 1 \right) \tag{3.36}$$

Using Taylor series expansion of e^x, (3.36) can be written as

$$\Psi_{S_0}(\mathbf{w})$$

$$= \lim_{\delta_\uparrow \to \infty} \overline{K} \left(\mathbb{E}\left\{ \int_0^{\delta_\uparrow} \sum_{m=1}^{\infty} \frac{(-1)^m |D_0^{-\frac{m\gamma}{2}} \mathbb{E}\{(B^0)^{2m}\} (\mathbb{E}\{H^{0^2}\})^m \|\mathbf{w}\|^{2m}}{4^m m!} \frac{2 D_0}{\delta_\uparrow^2 - \delta_\downarrow^2} d D_0 \right\} - 1 \right) \tag{3.37}$$

$$= \lambda_0 \pi \left(\sum_{m=1}^{\infty} \frac{(-1)^m |D_0^{-\frac{m\gamma}{2}} \{(B^0)^{2m}\} (\mathbb{E}\{H^{0^2}\})^m \|\mathbf{w}\|^{2m} (\delta_\downarrow^{-\gamma m - 2} - \delta_\uparrow^{-\gamma m - 2})}{4^m m!} \frac{2}{m\gamma - 2} \right) \tag{3.38}$$

valid for $\gamma > 2$. Assuming that the interferer emission amplitude B^0 has constant value $\overline{B}$, I get

$$\Psi_{S_0}(\mathbf{w}) = \lambda \pi \sum_{m=1}^{\infty} \frac{(-1)^m (\|\mathbf{w}\|^2 \sigma \overline{B})^m \delta_\downarrow^{-\gamma m + 2}}{4^m m!} \frac{2}{\gamma m - 2} \left(1 - \frac{\delta_\uparrow^{-\gamma m - 2}}{\delta_\downarrow} \right) \tag{3.39}$$

In Section 3.6.1, I discuss the impact of applying any general interferer emission amplitude distribution on the interference statistics. The multiplicative term $\frac{2}{m\gamma-2}\left(1 - \frac{\delta_\uparrow^{-\gamma m - 2}}{\delta_\downarrow}\right)$ prevents us from simplifying (3.39) into an exponential. Note that in reasonable to assume that for many wireless network scenarios $\delta_\uparrow \gg \delta_\downarrow$, in which case $\left(1 - \frac{\delta_\uparrow^{-\gamma m - 2}}{\delta_\downarrow}\right) \to 1$ leaving the term $\frac{2}{m\gamma-2}$. Similar to an approach used in [71], I approximate $\frac{2}{m\gamma-2}$ as an power series $\eta \beta^m$ for $m \geq 1$ and choose

parameters η_γ and β_γ to minimize the mean squared error (MSE)

$$\{\eta_\gamma, \beta_\gamma\} = \arg \min_{\eta \in \mathbb{R}, \beta \in \mathbb{R}} \sum_{m=1}^{\infty} \left(\frac{2}{m\gamma - 2} - \eta \beta^m \right)^2. \tag{3.40}$$

Using the non-linear unconstrained optimization toolbox functionality provided by MATLAB, I am able to determine the appropriate values for $\{\eta_\gamma, \beta_\gamma\}$ for any $\gamma > 2$ with MSE less than 10^{-4}. In the case where $\left(1 - \frac{\delta_\uparrow}{\delta_\downarrow}^{-\gamma m - 2} \right)$ cannot be ignored, I can again use the power series approximation to find parameters $\{\eta_\gamma, \beta_\gamma\}$ such that $\{\eta_\gamma, \beta_\gamma\} = \arg\min_{\eta \in \mathbb{R}, \beta \in \mathbb{R}} \sum_{m=1}^{\infty} \left(\frac{2}{m\gamma-2} \left(1 - \frac{\delta_\uparrow}{\delta_\downarrow}^{-\gamma m - 2} \right) - \eta \beta^m \right)^2.$

Using the aforementioned approximation, the log-characteristic exponent in (3.39) can be expressed as

$$\Psi_{S_0}(\mathbf{w}) = \lambda \pi \sum_{m=1}^{\infty} \frac{(-1)^m (\|\mathbf{w}\|^2 \sigma \overline{B})^m \delta_\downarrow^{-\gamma m + 2}}{4^m m!} \eta_\gamma \beta_\gamma^m \tag{3.41}$$

$$= \lambda \pi \delta_\downarrow^2 \eta_\gamma \left(e^{-\frac{\|\mathbf{w}\|^2 \delta_\downarrow^{-\gamma} \beta_\gamma \mathbb{E}\{H^{0^2}\} \overline{B}^2}{4}} - 1 \right) \tag{3.42}$$

$$= A_0 \left(e^{-\frac{\|\mathbf{w}\|^2 \Omega_0}{2}} - 1 \right). \tag{3.43}$$

Equation (3.41) is the log-characteristic function of a Middleton Class A where $A_0 = \lambda \pi \delta_\downarrow^2 \eta_\gamma$ is the overlap index indicating the impulsiveness of the interference, and $\Omega_0 = \frac{A \delta_\downarrow^{-\gamma} \beta_\gamma \mathbb{E}\{H^{0^2}\} \overline{B}^2}{2}$ is the mean intensity of the interference [115]. Thus, I can write (3.10) as

$$\Phi_{S_0}(\mathbf{w}) = e^{A_0 \left(e^{-\frac{\|\mathbf{w}\|^2 \Omega_0}{2}} - 1 \right)} \tag{3.44}$$

3.5.2 Evaluation of $\Phi_{S_n}(\mathbf{w})$ (Interference Contribution from S_n)

In this section, I derive contribution of interferer sets $S_i \forall i = 1, 2...N$ to the spatial joint statistics of interference. At each antenna n, the interference

from the exclusive set of interferers is identical to interference seen by a single antenna receiver surrounded by interferers distributed according to a Poisson Point Process. The statistics of such interference have been derived in [71] and shown to be well modeled by the univariate Middleton Class A distribution. Thus I can write (3.11) as

$$\Phi_{\mathcal{S}_n}(\mathbf{w}) = e^{A_n\left(e^{-\frac{|\varpi_n|^2\Omega_n}{2}}-1\right)} \tag{3.45}$$

where $A_n = \lambda_n \pi \delta_\downarrow \eta_\gamma$ and $\Omega_n = \frac{A_n \delta_\downarrow^{-\gamma}\mathbb{E}\{H^{n2}\}\overline{B}^2\beta_\gamma}{2}$ are the parameters of the Class A distribution. Combining (3.9), (3.44) and (3.45), I get the joint characteristic function of interference as

$$\Phi_{\mathbf{Z}}(\mathbf{w}) = e^{A_0\left(e^{-\frac{\|\mathbf{w}\|^2\Omega_n}{2}}-1\right)} \times \prod_{n=1}^{N} e^{A_n\left(e^{-\frac{|\varpi_n|^2\Omega_n}{2}}-1\right)}. \tag{3.46}$$

The corresponding probability density function can be written as

$$f(\mathbf{Z}) = \left\{\prod_{n=1}^{N}\left\{\sum_{m_n=1}^{\infty}\frac{e^{-A_n}(A_n)^{m_n}}{\sqrt{2\pi m_n\Omega_n}m_n!}e^{\frac{-|Z_n|^2}{2m_n\Omega_n}} + e^{-A_n}\delta(Z_n)\right\}\right\}$$
$$\times \left\{\sum_{m_0=1}^{\infty}\frac{e^{-A_0}(A_0)^{m_0}}{\sqrt{2\pi m_0\Omega_0}m_0!}e^{\frac{-\|\mathbf{Z}\|^2}{2m_0\Omega_0}} + e^{-A_0}\delta(\mathbf{Z})\right\} \tag{3.47}$$

where $\delta(\cdot)$ is the Dirac-delta function. It indicates the probability that there are no interferers in the annular region around the receiver, resulting in zero interference. In practical receivers, however, thermal background noise is always present and is well modeled by the Gaussian distribution. Assuming that antenna n observes independent thermal noise with variance ρ_n, I can incorporate

65

it into my model resulting in the following distribution

$$f(\mathbf{Z}) = \left\{ \prod_{n=1}^{N} \left\{ \sum_{m_n=0}^{\infty} \frac{e^{-A_n}(A_n)^{m_n}}{\sqrt{2\pi\Omega_n(m_n+\Gamma_n)}\,m_n!} e^{\frac{-|Z_n|^2}{2\Omega_n(m_n+\Gamma_n)}} \right\} \right\} \sum_{m_0=1}^{\infty} \frac{e^{-A_0}(A_0)^{m_0}}{\sqrt{2\pi m_0\Omega_0}\,m_0!} e^{\frac{-\|\mathbf{Z}\|^2}{2m_0\Omega_0}}$$

$$+ e^{-A_0} \prod_{n=1}^{N} \sum_{m_n=0}^{\infty} \frac{e^{-A_n}(A_n)^{m_n}}{\sqrt{2\pi m_n\Omega_n}\,m_n!} e^{\frac{-|Z_n|^2}{2\Omega_n(m_n+\Gamma_n)}} \tag{3.48}$$

where $\Gamma_n = \frac{\rho_n}{\Omega_n}$.

3.6 Impact of System Model Assumptions on Derivation

3.6.1 Interference Statistics in General Fading Channel Models

In developing the system model in Section 3.4, I assumed a Rayleigh distributed fast fading channel between interfering sources and the multi-antenna receiver. While the Rayleigh distribution is a reasonably accurate and frequently used model of fading channel amplitude, other distributions have also been used to characterize wireless channel amplitudes[146].

For unconstrained interferer location distribution, I do not require any assumptions on the channel amplitude distribution to derive interference statistics. When the interferer locations are constrained, the Rayleigh distribution of the fading channel between interferers and the receiver was used to simplify the integral of a Bessel function in (3.30) into the integral of an exponential function. Removing the Rayleigh distribution assumption would prevent this step in the proof. However, since I am primarily interested in the tail statistics of the interference distribution, and Fourier analysis shows that the behavior of the characteristic function Φ in the neighborhood of $\|\mathbf{w}\| \to 0$ governs the tail probability

66

of the random envelope[115]. An approximation was proposed in [114] for the log-characteristic function for ψ in the neighborhood of zero using

$$\mathbb{E}_x\{J_0(x)\} = e^{-\mathbb{E}_x\{x\}}(1 + \Lambda(x)) \tag{3.49}$$

where $\Lambda(x)$ is a correction factor expressed as

$$\Lambda(x) = \sum_{m=2}^{\infty} \frac{(\mathbb{E}\{x^2\})^k}{2^{2k}k!} \mathbb{E}_1 F_1(-k; 1; \frac{x}{\mathbb{E}\{x\}}) \tag{3.50}$$

where ${}_1F_1(\cdot; \cdot; \cdot)$ is the confluent hypergeometric function of the first kind. As $x \to 0$, the slowest decaying term in $\Lambda(x)$ is of the order $\mathcal{O}(x^4)$. Thus, as $\|\mathbf{w}\| \to 0$, I approximate $1 + \Lambda(|\overline{\omega}_n| D_0^{-\frac{\gamma}{2}} H_n^0 B^0) \approx 1$. Using (3.49) in (3.26) and ignoring higher order terms around the region $|\overline{\omega}_n| = 0$, I can show that

$$\Psi_{\mathbb{S}_0}(\mathbf{w}) = \overline{K}\left(\mathbb{E}\left\{\prod_{n=1}^N J_0\left(|\overline{\omega}_n| D_0^{-\frac{\gamma}{2}} H_n^0 B^0\right)\right\} - 1\right) \tag{3.51}$$

$$= \overline{K}\left(\mathbb{E}\left\{\prod_{n=1}^N \mathbb{E}_{H_n^0} J_0\left(|\overline{\omega}_n| D_0^{-\frac{\gamma}{2}} H_n^0 B^0\right)\right\} - 1\right) \tag{3.52}$$

$$\approx \overline{K}\left(\mathbb{E}\prod_{n=1}^N e^{-\left\{\left(|\overline{\omega}_n| D_0^{-\frac{\gamma}{2}} \mathbb{E}\{(H_n^0)^2\} B^0\right)^2\right\}} - 1\right) \tag{3.53}$$

$$= \overline{K}\left(\mathbb{E}_{D_0, B^0} e^{-\left\{\left(\|\mathbf{w}\|^2 D_0^{-\frac{\gamma}{2}} \mathbb{E}\{H_n^2\} B^0\right)^2\right\} - 1}\right) \tag{3.54}$$

In stepping from (3.53) to (3.54), I used the assumption that the fading channel is *i.i.d.* across the receive antennas, therefore $\mathbb{E}\{(H_n^0)^2\}$ is independent of n. Since (3.54) has the same form as (3.35), the rest of the joint interference statistics derivation continues from (3.35) as shown in Section 3.5, yielding joint statistics of the form given in (3.47).

67

3.6.2 Interference Statistics in General Interferer Emission Models

In deriving interferer statistics in the presence of guard zones, I assumed that the emission amplitude was constant in (3.39) in order to simplify the interference statistics into the form of a Middleton Class A distribution. Without making this assumption, (3.41) would be replaced by

$$\Psi_{\mathcal{S}_0}(\mathbf{w}) = \lambda \pi \delta_\downarrow^2 \eta_\gamma \mathbb{E}_{B^0} \left\{ e^{-\frac{\|\mathbf{w}\|^2 \delta_\downarrow^{-\gamma} \beta_\gamma \mathbb{E}\{H^{0^2}\}(B^0)^2}{4}} - 1 \right\} \tag{3.55}$$

As discussed in Section 3.6.1, in order to accurately model tail probabilities, I am concerned with the region around $\|\mathbf{w}\| \to 0$. In this region, I can use the approximation $e^x \approx 1 + x$, to arrive at

$$\mathbb{E}_{B^0} \left\{ e^{-\frac{\|\mathbf{w}\|^2 \delta_\downarrow^{-\gamma} \beta_\gamma \mathbb{E}\{H^{0^2}\}(B^0)^2}{4}} - 1 \right\} \approx \mathbb{E} \left\{ \frac{-\|\mathbf{w}\|^2 \delta_\downarrow^{-\gamma} \beta_\gamma \mathbb{E}\{H^{0^2}\}(B^0)^2}{4} \right\} \tag{3.56}$$

$$= \frac{-\|\mathbf{w}\|^2 \delta_\downarrow^{-\gamma} \beta_\gamma \mathbb{E}\{H^{0^2}\} \mathbb{E}\{(B^0)^2\}}{4} \tag{3.57}$$

Again, by using the approximation $1 + x \approx e^x$, I can combine (3.55) and (3.57) to get

$$\Psi_{\mathcal{S}_0}(\mathbf{w}) \approx \lambda \pi \delta_\downarrow^2 \eta_\gamma \left(e^{\frac{-\|\mathbf{w}\|^2 \delta_\downarrow^{-\gamma} \beta_\gamma \mathbb{E}\{H^{0^2}\} \mathbb{E}\{(B^0)^2\}}{4}} - 1 \right) \tag{3.58}$$

which has the same form as (3.41). Thus, even if the envelope of the interferer emission signal is randomly distributed, the interference statistics can be approximated using the Middleton Class A form, especially in the tail probability region.

3.6.3 Interference Statistics in Spatially Correlated Fading Channel Models

To derive the joint statistics of interference in Section 3.5, I assumed that the wireless fading channel between the interfering source and receiver is spatially independent and identically distributed across the multiple antennae in the receiver. This assumption may not be true if two antennae are close to each other. Spatial correlations in the wireless channel are routinely modeled during performance analysis of multi-antenna receivers[143]. In this section, I study the impact of channel correlation on the joint spatial interference statistics. I start from (3.25), which shows that the joint log-characteristic function of interference can be expressed as

$$
\Psi_{S_0}(\mathbf{w}) =
$$
$$
\overline{K} \left(\mathbb{E} \left\{ \prod_{n=1}^{N} \sum_{m_n=0}^{\infty} j^{m_n} \epsilon_{m_n} J_{m_n} \left(|\overline{\omega}_n| D^{-\frac{\gamma}{2}} H_{n,0}^0 B_{n,0}^0 \right) \cos \left(m_n \left(\chi^0 + \Theta_n^0 + \xi_{\omega,n} \right) \right) \right\} - 1 \right).
$$
$$
(3.59)
$$

In Section 3.5, I used the assumption that the fast-fading channel phase is uncorrelated across receive antennae, to show that all terms with $m_n > 0$ are equal to zero, resulting in the simplified product of terms expression in (3.26). If there is phase correlation between receive antennae u and v, then the terms containing $\mathbb{E} \left\{ \cos \left(k_u (\chi^0 + \Theta_u^0 + \xi_{\omega,u}) + k_v (\chi^0 + \Theta_v^0 + \xi_{\omega,v}) \right) \right\}$ are not equal to 0 for $k_u, k_v > 0$. However, assuming that the interferer emissions are uniformly distributed in phase χ^0, only the terms with $k_v = -k_u$ and $k_u = k_v = 0$ are non-zero,

and considering only these terms (3.59) reduces to

$$
\Psi_{\mathcal{S}_0}(\mathbf{w}) = \overline{K}\mathbb{E}\left\{\left(\prod_{\substack{n=1 \\ n\neq u,v}}^{N}J_0\left(|\overline{\omega}_n|D^{-\frac{\gamma}{2}}H_n^0 B^0\right)\right)\times \right.
$$

$$
\left. \sum_{m=1}^{\infty}J_m\left(|\overline{\omega}_u|D^{-\frac{\gamma}{2}}H_u^0 B^0\right)J_m\left(|\overline{\omega}_v|D^{-\frac{\gamma}{2}}H_v^0 B^0\right)\cos\!\left(m\left(\Theta_u^0-\Theta_v^0+\xi_{\omega,u}-\xi_{\omega,v}\right)\right)\right\}-1
$$

$$(3.60)$$

By applying the following identity,

$$
J_0\left(\sqrt{a^2+b^2-2ab\cos(x)}\right)=\sum_{m=0}^{\infty}J_m(a)J_m(b)\epsilon_m\cos(mx) \qquad (3.61)
$$

(3.60) can be expressed as

$$
\Psi_{\mathcal{S}_0}(\mathbf{w}) = \overline{K}\mathbb{E}\left\{\left(\prod_{\substack{n=1 \\ n\neq u,v}}^{N}J_0\left(|\overline{\omega}_n|D^{-\frac{\gamma}{2}}H_n^0 B^0\right)\right)\times \right.
$$

$$
J_0\left(\left(|\overline{\omega}_u|D^{-\frac{\gamma}{2}}H_u^0 B^0\right)^2+\left(|\overline{\omega}_v|D^{-\frac{\gamma}{2}}H_v^0 B^0\right)^2 \right.
$$

$$
\left.\left. +|\overline{\omega}_u||\overline{\omega}_u|D^{-\gamma}H_u^0 H_v^0 (B^0)^2\cos(\Theta_u^0-\Theta_v^0+\xi_{\omega,u}-\xi_{\omega,v})\right)\right\}-1 \qquad (3.62)
$$

I again use the approximation result provided in (3.49) to get

$$
\Psi_{\mathcal{S}_0}(\mathbf{w}) = \overline{K}\left(\mathbb{E}\left\{e^{-D_0^{-\gamma}(B^0)^2\sum_{n=1}^{N}\left(|\overline{\omega}_n|^2\mathbb{E}\left\{(H_n^0)^2\right\}\right)+|\overline{\omega}_u||\overline{\omega}_v|\mathbf{E}\{H_{u,0}^0 H_{v,0}^0\}\cos(\Theta_u^0-\Theta_v^0+\xi_{\omega,u}-\xi_{\omega,v})}\right\}-1\right)
$$

$$(3.63)$$

$$
=\overline{K}\left(\mathbb{E}\left\{e^{-D_0^{-\gamma}(B^0)^2\sum_{n=1}^{N}\left(|\overline{\omega}_n|^2\mathbb{E}\left\{(H_n^0)^2\right\}\right)}e^{-D_0^{-\gamma}(B^0)^2\omega_{u,I}\omega_{v,I}\mathbf{E}\{H_{u,0}^0 H_{v,0}^0\cos(\Theta_{u,0}-\Theta_{v,0})\}}\right.\right.
$$

$$
\times e^{-D_0^{-\gamma}(B^0)^2\omega_{u,Q}\omega_{v,Q}\mathbf{E}\{H_{u,0}^0 H_{v,0}^0\cos(\Theta_{u,0}-\Theta_{v,0})\}}
$$

$$
\times e^{-D_0^{-\gamma}(B^0)^2\omega_{u,I}\omega_{v,Q}\mathbf{E}\{H_{u,0}^0 H_{v,0}^0\sin(\Theta_{u,0}-\Theta_{v,0})\}}
$$

$$
\left.\left.\times e^{-D_0^{-\gamma}(B^0)^2\omega_{u,Q}\omega_{v,I}\mathbf{E}\{H_{u,0}^0 H_{v,0}^0\sin(\Theta_{u,0}-\Theta_{v,0})\}}\right\}-1\right) \qquad (3.64)
$$

Note that in addition to the $|\overline{\omega}_n|^2$ terms, $\Psi_{\mathbf{Z},S_0}(\mathbf{w})$ contains non-zero terms of the form $\omega_{u,R}\omega_{v,R}$, $\omega_{u,R}\omega_{v,I}$, $\omega_{u,I}\omega_{v,I}$, and $\omega_{u,I}\omega_{v,R}$. These terms indicates sample level correlation in the sum interference, for example the coefficient of the $\omega_{u,R}\omega_{v,R}$ term is indicative of correlation between $Y_{u,R}$ and $Y_{v,R}$. Analogous to the cross terms in multi-dimensional Gaussian distributions, this coefficient of the $\omega_{u,R}\omega_{v,R}$ term is equal to $\mathbb{E}\left\{Y_{u,R}Y_{v,R}\right\}$.

$$\Phi_{\mathbf{Z}}(\mathbf{w}) = e^{A_0\left(e^{-\frac{\mathbf{w}^T\mathbf{K}^{-1}\mathbf{w}}{2}}-1\right)} \times \prod_{n=1}^{N} e^{A_n\left(e^{-\frac{|\overline{\omega}_n|^2\Omega_n}{2}}-1\right)}. \tag{3.65}$$

The probability density function corresponding to the characteristic function in (3.46) can be written as

$$f(\mathbf{Z}) = \left\{\prod_{n=1}^{N}\left\{\sum_{m_n=1}^{\infty}\frac{e^{-A_n}(A_n)^{m_n}}{m_n!}e^{\frac{-|Z_n|^2}{\Omega_n}}\right\}\right\}\sum_{m_0=1}^{\infty}\frac{e^{-A_0}(A_0)^{m_0}}{m_0!}e^{\frac{-\mathbf{Z}^T\mathbf{K}^{-1}\mathbf{Z}}{\Omega_0}} \tag{3.66}$$

where the matrix $\mathbf{K}$ is a $2N\times 2N$ matrix. For all integers $u,v \in [1,N]$, the elements of $\mathbf{K}$ are given as

$$K_{2u,2v} = \mathbb{E}\left\{H_u^0 H_v^0 \cos(\Theta_u^0 - \Theta_v^0)\right\} \tag{3.67}$$

$$K_{2u+1,2v+1} = \mathbb{E}\left\{H_u^0 H_v^0 \cos(\Theta_u^0 - \Theta_v^0)\right\} \tag{3.68}$$

$$K_{2u,2v+1} = \mathbb{E}\left\{H_u^0 H_v^0 \sin(\Theta_u^0 - \Theta_v^0)\right\} \tag{3.69}$$

$$K_{2u+1,2v} = \mathbb{E}\left\{H_u^0 H_v^0 \sin(\Theta_u^0 - \Theta_v^0)\right\} \tag{3.70}$$

$$K_{2u,2u} = \mathbb{E}\left\{(H_u^0)^2\right\} \tag{3.71}$$

$$K_{2u+1,2u+1} = \mathbb{E}\left\{(H_u^0)^2\right\}. \tag{3.72}$$

Table 3.3: Parameter values used in simulations

Parameter	Description	Value
λ_{tot}	Per-antenna total intensity of interferers	0.01
γ	Power path-loss exponent	2.5
$\overline{B}$	Mean amplitude of interferer emissions	1.0
$\delta_\downarrow$	Radius of guard zone around receiver	1.5
$\mathbb{E}\{H^2\}$	Fast fading channel power	1.0

3.7   Simulation Results

To study the accuracy of my joint amplitude distribution model for constrained interferer distributions, I numerically simulate interference observed by a multi-antenna receiver operating in an interferer environment as described in Section 5.4. The receiver uses two antennae and the interferers exclusive to each antennae are distributed with equal densities, i.e. $\lambda_1 = \lambda_2 = \lambda_e$. I choose a value of λ_0 such that $\lambda_0 + \lambda_e = 0.01$, i.e. the density of total interferers observed by each antenna is the same, regardless of the choice of λ_0 or λ_e. This helps to normalize my data as the variance of interference observed at each antenna (proportional to $\lambda_0 + \lambda_e$) remains the same regardless of the value taken by λ_0 or λ_e. Table 3.3 lists the values for the rest of the simulation parameters.

Figure 3.2 shows a simulated random interference sample sequence observed at the two antennae over a span of 40 time samples using different values of λ_0 and λ_e and other parameters from Table 3.3. When the interference samples are generated with $\lambda_0 = 0$, they are independent across receive antennae, causing impulsive events (samples which have a large amplitude) to occur independently across the two antennae. Setting $\lambda_e = 0$, leads to high spatial de-

72
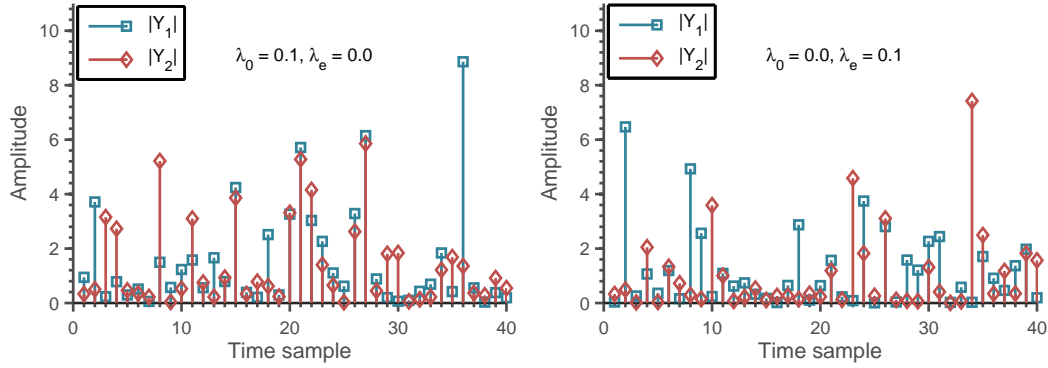
Figure 3.2: Time series plot of simulated interference at a 2−antenna receiver. $\lambda_0 = 0.1$ and $\lambda_1 = \lambda_2 = 0.0$ in the figure on the left, and $\lambda_0 = 0.0$ and $\lambda_1 = \lambda_2 = 0.1$ in the figure on the right.

pendence in the resulting interference, consequently, impulse events at the two receive antennae occur with different strengths but at the same location in time. Figure 3.3 shows a scatter plot of the amplitude of interference at two receive antenna, where the horizontal axis denotes the amplitude of interference samples at antenna 1 and the vertical axis denotes the amplitude of interference samples at antenna 2. As λ_0 increases, the interference sample points move towards the top left of the scatter plot area, indicating that impulsive events occur in a spatially dependent manner.

I use the Kullback-Liebler (KL) divergence as a metric to compare the empirical distribution of the simulated interference amplitude with prior work and my proposed statistical models. Although KL divergence is not a distance metric, it is often used to compare probability density distributions and various methods are available for its efficient computation[168]. A smaller KL divergence between two density distributions implies high similarity between the density functions.
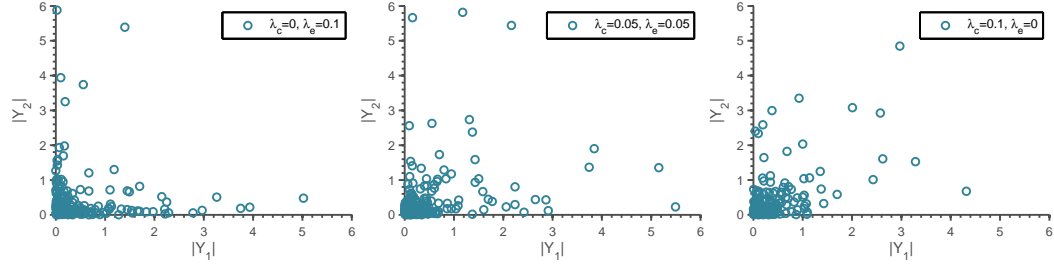
Figure 3.3: Scatter plot of simulated interference amplitude at a 2−antenna receiver.

Figure 3.4 shows the KL divergence calculated for different values of λ_0. The KL divergence between the empirically estimated distribution and the proposed distribution is lower than the KL divergence between the empirically estimated distribution and Models I, III from [47] for all values of λ_0. The KL divergence between the empirical interference distribution and Model I increases as λ_0 increases since Model I does not account for spatial dependence which increases with λ_0. Similarly, Model II only takes into account spatial dependence and its KL divergence increases as λ_0 decreases. The KL divergence between simulated interference data and multivariate Gaussian distribution of equal variance is very large, owing to the fact that the Gaussian distribution cannot accurately model the high frequency with which impulsive events occur in simulated interference. Note that in all comparisons the variance of the marginal distribution at each antenna is the same for purposes of normalization.

Next, I compare the tail probabilities of the numerically simulated distribution and the proposed distribution models. The tail probability is the complementary cumulative distribution function of a random variable and in per-

74
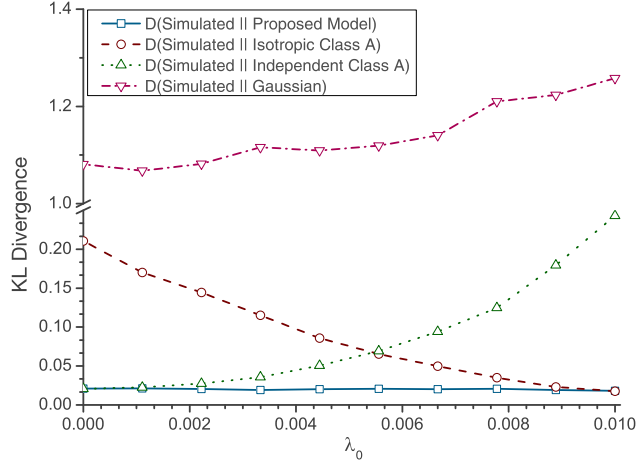
Figure 3.4: Estimated KL divergence between density distribution of simulated interference and Middleton Class A distribution vs. λ_0 ($\lambda_e = 0.01 - \lambda_0$), where a lower KL divergence means a better fit. $D(P\|Q)$ denotes the KL divergence between distributions P and Q. KL divergence is also calculated between the simulated interference distribution and models MCA.I (Independent Class A) and MCA.III (Isotropic Class A) from Table 2.2.

formance analysis of communication systems, the tail probability of interference is related to the outage performance of receivers. Given a threshold τ, I define tail probability as $\mathbb{P}(|Y_1| > \tau, \cdots, |Y_N| > \tau)$. Figure 3.5 shows a comparison of the tail probabilities of the numerically simulated distribution, my proposed distribution, and the Gaussian distribution for interference with and without guard zones, respectively. The tail probability of the multi-dimensional Middleton Class A distribution can be evaluated as a mixture of Gaussian tail probabilities. The tail probabilities of my proposed distribution match closely to simulated interference, while the Gaussian distribution is clearly unable to capture the large tail probabilities of impulsive interference.

75
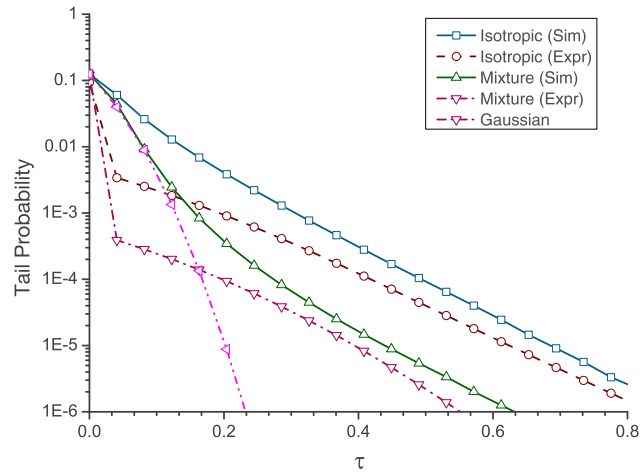
Figure 3.5: Tail probability vs. threshold τ for simulated interference in the presence of guard zones. The tail probability is compared between the numerically simulated interference ("Sim") and the tail of the proposed multi-variate Middleton Class A distribution ("Expr"). The tail probabilities are generated for isotropic interference ($\lambda_0 = 0.01, \lambda_e = 0.0$) and a mixture of isotropic and independent interference ($\lambda_0 = 0.001, \lambda_e = 0.009$). Remaining parameter values are given in Table 3.3.

Table 3.4: Channel models used in Figure 3.6

Channel Model	Parameters
Rayleigh fading $f(x) = \frac{x}{\sigma^2} e^{\frac{-x^2}{2\sigma^2}}$	$\sigma = 1$
Rician fading $f(x) = \frac{2(K+1)x}{\Omega} e^{\left(-K - \frac{(K+1)x^2}{\Omega}\right)} I_0\left(2\sqrt{\frac{K(K+1)}{\Omega}}x\right)$	$K = 2, \Omega = 1$
Nakagami fading $f(x) = \frac{2\mu^\mu}{\Gamma(\mu)\omega^\mu} x^{2\mu-1} e^{\left(-\frac{\mu}{\omega}x^2\right)}$	$\mu = 0.5, \omega = 1$

I also use KL divergence to study the impact of different channel models on the resulting spatial distribution of interference. Table 3.4 lists the channel models that are used for this study and the parameter values associated with each model. The system parameter values are chosen from Table 3.3. Figure 3.6 shows that the KL divergence with Rayleigh fading channel model is the lowest, which is to be expected. The KL divergence increases slightly upon changing the channel model, indicating that the approximation used in (3.49) is close to its true value. I claim that the differences in KL divergence in Figure 3.6 are small by referencing the significantly larger differences in KL divergence in Figure 3.4 that arise by not taking into account for spatial dependence or by using the Gaussian distribution to model impulsive data.

Finally, I simulate correlated fading channels to test whether my model correctly accounts for spatial correlation. I simulate correlation between the in-phase components of the channel between an interferer and the two receive antennae. The Pearson product moment correlation coefficient (PMCC) [137] between these two random variables is chosen as 0.3. Using (3.67), the PMCC
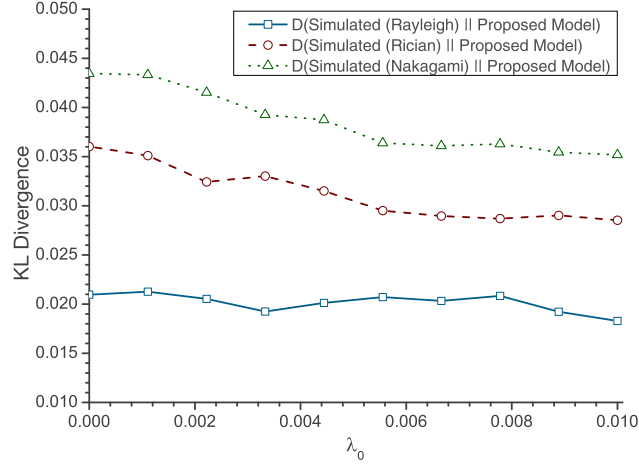
Figure 3.6: Estimated KL Divergence between simulated interference distribution and proposed model vs. λ_0, using different fast fading channel models. The density function corresponding to each channel model is provided in Table 3.4. $\lambda_e = 0.01 - \lambda_0$, and remaining parameters are given in Table 3.3. $D(P\|Q)$ denotes KL Divergence between distributions P and Q.

between the in-phase components of the two receive antennae has a predicted value of $\frac{0.3 * \lambda_0}{\lambda_0 + \lambda_e}$. In this test, I fix $\lambda_e = 0.04$, vary λ_0 between 0.0 and 0.1, and the remaining parameter values are given in Table 3.3. Figure 3.7 shows that the empirically estimated value of the PMCC follows the model prediction very accurately.

3.8   Conclusions

In this chapter, I proposed a statistical-physical framework for modeling interference observed by a multi-antenna receiver surrounded by interference causing emitters. This framework incorporates random distribution of interferer locations in two-dimensional space around the receiver with an interferer-
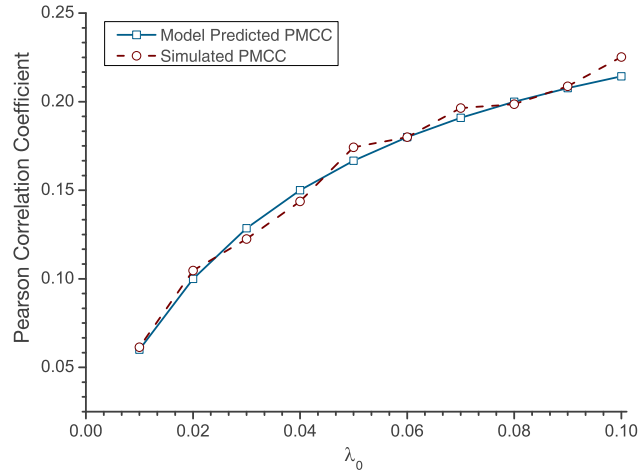
Figure 3.7: Estimated Pearson Product Moment Correlation Coefficient (PMCC) vs. λ_0. $\lambda_e = 0.04$ and other parameter values are given in Table 3.3.

free *guard zone*, and physical mechanisms describing the generation and propagation of interference through the wireless medium, such as fast fading and pathloss attenuation. This framework also incorporates partial statistical dependence of interference across the receive antennae and captures a continuum between spatially independent and spatially isotropic interference.

Using my proposed framework, I derived the joint statistics of interference observed across a multi-antenna receiver, with the resulting amplitude distribution modeling both spatially isotropic and spatially independent observations of interference as special cases. Depending on the region within which interferers are distributed, the interference statistics can be modeled using the Middleton Class A or the symmetric alpha stable distribution. Some of these distributions find use in designing interference mitigation algorithms or analyzing communication performance of receivers in the presence of interference. By

79

providing a link between network models and interference distribution, my proposed models can better inform such analysis and can be used in designing receivers that are better suited to the network and interference conditions in which they are expected to operate.

In the next chapter, I derive joint statistics of interference observed by a multi-antenna receiver operating within a network without any interferer-free guard zones. Such a network model can be applied to decentralized networks, such as sensor networks, or *ad hoc* networks, as well as interference from non-communicating devices.

Chapter 4

Statistical Modeling of Interference in Decentralized Networks

4.1 Introduction

In Chapter 3, I derived joint statistics of interference observed by multi-antenna receivers in centralized networks. In developing the network model, I assumed the presence of a central authority that limits interferers to be located outside of a finite area *guard zone* around the receiver. This is a reasonable model for out-of-cell CCI in networks where multiple access protocols within a cell can limit CCI from coordinated devices nearby an active user[79]. However, interference can arise from co-existing wireless protocols such as Bluetooth and Wi-Fi[184], and from non-communicating sources such as clocks and busses on a computational platform[147]. Such sources of interference are typically not in the control of a central coordinating authority and may be transmitting arbitrarily close to an active receiver[86].

In this chapter, I randomly distribute the active interferers surrounding a wireless receiver with no constraints imposed on the minimum distance between an interferer and the receiver. Such a system model resembles an *ad hoc* wireless network without any contention-based medium access control proto-

col[78]. The same model can also describe interference generated as platform noise[118], as interference causing components on the device platform can be located arbitrarily close to the wireless device.

Another key assumption in Chapter 3 was that the receiver antennae are colocated. In other words, I ignored separation between the antennae of the wireless receiver. For many small form-factor mobile wireless devices, such a simplification may be reasonable as the separation between the multiple receive antennae is significantly smaller than the distance between the device and other interfering sources. However, there exist network scenarios where the separation between the multiple receive antennae cannot be ignored and may have an impact on the nature of interference statistics. For example, cooperative MIMO receivers utilize geographically distributed antennae in order to mitigate the harmful impact of wireless fading on communication performance. Platform interference on embedded wireless devices arises from sources so close to the antennae, that inter-antenna separation is not significantly smaller than antenna-interferer separation. It is therefore imperative that joint statistical models of interference account for receive antenna separation, consequently I derive joint statistics of interference across two physically separate antennae located in a Poisson field of interferers.

4.2   Organization and Notation

Section 4.3 presents a concise survey of statistical models of interference in distributed antennae located in decentralized networks. Section 4.4 discusses

Table 4.1: Summary of key symbols used in this chapter.

Symbol	Description
Indexing Variables	
i	Interferer index in a set of interferers
n	Antenna index in a multi-antenna receiver
Sets	
$\mathcal{S}_0$	Set of interferers observed by all receive antennae
$\mathcal{S}_n$	Set of interferers observed by n^{th} receive antenna
Constants	
γ	Power pathloss exponent
λ_0, λ_n	Interferer distribution intensity Π_0, Π_n
Random Variables	
B, χ	Amplitude and phase of interferer emissions
H, Θ	Amplitude and phase of fast fading channel
$\mathbf{Y} = \mathbf{Y}_I + j\mathbf{Y}_Q$	Sum interference at receiver from all sets
$\mathbf{Y}_n = \mathbf{Y}_{n,I} + j\mathbf{Y}_{n,Q}$	Sum interference at receiver from set $\mathcal{S}_n$
$\Phi_{\overline{\mathbf{Z}}}(\mathbf{w})$	Joint characteristic function of $\overline{\mathbf{Z}}$
$\Psi_{\overline{\mathbf{Z}}}(\mathbf{w})$	Joint log-characteristic function of $\overline{\mathbf{Z}}$
$\omega_{n,I}, \omega_{n,Q}$	Frequency variables for $\Phi_{\overline{\mathbf{Z}}}(\mathbf{w})(n=1,2)$
$\mathbf{w}$	$[\omega_{1,I}, \omega_{1,Q}, \omega_{2,I}\omega_{2,Q}]$

the system model of interference generation and propagation. Section 4.5 derives interference statistics in a receiver with colocated multiple antennae. Section 4.6 derives interference statistics in a wireless receiver with distributed multiple antennae. In Section 4.8, I remove some of the system model assumptions and study the impact on interference statistics. Section 4.9 presents numerical simulations to corroborate my claims and Section 4.10 provides a short summary of the key takeaways from this chapter. Key symbols are summarized in Table 4.1.

4.3 Motivation and Prior Work

In typical communication receiver design, interference is usually modeled as a Gaussian distributed random variable [23]. While the Gaussian distribution is a good model for thermal noise at the receiver[65], interference has predominantly non-Gaussian statistics[115] and is well modeled using impulsive distributions such as symmetric alpha stable[140] and Middleton Class A distributions[114]. The impulsive nature of interference may cause significant degradation in communication performance of wireless receivers designed under the assumption of additive Gaussian noise[118].

The statistical techniques used in modeling interference can be divided into two categories: (1) statistical inference methods and (2) statistical-physical methods. Empirical approaches fit a mathematical model to interference signal measurements, without regard to the physical generation mechanisms behind the interference[141]. Statistical-physical models, on the other hand, model interference based on the physical principles that govern the generation and propagation of interference-causing emissions[86, 115]. Statistical-physical models can therefore be more useful than empirical models in designing robust receivers in the presence of interference[115].

In [149], interference from a Poisson field of interferers was modeled using the symmetric alpha stable distribution[140]. This result was later extended to show that interference observed by a multi-antenna receiver in a Poisson field of interferers follows the isotropic symmetric alpha stable distribution[86]. The authors assume that each receiver is surrounded by the same set of active inter-

Table 4.2: Key statistical models of interference observed by multi-antenna receivers in interference-limited networks without guard zones.

Model Name	Statistical Model
Symmetric alpha stable	Characteristic Function $\Phi_Z(\omega) = e^{-\sigma|\omega|^\alpha}$ α : Characteristic exponent. σ : Dispersion parameter.
Isotropic symmetric alpha stable	Characteristic Function: $\Phi_Z(\mathbf{w}) = e^{-\sigma\|\mathbf{w}\|^\alpha}$ α : Characteristic exponent σ : Dispersion parameter
Independent symmetric alpha stable	Characteristic Function: $\Phi_Z(\mathbf{w}) = e^{-\sigma\|\mathbf{w}\|_\alpha^\alpha}$ α : Characteristic exponent σ : Dispersion parameter

ferers, and receiver separation is ignored. The spherically isotropic alpha stable model is derived under both homogeneous and non-homogeneous distribution of interferers, with the signal propagation model incorporating pathloss, lognormal shadowing and Rayleigh fading.

Prior work on statistical modeling of interference in multi-antenna wireless systems has typically focused on using multi-variate extensions of single-antenna interference statistical models[47]. The two common approaches of generating multi-variate extensions of uni-variate distributions assume that either (a) interference is independent across the receive antennae, or (b) the multi-variate interference model is isotropic. Table 4.2 describes the uni-variate symmetric alpha stable distribution as well as the multi-variate isotropic and independent symmetric alpha stable distributions.

One of the recent strategies to increase data rate and communication reliability in the presence of interference is to use geographically distributed multiple antennae at the receiver[160]. Studies have since shown potential advantages such as improving wireless network capacity and reducing device power utilization[63, 129]. In distributed antennae systems (DAS), antenna modules are geographically distributed and each distributed antenna module is connected to a home base station (or central unit) via dedicated wires, fiber optics, or an exclusive RF link[39]. In particular, the terms cooperative MIMO, or relay communication, are connotative of the same RF link being used between the distributed antennae, and between the base station and each antenna.

In this chapter, I develop a network model where a receiver employing two distributed antennae is surrounded by a field of randomly distributed interferers, with signal propagation through this medium suffering from pathloss attenuation and fast fading. I derive the joint statistics of sum interference observed by the distributed antennae and provide closed form expressions approximating the joint characteristic function of interference. These joint statistics are useful in the many practical applications of distributed antennae receiver systems, and cooperative communications. Accurate models of interference statistics can inform design of receiver algorithms to combat interference and analysis of communication performance in the presence of interference.

4.4   System Model and List of Assumptions

In this section, I describe a interference limited multi-antenna wireless communication system via the following assumptions:

Assumption 4.1. *A wireless receiver with N antennae is observing interference.*

Assumption 4.2. *Interferers are located in a two-dimensional plane around the receiver.*

This assumption is used only for ease of analysis. Distributing interferers in a three-dimensional volume does not alter the nature of any results, other than certain parameter values.

Assumption 4.3. *Inteferers are either observed by all antennae, or by only one antenna.*

At each time snapshot, the active interfering sources are classified into $N+1$ independent sets $\mathcal{S}_0, \mathcal{S}_1, \cdots, \mathcal{S}_N$. $\mathcal{S}_0$ denotes the set of interferers that cause interference to every receive antenna. $\mathcal{S}_n \ \forall \ n = 1, \cdots, N$ denotes the set of interferers that are observed by antenna n alone. Under this assumption interference statistics lie in a continuum between spatially independent, or spatially isotropic. More justification for this assumption is provided in Section 3.4.

Assumption 4.4. *Interferers are distributed as a spatial Poisson Point Process.*

At each sampling time instant, the locations of the active interferers in $\mathcal{S}_n$ $\forall \ n = 0, \cdots, N$ are distributed according to a homogeneous spatial Poisson Point

87

Process in the two-dimensional plane around the receiver. The intensity of set $\mathcal{S}_n$ is denoted by $\lambda_n \ \forall \ n = 0, \ldots, N$. The Poisson Point Process distribution is usually applied to modeling the statistical distribution of interfering sources in wireless communication systems[12]. A spatial Poisson point process distribution of interferers allows each interferer set $\mathcal{S}_n$ to have potentially infinite number of interferers. The distance of each interferer from the origin provides an ordering function, ensuring that the interferers in each set are countable. In other words, the ith interferer in $\mathcal{S}_n$, located at coordinates $\mathbf{R}_{n,i}$, is defined by implicitly assuming $\|\mathbf{R}_{n,1}\|_2 < \|\mathbf{R}_{n,2}\|_2 < \|\mathbf{R}_{n,3}\|_2 < \cdots$.

Assumption 4.5. *The wireless signal energy decays according to the power-law path-loss model with a patloss coefficient of γ.*

Assumption 4.6. *There wireless channel between the interferer and receiver experiences Rayleigh fast-fading.*

The fast-fading channel between the interfering sources and the receiver is modeled using the Rayleigh distribution[65].

Assumption 4.7. *Additive thermal noise is ignored at the receiver.*

With high user density and frequency reuse, many communication systems are interference-limited; i.e., interference at the receiver is much stronger than the thermal noise component. Consequently, the resulting statistical model is applicable to interference-limited communication scenarios.

Assumption 4.8. *Inteferers may be arbitrarily close to the receiver.*
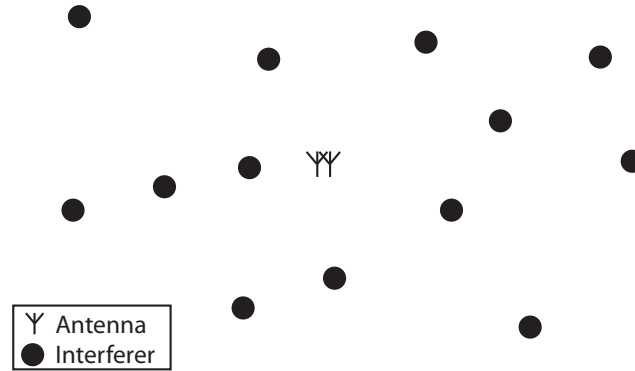
Figure 4.1: Illustration of interferer distribution around a 2-antenna receiver with colocated antennae at a sampling time instant.

The active interferers surrounding the wireless receiver a located with no constraints imposed on the minimum distance between an interferer and the receiver. Such a system model resembles an *ad hoc* network without any contention-based medium access control protocol[78]. The same model can also describe platform noise[118], as interfering sources on the device platform can be located arbitrarily close to the wireless device. The absence of guard-zones is vital to modeling interference in decentralized *ad hoc* networks, as well as interference from uncoordinated users in centralized networks. Figure 4.1 shows a snapshot of interferer distribution around two colocated antennae in a Poisson field of interferers.

4.5 Joint Statistics of Interference in Colocated Antennae

In this section, I derive the statistics of interference assuming that the wireless antennae are colocated. At each receive antenna n, the baseband sum

interference signal at any sampling time instant can be expressed as the sum total of the interference signal observed from common interferers and the interference signal from interferers visible only to antenna n. I can express the interference signal at the nth antenna as

$$Z_n = Z'_{0,n} + Z'_n \tag{4.1}$$

where Z_n, $Z'_{0,n}$ represent the sum interference signal from interfering sources in $\mathcal{S}_n$ (visible only to antenna n), and interfering sources in $\mathcal{S}_0$ (visible to all antennae), respectively. As shown in Section 3.5, the sum interference signal Z'_n from interferers in $\mathcal{S}_n$ can be written as

$$Z'_n = \sum_{i \in \mathcal{S}_n} B_i^n e^{j\chi_i^n} (D_{n,i})^{-\frac{\gamma}{2}} H_i^n e^{j\Theta_i^n}. \tag{4.2}$$

Z'_n is the sum of interfering signals $B_i^n e^{j\chi_i^n} (D_{n,i})^{-\frac{\gamma}{2}} H_i^n e^{j\Theta_i^n}$ emitted by each interferer $i \in \mathcal{S}_n$ located at $\mathbf{R}_{n,i}$. $B_i^n e^{j\chi_i^n}$ denotes interferer emissions from interfering source i where B_i^n is the emission signal envelope and χ_i^n is the phase of the emission. I assume that the signal envelope B_i^n is constant. $D_{n,i}$ denotes the distance between the receiver n and the interferer, and γ is the power pathloss coefficient ($\gamma > 2$), consequently, $(D_{n,i})^{-\frac{\gamma}{2}}$ indicates the reduction in interfering signal energy during propagation through the wireless medium. $H_i^n e^{j\Theta_i^n}$ denotes the complex fast-fading channel between the interferer and receiver n. For the fast fading channel model, I assume that the channel amplitude H_i^n follows the Rayleigh distribution, and that the channel phase Θ_i^n is uniformly distributed on $[0, 2\pi]$. H_i^n, Θ_i^n, B_i^n, and χ_i^n are assumed to be *i.i.d.* across all interfering sources $i \in \mathcal{S}_n$.

The signal from the common set of interferers $\mathcal{S}_0$ is expressed as

$$Z'_{0,n} = \sum_{i^0 \in \mathcal{S}_0} B_i^0 e^{j\chi_i^0} (D_{0,i})^{-\frac{\gamma}{2}} H_{n,i}^0 e^{j\Theta_{n,i}^0}. \tag{4.3}$$

Note that the difference between (4.2) and (4.3) is that the interferer emission signal $B_i^0 e^{j\chi_i^0}$ and the distance D_i^0 between interferer i and the receive antenna n , is independent of the antenna under observation (n). This is because I ignore inter-antenna spacing and assume all antennae are located at the origin. The channel between the interferer and n^{th} receiver, denoted by $H_{n,i}^0 e^{j\theta_{n,i}^0}$, is also assumed $i.i.d.$ across n and i.

Following the derivation in Section 3.5, I get the joint characteristic function of the interference vector $\mathbf{Y}$ as

$$\Phi_{\mathbf{Z}}(\mathbf{w}) = \Phi_{\mathcal{S}_0}(\mathbf{w}) \prod_{n=1}^{N} \Phi_{\mathcal{S}_n}(\mathbf{w}) \tag{4.4}$$

where,

$$\Phi_{\mathcal{S}_0}(\mathbf{w}) = \mathbb{E}\left\{ e^{j \sum_{n=1}^{N} |\overline{\omega}_n| \sum_{i=1}^{|\mathcal{S}_0|} D_{0,i}^{-\frac{\gamma}{2}} H_{n,i}^0 B_i^0 \cos(\chi_i^0 + \Theta_{n,i}^0 + \xi_{\omega,n})} \right\} \tag{4.5}$$

$$\Phi_{\mathcal{S}_n}(\mathbf{w}) = \mathbb{E}\left\{ e^{j |\overline{\omega}_n| \sum_{i=1}^{|\mathcal{S}_n|} D_i^{-\frac{\gamma}{2}} H_i^n B_i^n \cos(\chi_i^n + \Theta_i^n + \xi_{\omega,n})} \right\} \tag{4.6}$$

where $|\overline{\omega}_n| = \sqrt{\omega_{n,I}^2 + \omega_{n,Q}^2}$ and $\xi_{\omega,n} = \tan^{-1}\left(\frac{\omega_{n,I}}{\omega_{n,Q}}\right)$. Subsequently, I evaluate $\Phi_{\mathcal{S}_0}(\mathbf{w})$, and $\Phi_{\mathcal{S}_n}(\mathbf{w})$.

4.5.1 Evaluation of $\Phi_{\mathcal{S}_n}(\mathbf{w})$ (Interference Contribution from $\mathcal{S}_n$)

In order to evaluate $\Phi_{\mathcal{S}_n}(\mathbf{w})$, I rewrite (4.6) as

$$\Phi_{\mathcal{S}_n}(\mathbf{w}) = \mathbb{E}\left\{ e^{j|\overline{\omega}_n|\sum_{i=1}^{|\mathcal{S}_n|} D_{n,i}^{-\frac{\gamma}{2}} H_i^n B_i^n \cos(\chi_i^n + \Theta_i^n + \xi_{\omega,n})} \right\} \tag{4.7}$$

$$= \mathbb{E}\left\{ e^{j|\overline{\omega}_n|\sum_{i=1}^{|\mathcal{S}_n|} \mathrm{sgn}(\cos(\chi_{n,i} + \Theta_{n,i} + \xi_{\omega,n})) D_{n,i}^{-\frac{\gamma}{2}} H_{n,i} B_{n,i} |\cos(\chi_{n,i} + \Theta_{n,i} + \xi_{\omega,n})|} \right\} \tag{4.8}$$

where $\mathrm{sgn}(\cdot)$ denotes the sign function. (4.8) is the characteristic function evaluated at $|\overline{\omega}_n|$, of the random variable

$$T = \sum_{i=1}^{|\mathcal{S}_n|} \mathrm{sgn}(\cos(\chi_i^n + \Theta_i^n + \xi_{\omega,n})) D_{n,i}^{-\frac{\gamma}{2}} H_i^n B_i^n \left|\cos(\chi_i^n + \Theta_i^n + \xi_{\omega,n})\right| \tag{4.9}$$

$$= \sum_{i=1}^{P} E_i R_i^{-\frac{\gamma}{2}} W_i \tag{4.10}$$

where $P = |\mathcal{S}_n|$ is a Poisson random variable, $E_i = \mathrm{sgn}(\cos(\chi_i^n + \Theta_i^n + \xi_{\omega,n}))$, $R_i = D_{n,i}$, and $W_i = H_{n,i} B_{n,i} \left|\cos(\chi_i^n + \Theta_i^n + \xi_{\omega,n})\right|$. χ_i^n and Θ_i^n are independent random variables distributed uniformly over $[0, 2\pi]$. It is trivial then to see that for any value of $\xi_{\omega,n}$, the random variable $\cos(\chi_i^n + \Theta_i^n + \xi_{\omega,n})$ is positive or negative with equal probability. R_i is the distance from the origin of points in a Poisson point Process with intensity λ_n. Furthermore, W_i, R_i and ϵ_i are *i.i.d.* across i. From Theorem 1.4.2 in [140], T follows the symmetric alpha stable distribution with parameters $\alpha = \frac{2}{\gamma}$ and $\sigma_n = \left(C_\alpha^{-1} \lambda_n \mathbb{E}\{|W_n|^\alpha\}\right)^{1/\alpha}$. Here C_α is a constant defined as follows

$$C_\alpha = \begin{cases} \frac{1-\alpha}{\Gamma(2-\alpha)\cos(\pi\alpha/2)} & \text{if } \alpha \neq 1, \\ 2/\pi & \text{if } \alpha = 1. \end{cases}$$

4.5.2 Evaluation of $\Phi_{Y,\mathcal{S}_0}(\mathbf{w})$ (Interference Contribution from $\mathcal{S}_0$)

The contribution to the joint spatial statistics of interference from the interferers in $\mathcal{S}_0$ is expressed as the term $\Phi_{\mathcal{S}_0}(\mathbf{w})$ in the joint characteristic function of interference given by (4.4). In order to derive a closed form expression for (4.5), I use an approach similar to one proposed in [86]. Observe that (4.5) is the characteristic function of a random vector $\mathbf{U}$ with $2N$ elements, whose n^{th} and $n+1^{\text{th}}$ elements U_n and U_{n+1} are given as

$$U_n = \sum_{i_0 \in \mathcal{S}_0} B_{i_0}^0 D_{0,i_0}^{-\frac{\gamma}{2}} H_{n,i_0}^0 \cos(\chi_{i_0}^0 + \Theta_{n,i_0}^0) \tag{4.11}$$

$$= \sum_{i_0 \in \mathcal{S}_0} E_{i_0}' D_{0,i_0}^{-\frac{\gamma}{2}} W_{n,i_0} \tag{4.12}$$

where $E_{i_0}' = \text{sgn}(\cos(\chi_{i_0}^0 + \Theta_{n,i_0}^0))$ and $W_{n,i_0} = B_{i_0}^0 H_{n,i_0}^0 \cos(\chi_{i_0}^0 + \Theta_{n,i_0}^0)$, and

$$U_{n+1} = \sum_{i_0 \in \mathcal{S}_0} B_{i_0}^0 D_{0,i_0}^{-\frac{\gamma}{2}} H_{n,i_0}^0 \sin(\chi_{i_0}^0 + \Theta_{n,i_0}^0) \tag{4.13}$$

$$= \sum_{i_0 \in \mathcal{S}_0} E_{i_0}'' D_{0,i_0}^{-\frac{\gamma}{2}} W_{n+1,i_0} \tag{4.14}$$

where $E_{i_0}'' = \text{sgn}(\sin(\chi_{i_0}^0 + \Theta_{n,i_0}^0))$ and $W_{n,i_0} = B_{i_0}^0 H_{n,i_0}^0 \sin(\chi_{i_0}^0 + \Theta_{n,i_0}^0)$. I can create the vector $\mathbf{W}$ comprising of W_{n+1} ($n = 1, 2, \cdots, 2N$) with characteristic function $\Phi_{\mathbf{W}}(\cdot)$. U_n and U_{n+1} follow the symmetric alpha stable distribution with exponent $\alpha = \frac{2}{\gamma}$ and dispersion $\sigma_n = \left(C_\alpha^{-1} \mathbb{E}|W_n|^\alpha\right)^{1/\alpha}$. Since the characteristic exponent of each coordinate U_n is the same and is independent of n, any linear combination of $U_1, U_2 \ldots U_{2N}$ is a symmetric stable random vector. Using Theorem 2.1.5 in [140], $\mathbf{U}$ is a symmetric alpha stable vector. Furthermore, each coordinate U_n and U_{n+1} can be decomposed into a product of a univariate random variable $B_{i_0}^0 D_{0,i_0}^{-\gamma/2}$, and a Gaussian random variable $H_{n,i_0}^0 \cos(\chi_{i_0}^0 + \Theta_{n,i_0}^0)$ or

93

$H^0_{n,i_0} \sin(\chi^0_{i_0} + \Theta^0_{n,i_0})$, respectively. The Gaussian random variables are independent across the antenna index n. Since a random vector comprised of independent Gaussian random variables is spherically symmetric, it follows from [140] that $\mathbf{U}$ is spherically symmetric. Combining this result with the fact that $\mathbf{U}$ is a symmetric alpha stable random vector, I arrive at the result that $\mathbf{U}$ is a spherically symmetric alpha stable vector. I can then write (4.5) as

$$\Phi_{\mathcal{S}_0}(\mathbf{w}) = e^{-\sigma_0 \|\mathbf{w}\|^\alpha} \tag{4.15}$$

where $\alpha = \frac{4}{\gamma}$, $\|\mathbf{w}\|$ is the 2-norm of the vector $\mathbf{w}$, and $\sigma_0 = \lambda_0 \pi \int_0^\infty \frac{\Phi_{\mathbf{w}}(\|t\|)}{\|t\|^\alpha} dt$ [86].

Combining (4.4),(4.5), and (4.6), I arrive at the characteristic function of interference as

$$\Phi_{\mathbf{Z}}(\mathbf{w}) = e^{-\sigma_0 \|\mathbf{w}\|^\alpha} \prod_{n=1}^{N} e^{-\sigma_n |\overline{\omega}_n|^\alpha} \tag{4.16}$$

(4.16) is the characteristic function of random variable that is a mixture of independent and spherically isotropic symmetric alpha stable vectors. The dispersion parameters σ_0 and σ_n $n = 1, 2, \cdots, N$ depend linearly on the intensities λ_0 and λ_n $n = 1, 2, \cdots, N$, respectively. It is easy to see, that by setting λ_0 to 0, my model degenerates into spatially independent interference, while setting λ_n to 0 for all $n = 1, 2, \cdots, N$ causes isotropic interference at the receiver.

4.6 Joint Statistics of Interference in Distributed Antennae

In this section, I derive the joint statistics of interference observed by two distributed receive antennae in a Poisson field of interferers. In this scenario there are two antennae, one of which is located at the origin. The location of
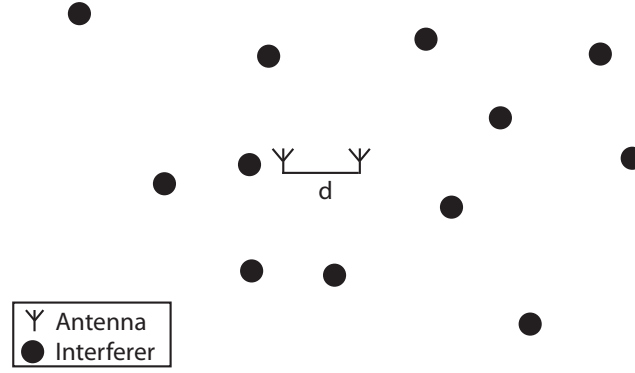
Figure 4.2: Illustration of interferer distribution around a 2-antenna receiver with colocated antennae at a sampling time instant.

the second antenna can be denoted by the two-dimensional vector coordinate $\mathbf{d}$. Figure 4.2 shows two separate antennae in a Poisson field of interferers. From (4.4), the joint characteristic function of interference in two distributed antennae can be written as

$$\Phi_{\mathbf{Z},\mathbf{d}}(\mathbf{w}) = \Phi_{\mathcal{S}_0,\mathbf{d}}(\mathbf{w})\Phi_{\mathcal{S}_1}(\mathbf{w})\Phi_{\mathcal{S}_2}(\mathbf{w}) \tag{4.17}$$

Observe that the characteristic function $\Phi_{\mathbf{Z},\mathbf{d}}(\mathbf{w})$ now reflects its dependence on antennae geometry via the subscript $\mathbf{d}$.

4.6.1 Evaluation of $\Phi_{\mathcal{S}_n}(\mathbf{w})$ (Interference contribution from $\mathcal{S}_n$)

Since the interferers are distributed as a homogeneous Poisson Point Process in two-dimensional space, the distribution of the independent set of interferers is invariant to translation of the antenna. Using the derivation of (4.6) in Section 4.5, I can write

$$\Phi_{\mathcal{S}_n}(\mathbf{w}) = e^{-\sigma_n|\overline{\omega}_n|^{\alpha}} \tag{4.18}$$

95

where σ_n and α have been defined in Section 4.5.

4.6.2   Evaluation of $\Phi_{\mathbf{Y},\mathcal{S}_0}(\mathbf{w})$ (Interference contribution from $\mathcal{S}_0$)

The key step in deriving joint statistics of interference in distributed antennae is the evaluation of $\Phi_{\mathcal{S}_0,\mathbf{d}}(\mathbf{w})$. First, I rewrite (4.5) to incorporate antenna locations to get

$$\Phi_{\mathcal{S}_0}(\mathbf{w}) = \mathbb{E}\left\{ e^{j\sum_{n=1}^2 |\bar{\omega}_n| \sum_{i=1}^{|\mathcal{S}_0|} D_{0,i}^{-\frac{\gamma}{2}} H_{n,i}^0 B_i^0 \cos(\chi_i^0 + \Theta_{n,i}^0 + \xi_{\omega,n})} \right\} \tag{4.19}$$

$$= \mathbb{E}\left\{ e^{j\sum_{n=1}^2 |\bar{\omega}_n| \sum_{i=1}^{|\mathcal{S}_0|} \|\mathbf{R}_{0,i} - \mathbf{d}_i\|^{-\frac{\gamma}{2}} H_{n,i}^0 B_i^0 \cos(\chi_i^0 + \Theta_{n,i}^0 + \xi_{\omega,n})} \right\}. \tag{4.20}$$

Note that $\mathbf{d}_i$ denotes the location coordinate of the ith receive antenna. In this case $\mathbf{d}_1 = \mathbf{0}$, and $\mathbf{d}_2 = \mathbf{d}$. Substituting $\mathbf{d}_i$ in (4.20), and expanding the summation yields

$$\Phi_{\mathcal{S}_0,\mathbf{d}}(\mathbf{w}) = \mathbb{E}\left\{ \prod_{i \in \mathcal{S}} \left(e^{\omega_{1,I} B_i^0 H_{1,i}^0 \cos(\chi_i^0 + \Theta_{1,i}^0)\|\mathbf{R}_i\|^{-\frac{\gamma}{2}} + \omega_{1,Q} B_i^0 H_{1,i}^0 \sin(\chi_i^0 + \Theta_{1,i}^0)\|\mathbf{R}_i\|^{-\frac{\gamma}{2}}} \right. \right. \tag{4.21}$$

$$\left. \left. \times\ e^{\omega_{2,I} B_i^0 H_{2,i}^0 \cos(\chi_i^0 + \Theta_{2,i}^0)\|\mathbf{R}_i - \mathbf{d}\|^{-\frac{\gamma}{2}} + \omega_{2,Q} B_i^0 H_{2,i}^0 \sin(\chi_i^0 + \Theta_{2,i}^0)\|\mathbf{R}_i - \mathbf{d}\|^{-\frac{\gamma}{2}}} \right) \right\}. \tag{4.22}$$

Noting that the $H_{1,i}^0$ and $H_{2,i}^0$ are Rayleigh distributed and $\chi_i^0 + \Theta_{1,i}^0$ and $\chi_i^0 + \Theta_{1,i}^0$ are *i.i.d.* uniformly distributed over $[0, 2\pi]$, the products $H_{1,i}^0 \cos(\chi_i^0 + \Theta_{1,i}^0)$, $H_{1,i}^0 \sin(\chi_i^0 + \Theta_{1,i}^0)$, $H_{2,i}^0 \cos(\chi_i^0 + \Theta_{2,i}^0)$, $H_{2,i}^0 \sin(\chi_i^0 + \Theta_{2,i}^0)$ are *i.i.d.* Gaussian random variables. Taking expectation over these Gaussian distributed random variables is akin to evaluating the characteristic function of a Gaussian distributed

96

random variable, which yields

$$
\Phi_{\mathcal{S}_0,\mathbf{d}}(\mathbf{w})
$$

$$
= \mathbb{E}\left\{\prod_{i\in\mathcal{S}_0} e^{-\omega_{1,I}^2(B_i^0)^2\sigma_H^2\|\mathbf{R}_i\|^{-\gamma}-\omega_{1,Q}^2(B_i^0)^2\sigma_H^2\|\mathbf{R}_i\|^{-\gamma}-\omega_{2,I}^2(B_i^0)^2\sigma_H^2\|\mathbf{R}_i-\mathbf{d}\|^{-\gamma}-\omega_{2,Q}^2(B_i^0)^2\sigma_H^2\|\mathbf{R}_i-\mathbf{d}\|^{-\gamma}}\right\}
$$
(4.23)

$$
= \mathbb{E}\left\{\prod_{i\in\mathcal{S}_0} e^{-|\omega_1|^2(B_i^0)^2\sigma_H^2\|\mathbf{R}_i\|^{-\gamma}-|\omega_2|^2(B_i^0)^2\sigma_H^2\|\mathbf{R}_i-\mathbf{d}\|^{-\gamma}}\right\}
$$
(4.24)

where $|\omega_n| = \sqrt{\omega_{n,I}^2 + \omega_{n,Q}^2}$. Next, I take the expectation over $(B_i^0)^2$, which is the equivalent to evaluating the characteristic function of an exponentially distributed random variable to get

$$
\Phi_{\mathcal{S}_0,\mathbf{d}}(\mathbf{w}) = \mathbb{E}\left\{\prod_{i\in\mathcal{S}_0} \frac{1}{1 + |\omega_1|^2\sigma_H^2\sigma_B^2\|\mathbf{R}_i\|^{-\gamma} + |\omega_2|^2\sigma_H^2\sigma_B^2\|\mathbf{R}_i - \mathbf{d}\|^{-\gamma}}\right\}
$$
(4.25)

Using the point generating functional property of Poisson Point Processes discussed in Appendix A (Definition A.3), the log-characteristic function $\Psi_{\mathcal{S}_0,\mathbf{d}}(\mathbf{w})$ can be written as

$$
\Psi_{\mathcal{S}_0,\mathbf{d}}(\mathbf{w}) = \log\left(\Phi_{\mathcal{S}_0,\mathbf{d}}(\mathbf{w})\right)
$$
(4.26)

$$
= -\lambda_0 \int_{\mathbb{R}^2} \left\{1 - \frac{1}{1 + |\omega_1|^2\sigma_H^2\sigma_B^2\|\mathbf{r}\|^{-\gamma} + |\omega_2|^2\sigma_H^2\sigma_B^2\|\mathbf{r} - \mathbf{d}\|^{-\gamma}} d\mathbf{r}\right\}
$$
(4.27)

The above integral denotes the interferer statistics observed across the receiver antennae. In the remainder of this section, I will attempt to solve the integral. I first look at the two extreme cases of $|\mathbf{d}| = 0$ and $|\mathbf{d}| \to \infty$, subsequently analyzing the general scenario of $|\mathbf{d}| > 0$.

4.6.2.1 Antennae are colocated ($\|\mathbf{d}\| = 0$)

In the first scenario, the receive antennae are assumed to be colocated; i.e., $\mathbf{d} = \mathbf{0}$. In Section 4.5, I showed that the joint statistics of resulting interference are distributed according to the isotropic symmetric alpha stable distribution. Setting $\mathbf{d} = \mathbf{0}$ in (4.27), I get

$$\Psi_{\mathcal{S}_0,\mathbf{0}}(\mathbf{w}) = -\lambda_0 \int_{\mathbb{R}^2} \left\{ 1 - \frac{1}{1 + |\omega_1|^2 \sigma_H^2 \sigma_B^2 \|\mathbf{r}\|^{-\gamma} + |\omega_2|^2 \sigma_H^2 \sigma_B^2 \|\mathbf{r}\|^{-\gamma}} d\mathbf{r} \right\} \tag{4.28}$$

$$= -\lambda_0 \int_{\mathbb{R}^2} \left\{ 1 - \frac{1}{1 + (|\omega_1|^2 + |\omega_2|^2) \sigma_H^2 \sigma_B^2 \|\mathbf{r}\|^{-\gamma}} d\mathbf{r} \right\} \tag{4.29}$$

$$= -\lambda_0 \int_{\mathbb{R}^2} \left\{ 1 - \frac{1}{1 + \|\mathbf{w}\|^2 \sigma_H^2 \sigma_B^2 \|\mathbf{r}\|^{-\gamma}} d\mathbf{r} \right\} \tag{4.30}$$

$$= -\lambda_0 \int_{\mathbb{R}^2} \left\{ 1 - \frac{1}{1 + \sigma_H^2 \sigma_B^2 \|\|\mathbf{w}\|^{4/\gamma} \mathbf{r}\|^{-\gamma}} d\mathbf{r} \right\} \tag{4.31}$$

By applying a change of variables $\mathbf{t} = \|\mathbf{w}\|^{4/\gamma} \mathbf{r}$ in the integration, I get

$$\Psi_{\mathcal{S}_0,\mathbf{0}}(\mathbf{w}) = -\|\mathbf{w}\|^{4/\gamma} \lambda \int_{\mathbb{R}^2} \left\{ 1 - \frac{1}{1 + \sigma_H^2 \sigma_B^2 \|\mathbf{t}\|^{-\gamma}} d\mathbf{t} \right\} \tag{4.32}$$

$$= -\|\mathbf{w}\|^{4/\gamma} \sigma_0 \tag{4.33}$$

$$= -\|\mathbf{w}\|^{\alpha} \sigma_0 \tag{4.34}$$

where $\sigma_0 = \lambda \int_{\mathbb{R}^2} \left\{ 1 - \frac{1}{1 + \sigma_H^2 \sigma_A^2 \|\mathbf{t}\|^{-\gamma}} d\mathbf{t} \right\}$, is the same as σ_0 evaluated in (4.16). Consequently, I can write the characteristic function $\Phi_{\mathcal{S}_0,\mathbf{0}}(\mathbf{w})$ as

$$\Phi_{\mathcal{S}_0,\mathbf{0}}(\mathbf{w}) = e^{-\|\mathbf{w}\|^{4/\gamma} \sigma_0} \tag{4.35}$$

which is the characteristic function of the isotropic symmetric alpha stable random variable as shown in Table 4.2, as well as Section 4.5. Predictably, the interference at two colocated wireless antennae in a Poisson field of interferers follows the isotropic symmetric alpha stable distribution.

4.6.2.2 Antennae are located infinitely far apart ($\|\mathbf{d}\| \to \infty$)

In this scenario, the receive antennae are separated by an extreme distance. Intuitively, one can see that the interference observed by these antennae should be statistically independent. And since it has been shown that the interference at each antenna follows the symmetric alpha stable distribution, the joint distribution of interference should follow the independent symmetric alpha stable multivariate distribution. I start from (4.27) , which is

$$\Psi_{\mathbb{S}_0,\mathbf{d}}(\mathbf{w}) = -\lambda \int_{\mathbb{R}^2} \left\{ 1 - \frac{1}{1 + |\omega_1^2|\sigma_H^2\sigma_A^2\|\mathbf{r}\|^{-\gamma} + |\omega_2^2|\sigma_H^2\sigma_A^2\|\mathbf{r}-\mathbf{d}\|^{-\gamma}} d\mathbf{r} \right\} \qquad (4.36)$$

When $\mathbf{d} \to \infty$, for any value of $\mathbf{r}$, either $\|\mathbf{r}\|^{-\gamma}$ or $\|\mathbf{r} - \mathbf{d}\|^{-\gamma}$ is 0. When $\mathbf{r}$ is in the neighborhood of $\mathbf{d}/2$, both are equal to 0. This allows us to write (4.36) as

$$\Psi_{\mathcal{S}_0,\infty}(\mathbf{w}) = \lim_{\mathbf{d} \to \infty} -\lambda_0 \int_{\mathbb{R}^2} \left\{ 1 - \frac{1}{1 + |\omega_1^2|\sigma_H^2\sigma_B^2\|\mathbf{r}\|^{-\gamma} + |\omega_2^2|\sigma_H^2\sigma_B^2\|\mathbf{r} - \mathbf{d}\|^{-\gamma}} d\mathbf{r} \right\} \quad (4.37)$$

$$= \lim_{\mathbf{d} \to \infty} -\lambda_0 \int_{\mathbb{R}^2} \left\{ 1 - \frac{1}{1 + |\omega_1|^2\sigma_H^2\sigma_B^2\|\mathbf{r}\|^{-\gamma}} - \frac{1}{|\omega_2^2|\sigma_H^2\sigma_B^2\|\mathbf{r} - \mathbf{d}\|^{-\gamma}} d\mathbf{r} \right\} \quad (4.38)$$

$$= -\lambda_0 \int_{\mathbb{R}^2} \left\{ 1 - \frac{1}{1 + \sigma_H^2\sigma_B^2\||\omega_1|^{2/\gamma}\mathbf{r}\|^{-\gamma}} d\mathbf{r} \right\}$$

$$- \lim_{\mathbf{d} \to \infty} \lambda_0 \int_{\mathbb{R}^2} \left\{ 1 \frac{1}{\sigma_H^2\sigma_B^2\||\omega_2|^{4/\gamma}(\mathbf{r} - \mathbf{d})\|^{-\gamma}} d\mathbf{r} \right\} \quad (4.39)$$

$$= -\lambda_0 \int_{\mathbb{R}^2} \left\{ |\omega_1|^{2/\gamma} 1 - \frac{1}{1 + \sigma_H^2\sigma_A^2\|\mathbf{t}_1\|^{-\gamma}} d\mathbf{t}_1 \right\}$$

$$- \lim_{\mathbf{d} \to \infty} \lambda_0 \int_{\mathbb{R}^2} \left\{ |\omega_2|^{2/\gamma} 1 \frac{1}{\sigma_H^2\sigma_A^2\|\mathbf{t}_2 - \mathbf{d}\|^{-\gamma}} d\mathbf{t}_2 \right\} \quad (4.40)$$

$$= -\lambda_0 |\omega_1|^{4/\gamma}\sigma_0 - \lambda_0|\omega_2|^{4/\gamma}\sigma_0 \quad (4.41)$$

Subsequently, I can write the characteristic function as

$$\Phi_{\mathcal{S}_0,\infty}(\mathbf{w}) = e^{-\|\omega_1\|^{4/\gamma}\sigma_0 + \|\omega_2\|^{4/\gamma}\sigma_0} \quad (4.42)$$

$$= e^{-\|\omega_1\|^{\alpha}\sigma_0 + \|\omega_2\|^{\alpha}\sigma_0} \quad (4.43)$$

which is the characteristic function of the independent symmetric alpha stable distribution as shown in Table 4.2.

4.6.2.3 Antennae are separated by a finite distance ($\|\mathbf{d}\| > 0$)

In the final case, I consider the scenario where the receive antennae are separated, however, the separation is not close enough to 0 or large enough that I can approximate the interference statistics by the $\Phi_{\mathcal{S}_0,\mathbf{0}}(\mathbf{w})$ or $\Phi_{\mathcal{S}_0,\infty}(\mathbf{w})$. Again, I have to solve the integral

$$\Psi_{\mathcal{S}_0,\mathbf{d}}(\mathbf{w}) = -\lambda_0 \int_{\mathbb{R}^2} \left\{ 1 - \frac{1}{1 + |\omega_1|^2 \sigma_H^2 \sigma_B^2 \|\mathbf{r}\|^{-\gamma} + |\omega_2|^2 \sigma_H^2 \sigma_B^2 \|\mathbf{r}-\mathbf{d}\|^{-\gamma}} d\mathbf{r} \right\}. \quad (4.44)$$

I am not aware of a closed form solution to (4.44). While there are many methods available for approximating integrals, I choose to approximate $\Psi_{\mathcal{S}_0,\mathbf{d}}(\mathbf{w})$ in (4.44) by $\hat{\Psi}_{\mathcal{S}_0,\mathbf{d}}(\mathbf{w})$, given as

$$\hat{\Psi}_{\mathcal{S}_0,\mathbf{d}}(\mathbf{w}) = v(\mathbf{d})\Psi_{\mathcal{S}_0,\mathbf{0}}(\mathbf{w}) + (1 - v(\mathbf{d}))\Psi_{\mathcal{S}_0,\infty}(\mathbf{w}) \quad (4.45)$$

$$= \sigma_0 \left(-v(\mathbf{d})\|\mathbf{w}\|^\alpha - (1 - v(\mathbf{d}))(|\omega_1|^\alpha - |\omega_2|^\alpha) \right) \quad (4.46)$$

$$= \sigma_0 \left(-v(\mathbf{d})\|\mathbf{w}\|^\alpha - (1 - v(\mathbf{d}))\|\mathbf{w}\|_\alpha^\alpha \right). \quad (4.47)$$

This approximation is equivalent to assuming that the joint statistics of interference across the two antennae are a weighted mixture of isotropic and independent interference, with the weights given as $w(\delta)$ and $1 - w(\delta)$, respectively. When the antennae are colocated ($\delta = 0$), interference is demonstrably jointly isotropic thus $v(0) = 1$, and when the antennae are far apart ($\|\mathbf{d}\| \to \infty$), interference is demonstrably jointly independent and consequently $v(\infty) = 0$.

The optimal weighting function $v(\mathbf{d})$ would ideally be evaluated as

$$v(\mathbf{d}) = \arg\min_{\mathbb{R}} \int_{\mathbb{R}^N} \left| \Psi_{S_0,\mathbf{d}}(\mathbf{w}) - \hat{\Psi}_{S_0,\mathbf{d}}(\mathbf{w}) \right|^2 d\mathbf{w} \tag{4.48}$$

$$= \arg\min_{\mathbb{R}} \int_{\mathbb{R}} \int_{\mathbb{R}} \int_{\mathbb{R}^2} \left| \frac{1}{1 + |\omega_1|^2 \sigma_H^2 \sigma_B^2 \|\mathbf{r}\|^{-\gamma} + |\omega_2|^2 \sigma_H^2 \sigma_B^2 \|\mathbf{r}-\mathbf{d}\|^{-\gamma}} \right.$$

$$- \frac{1-v}{1 + |\omega_1^2| \sigma_H^2 \sigma_A^2 \|\mathbf{r}\|^{-\gamma}} - \frac{1-v}{1 + |\omega_2^2| \sigma_H^2 \sigma_A^2 \|\mathbf{r}\|^{-\gamma}}$$

$$\left. - \frac{v}{1 + (|\omega_1^2| + |\omega_2^2|)\sigma_H^2 \sigma_A^2 \|\mathbf{r}\|^{-\gamma}} \right|^2 d\mathbf{r} d|\omega_1|^2 d|\omega_2|^2. \tag{4.49}$$

The solution to the above optimization problem can be written as

$$v(\mathbf{d}) =$$

$$\frac{\iint\limits_{\mathbb{R}\mathbb{R}\mathbb{R}^2}\frac{1}{1 + |\omega_1|^2 \sigma_H^2 \sigma_B^2 \|\mathbf{r}\|^{-\gamma} + |\omega_2|^2 \sigma_H^2 \sigma_B^2 \|\mathbf{r}-\mathbf{d}\|^{-\gamma}} - \frac{1}{1 + |\omega_1|^2 \sigma_H^2 \sigma_A^2 \|\mathbf{r}\|^{-\gamma}} - \frac{1}{1 + |\omega_2|^2 \sigma_H^2 \sigma_A^2 \|\mathbf{r}\|^{-\gamma}} d\mathbf{r} d|\omega_1|^2 d|\omega_2|^2}{\int\limits_{\mathbb{R}}\int\limits_{\mathbb{R}}\int\limits_{\mathbb{R}^2}\frac{1}{1 + |\omega_1^2| \sigma_H^2 \sigma_A^2 \|\mathbf{r}\|^{-\gamma}} + \frac{1}{1 + |\omega_2^2| \sigma_H^2 \sigma_A^2 \|\mathbf{r}\|^{-\gamma}} - \frac{1}{1 + (|\omega_1^2| + |\omega_2^2|)\sigma_H^2 \sigma_A^2 \|\mathbf{r}\|^{-\gamma}} d\mathbf{r} d|\omega_1|^2 d|\omega_2|^2}.$$

$$\tag{4.50}$$

I cannot solve this problem in closed-form, but $v(\mathbf{d})$ can be easily evaluated numerically. Using curve fitting solutions provided by MATLAB, I am able to well approximate $v(\mathbf{d})$ as

$$v(\mathbf{d}) = e^{-a(\gamma)d^b(\gamma)}. \tag{4.51}$$

Numerically evaluating the minimization function in MATLAB and finding the closest weights, I can reduce the square error given in (4.48). Figure 4.3 shows the square error for the approximation for different values of $\|\mathbf{d}\|$, while Figure 4.4 shows the error as a function of ω_1 and ω_2. Since the fitting function matches exactly at $\|\mathbf{d}\| = 0$ and when $\|\mathbf{d}\|$ grows very large, the square error term in those
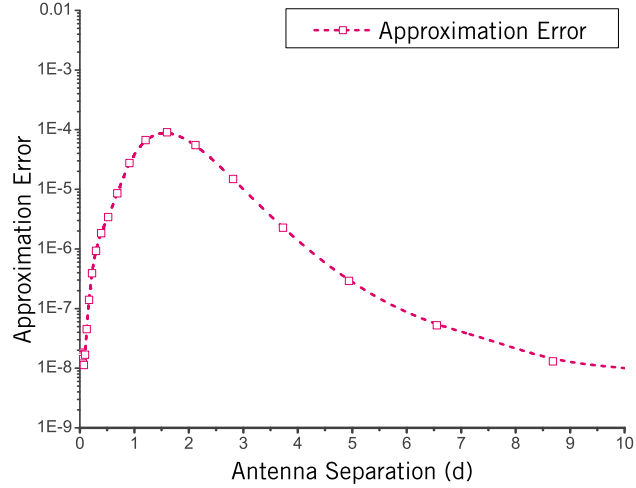
Figure 4.3: Mean square error of integral approximation in (4.48) vs. distance between receive antennae.

regions is very close to 0. Figure 4.5 shows the weight $v(\mathbf{d})$ for different values of $\|\mathbf{d}\|$. Figure 4.6 shows the values of the fitting parameters.

Thus, the joint statistics of interference across two separate antennae are approximated as

$$\Psi_{\mathcal{S}_0,\mathbf{d}}(\mathbf{w}) \approx -\sigma_0(v(\mathbf{d}\|\mathbf{w}\|^\alpha + (1-v(\mathbf{d})\|\mathbf{w}\|_\alpha^\alpha) \tag{4.52}$$

and consequently,

$$\Phi_{\mathcal{S}_0,\mathbf{d}}(\mathbf{w}) = e^{-\sigma_0(v(\mathbf{d}\|\mathbf{w}\|^\alpha + (1-v(\mathbf{d})\|\mathbf{w}\|_\alpha^\alpha)} \tag{4.53}$$

By combining (4.17), (4.20), and (4.6), I get

$$\Phi_{\mathbf{Z}}(\mathbf{w}) = e^{-\sigma_0 v(\mathbf{d}\|\mathbf{w}\|^\alpha - (\sigma_0(1-v(\mathbf{d})+\sigma_n)\|\mathbf{w}\|_\alpha^\alpha}. \tag{4.54}$$

Thus, I have derived the joint statistics of interference observed across two physically separate wireless antennae and shown the intuitively satisfying

103
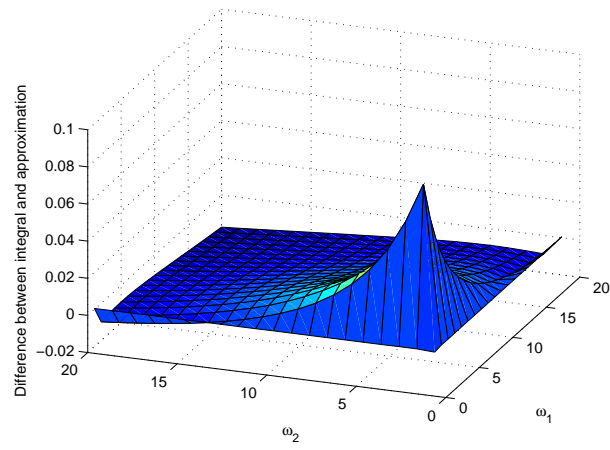
Figure 4.4: Difference between (4.44) and approximating function (4.45) vs. characteristic frequency.
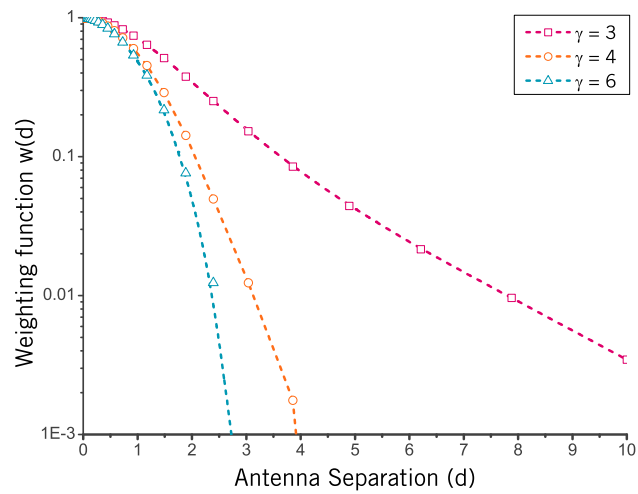
Figure 4.5: Weighting function $v(\mathbf{d})$ vs. distance $\|\mathbf{d}\|$ between receive antennae.
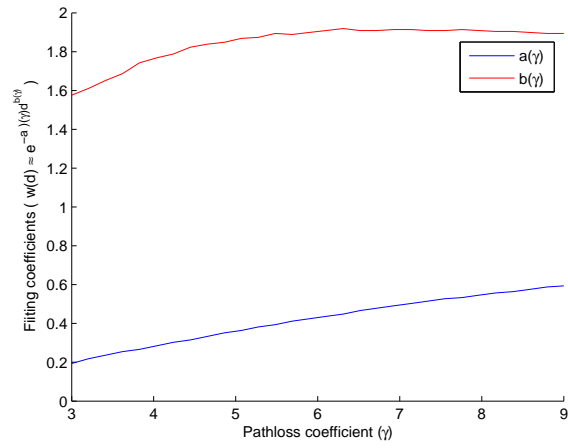
Figure 4.6: Fitting parameters $a(\gamma)$ and $b(\gamma)$ vs. power pathloss exponent γ.
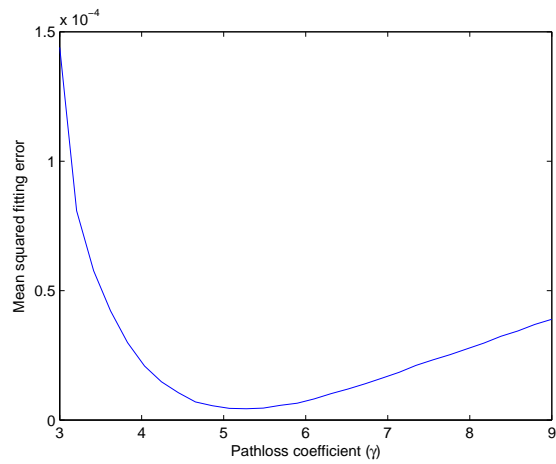
Figure 4.7: Mean squared fitting error between weighting function and $e^{-a(\gamma)d^{b(\gamma)}}$ vs. γ.

result that the statistics move within a continuum between spatially isotropic and spatially independent, as the receivers move from being colocated to being infinitely far apart.

4.7 Joint Statistics of Interference Observed by More than Two Antennae

In the previous section, I derived the joint statistics of interference observed across two physically separate antennae. In order to extend this result to N antennae where N may be greater than 2, I write the interference observed at the Nth antenna as

$$Z_n = \sum_{i \in \mathcal{S}} B_i^0 e^{j\chi_i^0} \|\mathbf{R}_i - \mathbf{d}_n\|^{-\frac{\gamma}{2}} H_{n,i}^0 e^{j\Theta_{n,i}^0} \tag{4.55}$$

where $B_i^0 e^{j\chi_i^0}$ is the interferer emission, $H_{n,i}^0 e^{j\Theta_{n,i}^0}$ is the fast fading channel between the interferer and the nth receive antenna, and $\mathbf{x}_n$ is the two dimensional coordinate of the nth antenna. Following the same steps as I did in Section 4.6, I arrive at the log-characteristic function

$$\Psi_{\mathcal{S}_0}(\mathbf{w}) = -\lambda \int_{\mathbb{R}^2} \left\{ 1 - \frac{1}{1 + \sum\limits_{n=1}^{N} |\omega_n^2| \sigma_H^2 \sigma_A^2 \|\mathbf{r} - \mathbf{d}_n\|^{-\gamma}} \right\} d\mathbf{r} \tag{4.56}$$

Solving the above integral is non-trivial and a worthy subject for future work.

106

4.8 Impact of System Model Assumptions

4.8.1 Interference Statistics in General Fading Channel Models

In developing my system model in Section 4.4, I assumed a Rayleigh distribution for the fading channel amplitude between the interfering source and the multi-antenna receiver. While the Rayleigh distribution is a reasonably accurate and widely used model of fading channels, other distributions have also been widely used to characterize wireless channel amplitudes[146].

I can rewrite (4.5) and (4.6) as

$$
\Phi_{S_0}(\mathbf{w}) = \mathbb{E}\left\{ e^{j\sum_{n=1}^{N}|\overline{\omega}_n|\sum_{i=1}^{|S_0|} D_{0,i}^{-\frac{\gamma}{2}} H_{n,i}^0 B_i^0 \cos(\chi_i^0 + \Theta_{n,i}^0 + \xi_{\omega,n})} \right\}
\tag{4.57}
$$

The number of interferers k within the annular region is a Poisson random variable with mean $\lambda_0 \pi(\delta_\uparrow^2 - \delta_\downarrow^2)$ ($\delta_\downarrow \to 0$ and $\delta_\uparrow \to \infty$). Combining this notion with (4.57), I can expand (4.57) as the sum of k $i.i.d.$ interference signals, with k being a Poisson distributed integer. Thus, I obtain

$$
\Phi_{S_0}(\mathbf{w}) = \sum_{k=0}^{\infty} \mathbb{E}\left\{ e^{j\sum_{n=1}^{N}|\overline{\omega}_n||D_0^{-\frac{\gamma}{2}} H_n^0 B^0 \cos(\chi^0 + \Theta_n^0 + \xi_{\omega,n})} \right\}^k e^{-\lambda_0\pi(\delta_\uparrow^2 - \delta_\downarrow^2)} \frac{\left(\lambda_0\pi(\delta_\uparrow^2 - \delta_\downarrow^2)\right)^k}{k!}
\tag{4.58}
$$

$$
= e^{-\lambda_0\pi(\delta_\uparrow^2 - \delta_\downarrow^2)} \sum_{k=0}^{\infty} \frac{\left[\left(\lambda_0\pi(\delta_\uparrow^2 - \delta_\downarrow^2)\right) \mathbb{E}\left\{ e^{j\sum_{n=1}^{N}|\overline{\omega}_n||D_0^{-\frac{\gamma}{2}} H_n^0 B^0 \cos(\chi^0 + \Theta_n^0 + \xi_{\omega,n})} \right\} \right]^k}{k!}
\tag{4.59}
$$

$$
= e^{-\lambda_0\pi(\delta_\uparrow^2 - \delta_\downarrow^2)} e^{\mathbb{E}\left\{ e^{j\sum_{n=1}^{N}|\overline{\omega}_n||D_0^{-\frac{\gamma}{2}} H_n^0 B^0 \cos(\chi^0 + \Theta_n^0 + \xi_{\omega,n})} \right\} \lambda_0\pi(\delta_\uparrow^2 - \delta_\downarrow^2)}
\tag{4.60}
$$

$$
= e^{\left[\mathbb{E}\left\{ e^{j\sum_{n=1}^{N}|\overline{\omega}_n||D_0^{-\frac{\gamma}{2}} H_n^0 B^0 \cos(\chi^0 + \Theta_n^0 + \xi_{\omega,n})} \right\} - 1 \right] \lambda_0\pi(\delta_\uparrow^2 - \delta_\downarrow^2)}
\tag{4.61}
$$

107

By taking the logarithm of $\Phi_{S_0}(\mathbf{w})$ in (4.61), the log-characteristic function is

$$\Psi_{S_0}(\mathbf{w}) \triangleq \log \Phi_{S_0}(\mathbf{w}) \tag{4.62}$$

$$= \lambda_0 \pi (\delta_\uparrow^2 - \delta_\downarrow^2) \left(\mathbb{E} \left\{ e^{j \sum_{n=1}^N |\overline{\omega}_n| D_0^{-\frac{\gamma}{2}} H_n^0 B^0 \cos(\chi^0 + \Theta_n^0 + \xi_{\omega,n})} \right\} - 1 \right) \tag{4.63}$$

$$= \lambda_0 \pi (\delta_\uparrow^2 - \delta_\downarrow^2) \left(\mathbb{E} \left\{ \prod_{n=1}^N e^{j |\overline{\omega}_n| D_0^{-\frac{\gamma}{2}} H_n^0 B^0 \cos(\chi^0 + \Theta_n^0 + \xi_{\omega,n})} \right\} - 1 \right). \tag{4.64}$$

(4.64) can be reduced to

$$\Psi_{S_0}(\mathbf{w}) = \lambda_0 \pi (\delta_\uparrow^2 - \delta_\downarrow^2) \left(\mathbb{E} \left\{ \prod_{n=1}^N J_0 \left(|\overline{\omega}_n| D_0^{-\frac{\gamma}{2}} H_n^0 B^0 \right) \right\} - 1 \right). \tag{4.65}$$

This step is discussed in detail in Section 3.5. Next, I use the identity

$$e^{j a \cos(b)} = \sum_{m=0}^\infty j^m \epsilon_m J_m(a) \cos(mb) \tag{4.66}$$

where $\epsilon_0 = 1$, $\epsilon_m = 2$ for $m \geq 1$, and $J_m(\cdot)$ denotes the Bessel function of order m. Combining (4.66) and (4.64), the log-characteristic function $\Psi_{\mathbf{Y}, S_0}(\mathbf{w})$ can be expressed as

$$\Psi_{S_0}(\mathbf{w}) =$$
$$\overline{K} \left(\mathbb{E} \left\{ \prod_{n=1}^N \sum_{m_n=0}^\infty j^{m_n} \epsilon_{m_n} J_{m_n} \left(|\overline{\omega}_n| D_0^{-\frac{\gamma}{2}} H_n^0 B^0 \cos \left(m_n \left(\chi^0 + \Theta_n^0 + \xi_{\omega,n} \right) \right) \right) \right\} - 1 \right)$$
$$\tag{4.67}$$

where $\overline{K} = \lambda_0 \pi (\delta_\uparrow^2 - \delta_\downarrow^2)$. Since I am interested in the tail statistics of interference distribution and from Fourier analysis, the behavior of the characteristic function Φ in the neighborhood of $\|\mathbf{w}\| \to 0$ governs the tail probability of the random envelope[115]. An approximation was proposed by Middleton [114] for the log-characteristic function for ψ in the neighborhood of zero using

$$\mathbb{E}_x \{J_0(x)\} = e^{-\mathbb{E}_x\{x\}} (1 + \Lambda(x)) \tag{4.68}$$

108

where $\Lambda(x)$ is a correction factor expressed as

$$\Lambda(x) = \sum_{m=2}^{\infty} \frac{(\mathbb{E}\{x^2\})^k}{2^{2k} k!} {}_1F_1(-k;1;\frac{x}{\mathbb{E}\{x\}}) \tag{4.69}$$

where ${}_1F_1(\cdot;\cdot;\cdot)$ is the confluent hypergeometric function of the first kind. As $x \to 0$, the slowest decaying term in $\Lambda(x)$ is of the order $O(x^4)$. Thus, as $\|\mathbf{w}\| \to 0$, I approximate $1 + \Lambda(|\overline{\omega}_n| D_0^{-\frac{\gamma}{2}} H_n^0 B^0) \approx 1$. Using (4.68) in (4.65) and ignoring higher order terms around the region $|\overline{\omega}_n| = 0$, I get

$$\Psi_{\mathcal{S}_0}(\mathbf{w}) = \lambda_0 \pi (\delta_\uparrow^2 - \delta_\downarrow^2) \left(\mathbb{E}\left\{ \prod_{n=1}^{N} J_0\left(|\overline{\omega}_n| D_0^{-\frac{\gamma}{2}} H_n^0 B^0 \right) \right\} - 1 \right) \tag{4.70}$$

$$= \lambda_0 \pi (\delta_\uparrow^2 - \delta_\downarrow^2) \left(\mathbb{E}\left\{ \prod_{n=1}^{N} e^{-|\overline{\omega}_n| D_0^{-\frac{\gamma}{2}} H_n^0 B^0} \right\} - 1 \right) \tag{4.71}$$

and the remainder of the derivation follows in the same manner as shown in Sections 4.5 and 4.6.

4.8.2 Interference Statistics in General Interferer Emissions

In deriving interferer statistics, I assumed that the emission amplitude was Gaussian distributed in (4.55) in order to simplify the interference statistics into the form of a Middleton Class A distribution. Without making this assumption, (4.25) would be replaced by

$$\Phi_{\mathcal{S}_0,\mathbf{d}}(\mathbf{w}) = \mathbb{E}\left\{ \prod_{i \in \mathcal{S}} e^{|\omega_1|^2 B_i^2 \sigma_H^2 \|\mathbf{R}_i\|^{-\gamma} + |\omega_2|^2 B_i^2 \sigma_H^2 \|\mathbf{R}_i - \mathbf{x}\|^{-\gamma}} \right\} \tag{4.72}$$

$$= \mathbb{E}\left\{ \prod_{i \in \mathcal{S}} \phi_{B^2}\left(|\omega_1|^2 \sigma_H^2 \|\mathbf{R}_i\|^{-\gamma} + |\omega_2|^2 \sigma_H^2 \|\mathbf{R}_i - \mathbf{x}\|^{-\gamma} \right) \right\} \tag{4.73}$$

where $\phi_{B^2}(\cdot)$ is the characteristic function of the interferer emission power. Subsequently, after taking the log of the characteristic function and applying the

point generating functional property, (4.72) can be written as

$$\Psi_{\mathcal{S}_0,\mathbf{d}}(\mathbf{w}) = -\lambda \int_{\mathbb{R}^2} \phi_{B^2} \left(|\omega_1|^2 \sigma_H^2 \|\mathbf{R}_i\|^{-\gamma} + |\omega_2|^2 \sigma_H^2 \|\mathbf{R}_i - \mathbf{x}\|^{-\gamma} \right) \qquad (4.74)$$

Again, I can apply the approximation used in (4.45). From here on, the derivation of the joint statistics for the three cases discussed under Section 4.6 follows the same path, with a change in some of the constants.

4.9 Simulation Results

To study the accuracy of my joint amplitude distribution model for constrained interferer distributions, I numerically simulate interference observed by a multi-antenna receiver operating in an interferer environment as described in Section 4.4.

First, I compare the tail probabilities of the numerically simulated distribution and my proposed distribution models. The tail probability is the complementary cumulative distribution function of a random variable and in performance analysis of communication systems, the tail probability of interference is related to the outage performance of receivers. Given a threshold τ, I define tail probability as $\mathbb{P}(|Y_1| > \tau, \cdots, |Y_N| > \tau)$. Figure 4.8 shows a comparison of the tail probabilities of the numerically simulated distribution, my proposed distribution, and the Gaussian distribution, respectively. The tail probabilities of my proposed distribution match closely to simulated interference, while the Gaussian distribution is clearly unable to capture the large tail probabilities of impulsive interference.

110

Table 4.3: Parameter values used in simulations

Parameter	Description	Value
λ_{tot}	Per-antenna total intensity of interferers	0.01
γ	Power path-loss exponent	2.5
$\overline{B}$	Mean amplitude of interferer emissions	1.0
$\delta_{\downarrow}$	Radius of guard zone around receiver	1.5
$\mathbb{E}\{H^2\}$	Fast fading channel power	1.0

In Figure 4.8, the receiver uses two antennae and the interferers exclusive to each antennae are distributed with equal densities, i.e. $\lambda_1 = \lambda_2 = \lambda_e$. I choose a value of λ_0 such that $\lambda_0 + \lambda_e = 0.01$, i.e. the density of total interferers observed by each antenna is the same, regardless of the choice of λ_0 or λ_e. This helps to normalize my data as the variance of interference observed at each antenna (proportional to $\lambda_0 + \lambda_e$) remains the same regardless of the value taken by λ_0 or λ_e. Table 4.3 lists the values for the rest of the simulation parameters.

In Figure 4.9, the receiver uses two antennae and interferers are observed by all antennae, i.e. $\lambda_1 = \lambda_2 = 0$. $\lambda_0 = 0.01$. Figure 4.9 shows the simulated and the predicted tail probability of interference at $\tau = 1$ vs. the distance between the receiver antennae. The simulated and predicted values match very well, thereby validating the approximations needed to arrive at closed form solutions for interference statistics across two distributed antennae. Table 4.3 lists the values for the rest of the simulation parameters.
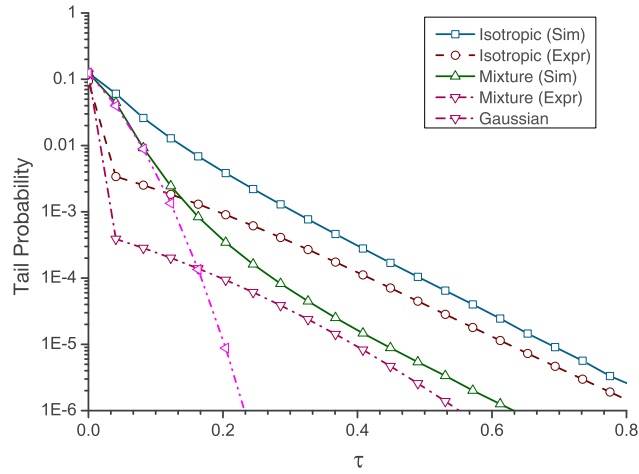
Figure 4.8: Tail probability vs. threshold τ for simulated interference in the absence of guard zones. The tail probability is compared between the numerically simulated interference ("Sim") and the tail of the proposed multi-variate Symmetric alpha stable distribution ("Expr"). The tail probabilities are generated for isotropic interference ($\lambda_0 = 0.01, \lambda_e = 0.0$) and a mixture of isotropic and independent interference ($\lambda_0 = 0.001, \lambda_e = 0.009$). Remaining parameter values are given in Table 4.3.
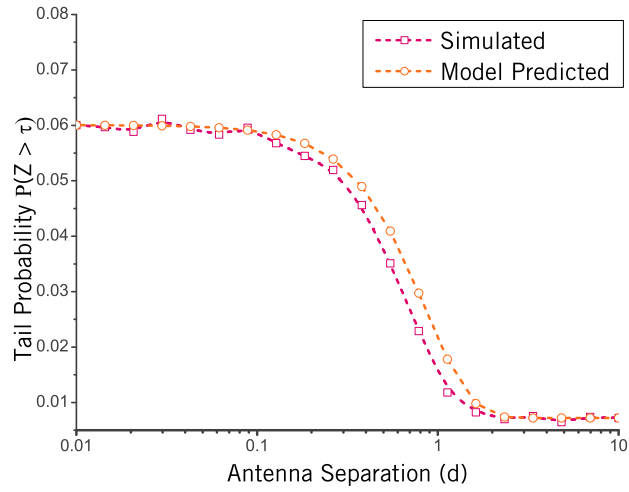
Figure 4.9: Tail probability vs. antennae separation $|\mathbf{d}|$ for simulated interference in the absence of guard zones. The tail probability is compared between the numerically simulated interference ("Sim") and the tail of the proposed multi-variate Symmetric alpha stable distribution ("Expr"). The tail probabilities are generated for isotropic interference $(\lambda_0 = 0.01, \lambda_e = 0.0)$. Remaining parameter values are given in Table 4.3.

4.10 Conclusions

In this chapter, I derived joint statistics of interference in a multi-antenna receiver located in a field of Poisson distributed interferers. I model a decentralized wireless network; i.e., the interferers can be arbitrarily close to the receiver. The joint statistics of interference are well modeled by the multi-dimensional symmetric alpha stable distribution. In my proposed framework, the resulting interference is a mixture of a spatially isotropic and spatially independent symmetric alpha stable random vector.

I also derived the joint amplitude statistics of interference observed by two physically separate wireless antennae placed in a Poisson field of interferers. Depending on the distance between the antennae, the proposed amplitude distribution exists in a continuum between the statistically isotropic bivariate symmetric alpha stable distribution and the statistically independent bivariate symmetric alpha stable distribution. My proposed distribution reduces to isotropic and independent statistics when the wireless antennae are colocated or extremely far apart, respectively. I discussed the impact of some of my system model assumptions on the interference statistics and showed that my proposed distribution is quite robust to the choice of fading channel or interferer emission statistics. Finally, I present some initial discussion on extending my results to modeling joint statistics of interference across more than two wireless antennae.

The statistical models of interference resulting from this chapter can be used to improve communication systems employing colocated or distributed antennae operating in the presence of interference. In the next chapter, I ana-

lyze communication performance of various conventional receiver diversity algorithms in the presence of multi-antenna interference.

Chapter 5

Communication Performance of
Interference-Limited Networks Without Guard Zones

5.1 Introduction

Wireless transceivers suffer degradation in communication performance due to interference generated by both human-made and natural sources[73]. Human-made sources of interference include uncoordinated wireless devices operating in the same frequency band (co-channel interference) [44], devices communicating in adjacent frequency bands (adjacent channel interference), and computational platform subsystems radiating clock frequencies and their harmonics[147]. Dense spatial reuse of the available radio spectrum, which is key in meeting increasing demand in user data rates[13], also causes severe co-channel interference and may limit communication system performance.

Recent communication standards and research have focused on the use of multiple receive antennae to increase data rate and communication reliability in wireless networks. Single input multiple output (SIMO) communication systems can achieve higher data rates with fewer errors through *spatial diversity*; i.e., receiving multiple copies of the signal increases the chance that some of these copies are relatively impairment free. Consequently, wireless receivers with

multiple antennae are increasingly being deployed in networks that are rife with interference due to resource re-use[44, 73]. Multi-antenna wireless receivers have generally been designed and their communication performance analyzed under the assumption of additive Gaussian noise. While the Gaussian distribution is a good statistical model for thermal noise at the receiver, interference has predominantly non-Gaussian statistics. This mismatch between design assumptions and the actual interference statistics may degrade the communication performance of multi-antenna wireless receivers. Since communication systems utilizing multiple antennae are being deployed on mobile platforms, it becomes essential to characterize the relative performance of spatial diversity techniques in the presence of interference.

In this chapter, I analyze the uncoded communication performance of diversity combining techniques in the presence of interference modeled via statistical-physical mechanisms of interferer distribution, interference generation, and interference propagation. The diversity combining receivers under study are the equal gain combiner (EGC), fixed weight combiner (FWC), maximum ratio combiner (MRC), selection combiner (SC), and the post-detection combiner (PDC). A detailed discussion on each of these receivers can be found in Sections 5.5 and 5.6. Evaluating the performance of these diversity combining algorithms in interference highlights the relative merits or disadvantages of different algorithms in different interference environments.

Communication standards typically employ some form of error correction coding. In the presence of coding, communication performance metrics

117

such as channel capacity or mutual information[43] are more relevant for link level analysis. Closed form expressions for SIMO channel capacity in symmetric alpha stable interference are not analytically expressible, given the lack of closed form density functions for the symmetric alpha stable distributions. Analysis of communication performance in presence of coding also requires accurate statistical-physical modeling of interference in the time domain, whereas in this dissertation interference is assumed to be statistically independent across time samples. I evaluate uncoded communication performance as the ccdf of signal to interference ratio (SIR) at the receiver, referred to as outage probability. Outage probability provides a baseline physical layer performance metric for different receiver diversity combining structures, and can even inform analysis of coded communication performance when used in conjunction with coding gain[146]. Outage probability is also used in analysis of network level performance, where it is the basis of evaluating metrics such as network capacity, area spectral efficiency[8] or transmission capacity[172].

5.2 Organization and Notation

In Section 5.3 I discuss the key contributions and limitations of prior work on communication performance in interference limited systems. Section 5.4 details my system model for interferer location distribution, and interference generation and propagation. In Section 5.5 I derive the outage probability of pre-detection diversity combining techniques. I derive closed-form outage probability expressions for fixed weight combining, maximum ratio combining and

118

selection combining. In Section 5.6 I derive the outage probability expression for a post detection combining receiver. Section 5.7 presents numerical simulations to compare my closed-form outage probability to simulated outage in a multi-antenna receiver located within a space containing Poisson distributed interferers. I conclude by a summary of the key contributions and insights in Section 5.8.

5.3 Prior Work

Prior work on analyzing communication performance of receiver diversity algorithms in the presence of interference has usually focused on bit-error rate (BER) analysis of various reception schemes in the presence of additive impulsive noise. Typical statistical distributions that model impulsive noise are the spherically invariant symmetric alpha-stable distribution[86], spherically invariant Middleton Class A distribution[47], and multi-dimensional independent Middleton Class A noise model[47]. These statistical distributions model two extreme cases of interference statistics; i.e, interference is either statistically invariant across antennae or statistically independent across receiver antennae.

In [88], the isotropic symmetric alpha-stable noise model was used to evaluate BER by using the Cauchy distribution to model alpha stable noise. This work was extended in [134] to more reception techniques, but only considered BPSK modulation. In [152], the authors investigated the performance of different diversity combining techniques over fading channels with impulsive noise modeled using either isotropic or independent multi-dimensional Middleton Class

A distribution. In [77], the authors analyze performance bounds for optimum and sub-optimum receivers in the presence of Middleton Class A impulsive noise over non-fading channels. In [41], the authors evaluate performance bounds of 2×2 MIMO communication with Alamouti codes using a generalized statistical-physical interference model from [113]. In [102] the performance of maximum ratio combining techniques was investigated in multi-user environments and in presence of receiver channel estimation error. While the authors did use the notion of statistical-physical interference propagation mechanisms, they assumed a fixed number and locations of the interference generating sources. In [7], a statistical-physical model similar to mine was used to study performance of optimum diversity combining. However, this model also assumed that interference was isotropic and the optimum receiver was impractical to implement as it required information about interferer locations at each sampling instant. By using impulsive statistical distributions to model interference, communication performance analysis can provide a link between communication performance and noise parameters. On the other hand, starting from a statistical-physical noise generation mechanism, performance analysis can provide a link between communication performance and network parameters such as user density and user distribution. Table 2.3 provides a summary of the interference models and receiver algorithms studied with regards to BER analysis.

In wireless systems, communication performance analysis can also apply to the performance of the overall network. Early studies on interference-limited MIMO networks modeled interference as the sum signal from multiple finite

120

sources, but did not model a decentralized network of randomly distributed interfering sources [26, 30, 46]. Such an interference generation model was most appropriate for interference in the downlink of single-tier networks, with uniformly placed basestations as the dominant interfering sources.

More recently, decentralized network models have been formulated with interferers and receivers randomly distributed as a Poisson Point Process[83], and using tools from stochastic geometry and Laplace transforms, statistical analysis is carried out on the received signal and interference power at a node[172]. These studies typically evaluate the network capacity trends for single-antenna[57] and multi-antenna networks[83] with a large number of users, and incorporate both physical layer as well as access control techniques into their analysis. For example, transmission capacity under linear diversity combination techniques such as maximum ratio combining, maximum ratio transmission, and orthogonal space-time block codes were studied in [83]. Transmission capacity assuming no channel state information at the transmitter and cancellation of interference from nearby users was studied in [164]. In [91], transmission capacity comparisons were made between receivers that performed some level of interference cancellation vs. receivers that simply treated interference as noise. In terms of the impact of access control on transmission capacity, [84] derives transmission capacity in the presence of interference mitigation through carrier sensing. These studies use outage probability expressions to analyze network performance rely heavily on a homogeneous Poisson Point Process distribution of the user nodes, although there does exist prior work using non-Poisson distributions

to model user locations[60].

My approach uses a system model that is based on the amplitude of the desired signal and interference observed at a multi-antenna receiver. One of its benefits is the ease of deriving accurate closed form expressions of outage probability, especially with different statistical distributions of the fading channel and the interfering source emissions. The disadvantage of this approach is that certain approximations are accurate only in the low outage probability regime, however, simulation results and derived expressions match well even when outage probability is high. Later, in Section 5.5, I show that some of the derived outage probability results using amplitude statistics exhibit similar trends as the closed form outage probability expressions for diversity combiners derived using power statistics[83]. Thus, the alternate approaches in prior work and proposed in this dissertation offer different benefits, with communication performance analysis using amplitude statistics being amenable to incorporating different fading and interfering emission distributions, and receiver algorithms, while analysis using signal power statistics being useful in translating link performance analysis into network performance results[172].

5.4   System Model

Figure 5.1 illustrates the interferer placement model for a 3-antenna receiver. The key assumptions are:

Assumption 5.1. *The communication link comprises of one transmit antenna and N receive antennae.*
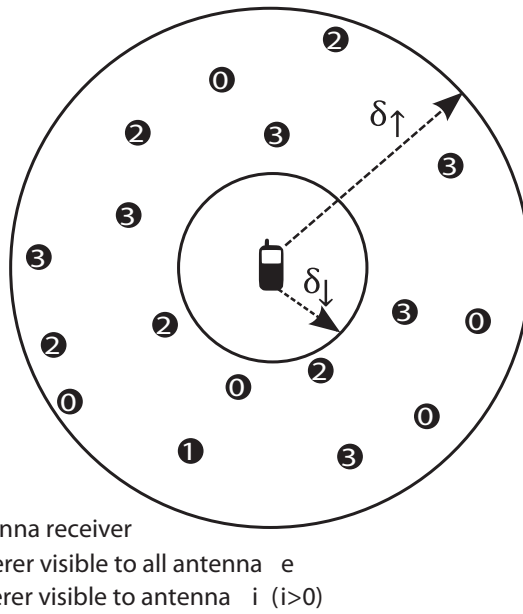
Figure 5.1: System model of a 3−antenna receiver located in a field of randomly distributed interferers. The interferers are classified according to the receiver antenna impacted by their emissions.

Assumption 5.2. *The interferers are located in a two-dimensional plane around the receiver.*

Assumption 5.3. *At each time snapshot, the active interfering sources are classified into $N+1$ independent sets $\mathcal{S}_0, \mathcal{S}_1, \cdots, \mathcal{S}_N$.*

$\mathcal{S}_0$ denotes the set of interferers that cause interference to every receive antenna. $\mathcal{S}_n \ \forall \ n = 1, \cdots, N$ denotes the set of interferers that are observed by antenna n alone. This also models antenna separation using the results derived in Chapter 4.

Assumption 5.4. *At each sampling time instant, the locations of the active interferers in $\mathcal{S}_n \ \forall \ n = 0, \cdots, N$ are distributed according to a homogeneous spatial Poisson Point Process in the two-dimensional plane around the receiver.*

The intensity of set $\mathcal{S}_n$ is denoted by $\lambda_n \ \forall \ n = 0, \ldots, N$. The distance of each interferer from the origin provides an ordering function.

Assumption 5.5. *As the wireless signal traverses through the environment, its energy decays according to the power-law path-loss model [65] with a coefficient of γ.*

Assumption 5.6. *The fast-fading channel between the transmitting source and the receiver as well as other interfering sources and the receiver is modeled using the Rayleigh distribution[65].*

Assumption 5.7. *Additive thermal noise is ignored at the receiver; i.e., the communication system is considered to be interference limited.*

5.4.1 Signal and Interference Representation

The received signal in a $1 \times N$ SIMO communication system can be denoted in vector form as

$$\mathbf{R} = \mathbf{G}s + \mathbf{Z} \tag{5.1}$$

where $\mathbf{R}$ is a complex $1 \times N$ vector where each element R_n denotes the received signal at n^{th} of the N receive antennae. The nth receive antenna observes the transmitted signal s after it has encountered a Rayleigh fading medium G_n and additive interference Y_n. In (5.1), random variables G_n and Z_n are stacked to form $1 \times N$ vectors $\mathbf{G}$ and $\mathbf{Z}$, respectively.

In Section 5.4, I classified interfering sources into different sets, such that each receive antenna observes interference from two sets that contain (1) interferers are observed by all antennae, and (2) interferers are observed only by said antenna, respectively. Following this system model, the total interference at antenna n, denoted by Z_n, can be expressed as

$$Z_n = \sum_{i_0 \in \mathcal{S}_0} B_{i_0}^0 D_{0,i_0}^{-\frac{\gamma}{2}} H_{n,i_0}^0 e^{j(\chi_{i_0}^0 + \Theta_{n,i_0}^0)} + \sum_{i \in \mathcal{S}_n} B_i^n D_{n,i}^{-\frac{\gamma}{2}} H_i^n e^{j(\chi_i^n + \Theta_i^n)} \tag{5.2}$$

where $B_{i_0}^0 e^{j(\chi_{i_0}^0)}$ indicates the emission from the i_0^{th} interferer in set $\mathcal{S}_0$, and $B_i^n e^{j(\chi_i^n)}$ indicates the emission from the ith interferer in set $\mathcal{S}_n$. H_i^n is the Rayleigh fading channel between the ith interferer and the nth receive antenna, the other receive antennae do not observe interferer i. Since the interferers in set $\mathcal{S}_0$ are observed by all receive antennae, the Rayleigh fading channel between the interferer and the nth receive antenna is denoted by H_{n,i_0}^0. D_{n,i_n} denotes the distance between the ith interferer in set $\mathcal{S}_n$ and the receiver. γ is power path-loss parameter.
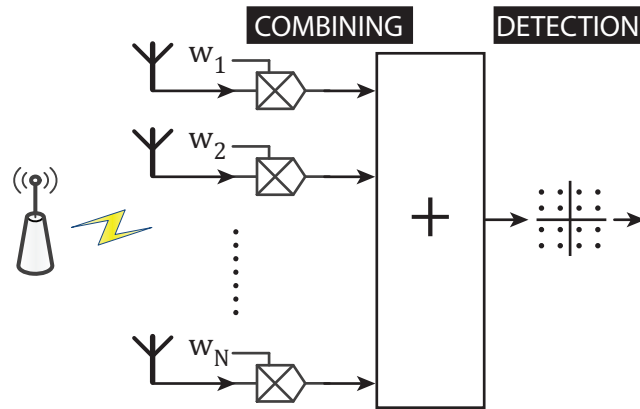
Figure 5.2: Block diagram of a receiver in which diversity combining is performed before symbol detection.

In the following sections, I derive the outage performance of various linear and non-linear diversity combining techniques. The expression for the outage probability of each receiver allows us to study the impact of network parameters such as interferer density, path-loss exponent, and interferer field correlation on outage performance.

5.5 Outage Performance of Conventional Linear Multi-Antenna Receivers

In this section, I evaluate the outage performance of linear diversity combining receivers, placed within a field of Poisson distributed interferers as described in Section 5.4. In such a receiver, the signal samples at the multiple receive antennae are linearly combined before symbol detection, as shown in Figure 5.2. During diversity combining, the signal output from each antenna

n is multiplied by a corresponding complex scalar weight w_n and the result is summed across all N receive antennae. The key behind different diversity combining schemes lies in the selection of the weights $w_i \ \forall \ i = 1, 2, \ldots, N$, henceforth denoted in vector form as the *weight vector* $\mathbf{w} = [w_1 \quad w_2 \quad \ldots \quad w_n]^T$. To maintain linearity, $\mathbf{w}$ is either a constant value, or depends on the channel $\mathbf{G}$ if the receiver has channel state information.

For a general weight vector $\mathbf{w}$, the output of the linear diversity combiner can be expressed as

$$v = \mathbf{w}^T \mathbf{R} \tag{5.3}$$

$$= s \sum_{n=1}^{N} w_n G_n + \sum_{n=1}^{N} w_n Z_n \tag{5.4}$$

$$= s \sum_{n=1}^{N} w_n G_n + \sum_{i_0 \in \mathcal{S}_0} \sum_{n=1}^{N} w_n B_{i_0}^0 D_{0,i_0}^{-\frac{\gamma}{2}} H_{n,i_0}^0 e^{j(\chi_{i_0}^0 + \Theta_{n,i_0}^0)} + \sum_{n=1}^{N} w_n \sum_{i \in \mathcal{S}_n} B_i^n D_{n,i}^{-\frac{\gamma}{2}} H_i^n e^{j(\chi_i^n + \Theta_i^n)} \tag{5.5}$$

$$= s \sum_{n=1}^{N} w_n G_n + \sum_{i_0 \in \mathcal{S}_0} B_{i_0}^0 D_{0,i_0}^{-\frac{\gamma}{2}} \sum_{n=1}^{N} w_n H_{n,i_0}^0 e^{j(\chi_{i_0}^0 + \Theta_{n,i_0}^0)} + \sum_{i \in \mathcal{S}_n} B_i^n D_{n,i}^{-\frac{\gamma}{2}} \sum_{n=1}^{N} w_n H_i^n e^{j(\chi_i^n + \Theta_i^n)}. \tag{5.6}$$

The SIR at combiner output can then be written as

$$\mathrm{SIR}_\mathbf{w} =$$
$$\frac{E_s \left| \sum_{n=1}^{N} w_n G_n \right|^2}{\left| \sum_{i_0 \in \mathcal{S}_0} B_{i_0}^0 D_{0,i_0}^{-\frac{\gamma}{2}} \sum_{n=1}^{N} w_n H_{n,i_0}^0 e^{j(\chi_{i_0}^0 + \Theta_{n,i_0}^0)} + \sum_{i \in \mathcal{S}_n} B_i^n D_{n,i}^{-\frac{\gamma}{2}} \sum_{n=1}^{N} w_n H_i^n e^{j(\chi_i^n + \Theta_i^n)} \right|^2}. \tag{5.7}$$

I define the outage probability as

$$P_\mathbf{w}^{\mathrm{out}}(\theta) = \mathbb{E}_{\mathrm{SIR}_\mathbf{w}} \left[\mathbb{P}(\mathrm{SIR}_\mathbf{w} < \theta) \right] \tag{5.8}$$

where θ is the SIR threshold for correct detection. The outage probability can then be written as

$$P_{\mathbf{w}}^{\text{out}}(\theta)$$

$$= \mathbb{E}\left[\mathbb{P}\left(E_s \left| \sum_{n=1}^{N} w_n G_n \right|^2 \times \right.\right.$$

$$\left.\left. \frac{1}{\left| \sum_{i_0 \in \mathbb{S}_0} B_{i_0}^0 D_{0,i_0}^{-\frac{\gamma}{2}} \sum_{n=1}^{N} w_n H_{n,i_0}^0 e^{j(\chi_{i_0}^0 + \Theta_{n,i_0}^0)} + \sum_{i \in \mathbb{S}_n} B_i^n D_{n,i}^{-\frac{\gamma}{2}} \sum_{n=1}^{N} w_n H_i^n e^{j(\chi_i^n + \Theta_i^n)} \right|^2} < \theta \right)\right] \tag{5.9}$$

$$= \mathbb{E}\left[\mathbb{P}\left(\left| \sum_{i_0 \in \mathbb{S}_0} B_{i_0}^0 D_{0,i_0}^{-\frac{\gamma}{2}} \sum_{n=1}^{N} w_n H_{n,i_0}^0 e^{j(\chi_{i_0}^0 + \Theta_{n,i_0}^0)} + \sum_{i \in \mathbb{S}_n} B_i^n D_{n,i}^{-\frac{\gamma}{2}} \sum_{n=1}^{N} w_n H_i^n e^{j(\chi_i^n + \Theta_i^n)} \right|^2 \right.\right.$$

$$\left.\left. > \frac{E_s \left| \sum_{n=1}^{N} w_n G_n \right|^2}{\theta} \right)\right] \tag{5.10}$$

$$= \mathbb{E}\left[\mathbb{P}\left(\left| \sum_{i_0 \in \mathbb{S}_0} B_{i_0}^0 D_{0,i_0}^{-\frac{\gamma}{2}} \sum_{n=1}^{N} w_n H_{n,i_0}^0 e^{j(\chi_{i_0}^0 + \Theta_{n,i_0}^0)} + \sum_{i \in \mathbb{S}_n} B_i^n D_{n,i}^{-\frac{\gamma}{2}} \sum_{n=1}^{N} w_n H_i^n e^{j(\chi_i^n + \Theta_i^n)} \right| \right.\right.$$

$$\left.\left. > \frac{E_s \left| \sum_{n=1}^{N} w_n G_n \right|}{\sqrt{\theta}} \right)\right]. \tag{5.11}$$

Since the union of independent Poisson Point Processes is another Poisson Point Process with intensity equal to the sum of intensities of the component processes[19], I can write (5.11) as

$$P_{\mathbf{w}}^{\text{out}}(\theta) = \mathbb{E}\left[\mathbb{P}\left(\left| \sum_{i \in \cup_{n=0}^{N} \mathbb{S}_n} x_i'(d_i')^{-\gamma/2} h_i' \right| > \frac{E_s \left| \sum_{n=1}^{N} w_n G_n \right|}{\sqrt{\theta}} \right)\right] \tag{5.12}$$

128

where d_i' is the distance from origin of each point (indexed by i) in the combined process, x_i' is a random variable indicating the interferer source emissions, and H_i' is a $N+1$ term complex Gaussian mixture random variable with variances $\|w\|^2\sigma_I^2, |w_1|^2\sigma_I^2, |w_2|^2\sigma_I^2, \ldots |w_N|^2\sigma_I^2$, and mixing probabilities $\frac{\lambda_0}{\sum_{n=0}^N \lambda_n}, \frac{\lambda_1}{\sum_{n=0}^N \lambda_n}, \ldots \frac{\lambda_n}{\sum_{n=0}^N \lambda_n}$, respectively. $\sum_{i\in \cup_{n=0}^N S_n} x_i'\|d_i'\|^{-\gamma}h_i'$ is a random variable that follows the isotropic symmetric alpha-stable distribution, as shown in Chapter 4. Using the ccdf of an isotropic symmetric alpha-stable random variable, I can express (5.12) as

$$P_{\mathbf{w}}^{\text{out}}(\theta) \approx \pi \left(\sum_{n=0}^N \lambda_n\right) \mathbb{E}\left[(x_0')^\alpha\right] \mathbb{E}\left[|H_0'|^\alpha\right] \mathbb{E}\left[\left(\frac{E_s\left|\sum_{n=1}^N w_n G_n\right|}{\sqrt{\theta}}\right)^{-\alpha}\right] \quad (5.13)$$

where $\alpha = \frac{4}{\gamma}$, and $\Gamma(\cdot)$ is the well-known Gamma function[3]. Note that the ccdf result used in (5.13) is an approximate result with low approximation error when θ is small, consequently, my results are useful in low-outage regimes. Next, I simplify (5.13) under the assumption that the fast-fading channel between transmitter and receiver, and interferer and receiver is a complex Gaussian random variable. Taking expectation over h_0' and $G_n \; \forall \; n = 1, \cdots, N$, I get

$$P_{\mathbf{w}}^{\text{out}}(\theta) \approx \pi 2^{\frac{\alpha}{2}}\Gamma(1+\frac{\alpha}{2})\mathbb{E}[X^\alpha]\left(\left(\sum_{n=1}^N \lambda_n|w_n|^\alpha\sigma_I^\alpha\right) + \lambda_0\|\mathbf{w}\|_2^\alpha\sigma_I^\alpha\right) \times$$

$$\mathbb{E}\left[\left(\frac{E_s\left|\sum_{n=1}^N w_n G_n\right|}{\sqrt{\theta}}\right)^{-\alpha}\right] \quad (5.14)$$

$$= \pi E_s^{-\alpha}\sigma_S^{-\alpha}\sigma_I^\alpha\Gamma(1+\frac{\alpha}{2})\Gamma(1-\alpha/2)\mathbb{E}[X^\alpha]\frac{\sum_{n=1}^N \lambda_n|w_n|^\alpha + \lambda_0\|\mathbf{w}\|_2^\alpha}{\|\mathbf{w}\|_2^\alpha}\theta^{\frac{\alpha}{2}}. \quad (5.15)$$

129

From (5.15), I can make intuitively satisfying observations such as the outage probability is directly proportional to the detection SIR threshold θ, and interferer density λ_n ($n = 0, 1, \ldots, N$), whereas it is inversely proportional to the signal power E_s. The following subsections analyze the outage probability for some typical diversity combining receivers.

5.5.1 Linear Receivers Lacking Channel Information

Fixed Weight Combining: A receiver with no channel state information and no knowledge of interference statistics may choose to use the same weight on all antennae outputs. The outage probability for a receiver using a weight vector **w** is provided in (5.15). In fixed weight diversity combining, **w** remains constant and independent from the received signal. If all the weights are equal to 1, the outage performance of such a scheme is given as

$$P_{\text{FWC}}^{\text{out}}(\theta) \approx \pi E_s^{-\alpha} \sigma_S^{-\alpha} \sigma_I^{\alpha} \Gamma(1 + \frac{\alpha}{2}) \Gamma(1 - \alpha/2) \mathbb{E}[X^{\alpha}] \frac{\sum_{n=1}^{N} \lambda_n + \lambda_0 N^{\frac{\alpha}{2}}}{N^{\frac{\alpha}{2}}} \theta^{\frac{\alpha}{2}}. \qquad (5.16)$$

I consider a reasonable scenario where the intensity of each of the interferer sets $\mathcal{S}_n \ \forall \ n = 1, \ldots, N$ is equal to λ_e. Applying to (5.16), I get

$$P_{\text{FWC}}^{\text{out}}(\theta) \approx \pi E_s^{-\alpha} \sigma_S^{-\alpha} \sigma_I^{\alpha} \Gamma(1 + \frac{\alpha}{2}) \Gamma(1 - \alpha/2) \mathbb{E}[X^{\alpha}] (\lambda_e N^{1 - \frac{\alpha}{2}} + \lambda_0) \theta^{\frac{\alpha}{2}}. \qquad (5.17)$$

From (5.17), I can deduce that the common set of interferers does not provide any diversity gain in outage performance, while interference from the independent set of interferers actually worsens outage performance upon increasing the number of receive antennae. This reduction in outage performance is due to *interference diversity* where increasing the number of receive antennae increases

130

the chances that one of them might be suffering from an impulsive interference event which corrupts the entire combiner output. Also note that when interference statistics are close to Gaussian distribution the $N^{1-\frac{\alpha}{2}}$ term disappears and the combiner has no diversity gain or loss, a well-known fact [23] which acts as a confirmation of my results.

Random Antenna Selection: Another receiver with no channel state information may simply choose to decode a receive antenna at random. Thus the weight vector is a random vector with a single element equal to 1 and the remaining elements equal to zero. Using $\mathbf{1}_n$ to denote a vector with the nth element equal to 1 and remaining elements equal to 0, the outage probability of the random antenna selection receiver is

$$P_{RAS}^{\text{out}}(\theta) = \sum_{n=1}^{N} \frac{P_{\mathbf{w}=\mathbf{1}_n}^{\text{out}}(\theta)}{N} \tag{5.18}$$

$$= \sum_{n=1}^{N} \pi E_s^{-\alpha} \sigma_S^{-\alpha} \sigma_I^{\alpha} \Gamma(1+\frac{\alpha}{2}) \Gamma(1-\alpha/2) \mathbb{E}\left[X^\alpha\right](\lambda_n + \lambda_0) \theta^{\frac{\alpha}{2}} \tag{5.19}$$

$$= \pi E_s^{-\alpha} \sigma_S^{-\alpha} \sigma_I^{\alpha} \Gamma(1+\frac{\alpha}{2}) \Gamma(1-\alpha/2) \mathbb{E}\left[X^\alpha\right] \left(\sum_{n=1}^{N} \frac{\lambda_n}{N} + \lambda_0 \right) \theta^{\frac{\alpha}{2}}. \tag{5.20}$$

5.5.2   Linear Receivers With Channel Information

Maximum Ratio Combining: In this diversity combining technique, the receiver chooses a weight vector directly proportional to the channel conjugate and inversely proportional to interference power. Assuming *i.i.d.* interferer emissions and *i.i.d.* fading between interferer and receiver, the interference power at each antenna would be proportional to $\lambda_0 + \lambda_n$. Thus the nth element of the

131

combining weight vector w_n would be given by $w_n = \frac{G_n^*}{\lambda_0 + \lambda_n}$. Again assuming that $\lambda_n = \lambda_e \ \forall \ n$, and inserting the MRC weight vector into (5.14), the outage probability of MRC combining can be expressed as

$$P_{\text{MRC}}^{\text{out}}(\theta) \approx \pi \sigma_I^\alpha 2^{\frac{\alpha}{2}} \Gamma(1 + \frac{\alpha}{2}) \mathbb{E}[X^\alpha] \mathbb{E}\left[\frac{\sum_{n=1}^N \lambda_n |G_n|^\alpha + \lambda_0 \|\mathbf{G}\|^\alpha}{\|\mathbf{G}\|^{2\alpha}}\right] \theta^{\frac{\alpha}{2}} \tag{5.21}$$

$$= \pi E_s^{-\alpha} \sigma_I^\alpha 2^{\frac{\alpha}{2}} \Gamma(1 + \frac{\alpha}{2}) \mathbb{E}[X^\alpha] \mathbb{E}\left[\frac{\sum_{n=1}^N \lambda_n |G_n|^\alpha}{\|\mathbf{G}\|_2^{2\alpha}} + \frac{\lambda_0}{\|\mathbf{G}\|_2^\alpha}\right] \theta^{\frac{\alpha}{2}}. \tag{5.22}$$

For the special case where intensities of the independent set of interferers $\lambda_n (n = 1, \ldots, N)$ are equal to λ_e, I can compact (5.21) to

$$P_{\text{MRC}}^{\text{out}}(\theta) \approx \pi E_s^{-\alpha} \sigma_I^\alpha 2^{\frac{\alpha}{2}} \Gamma(1 + \frac{\alpha}{2}) \mathbb{E}[X^\alpha] \mathbb{E}\left[\frac{\lambda_e \|\mathbf{G}\|_\alpha^\alpha}{\|\mathbf{G}\|_2^{2\alpha}} + \frac{\lambda_0}{\|\mathbf{G}\|_2^\alpha}\right] \theta^{\frac{\alpha}{2}} \tag{5.23}$$

Note that channel diversity does provide some improvement in outage performance, especially in the case of isotropic interference. By setting $\lambda_e = 0$, the MRC outage probability reduces to

$$P_{\text{MRC,isotropic}}^{\text{out}}(\theta) \approx \pi E_s^{-\alpha} \sigma_I^\alpha 2^{\frac{\alpha}{2}} \Gamma(1 + \frac{\alpha}{2}) \mathbb{E}[X^\alpha] \mathbb{E}\left[\frac{\lambda_0}{\|\mathbf{G}\|_2^\alpha}\right] \theta^{\frac{\alpha}{2}} \tag{5.24}$$

Noting that $\|\mathbf{G}\|_2^2$ is a sum of exponentially distributed random variables, which in turn follows the Erlang density distribution. Thus, the $\frac{-\alpha}{2}^{\text{th}}$ moment of $\|\mathbf{G}\|_2^2$ can be substituted in (5.24), yielding

$$P_{\text{MRC,isotropic}}^{\text{out}}(\theta) \approx \pi E_s^{-\alpha} \sigma_I^\alpha 2^{\frac{\alpha}{2}} \Gamma(1 + \frac{\alpha}{2}) \mathbb{E}[X^\alpha] \frac{\lambda_0 2^{\frac{-\alpha}{2}} \Gamma(N - \frac{\alpha}{2})}{\Gamma(N)} \theta^{\frac{\alpha}{2}} \tag{5.25}$$

The spatially isotropic interference model is used in [83] to derive the outage probability for maximum ratio combining. [83] models statistics of received interference power as compared to this dissertation that models received amplitude statistics. The MRC outage probability in this dissertation (eq. (5.25)) and

132

the MRC outage probability expression derived in [83] (Theorem 1) are identical in their linear dependence on the interferer intensity λ, and their dependence on $\theta^{\alpha/2}$, where θ is the SIR threshold. The contrasting terms arise in the terms involving number of antennae N; while (5.25) contains $\frac{\Gamma(N-\frac{\alpha}{2})}{\Gamma(N)}$ in the derived expression, [83] contains $\left(1 + \sum_{n=1}^{N-1} \frac{1}{n!} \prod_{k=0}^{n-1} \left(k - \frac{\alpha}{2}\right)\right)\Gamma(1-\alpha/2)$ in the derived expression. While these two terms look dissimilar, numerical evaluation shows that these expressions are identical. Thus, the outage probability expressions in this dissertation and [83] lead to the same result via different approaches.

Equal Gain Combining: In this diversity combining technique, the receiver chooses a weight vector with each element having an absolute value of 1 and the same phase as the channel conjugate. Thus, in essence the receiver is only estimating the channel phase and ensuring that the signals from the multiple antennae are combined in a phase coherent manner. The nth element of the combining weight vector w_n would be given by $w_n = \frac{G_n^*}{|G_n|}$. Substituting this weight vector into (5.14), the outage probability of EGC combining can be expressed as

$$P_{\text{EGC}}^{\text{out}}(\theta) \approx \pi E_s^{-\alpha} \sigma_I^\alpha 2^{\frac{\alpha}{2}} \Gamma(1-\alpha/2) \mathbb{E}\left[X^\alpha\right] \mathbb{E}\left[\frac{\left(\sum_{n=1}^N \lambda_n\right) + N^{\frac{\alpha}{2}} \lambda_0}{\|\mathbf{G}\|_1^\alpha}\right] \theta^{\frac{\alpha}{2}}. \qquad (5.26)$$

Note that channel diversity does provide some improvement in outage performance, especially in the case of isotropic interference.

Selection Combining: Selection combining is a technique where the receiver chooses to decode the signal from one antenna. The advantages of selection combining are that no gain and phase multiplication block is needed

133

in the receiver hardware, at the cost of negatively impacting the communication performance since the signal energy from other antennae is not used. In the pre-detection diversity combining setting, I study the sub-optimal selection combiner which selects the receive antenna with the strongest channel. In this combiner, the weight vector has value 1 at the antenna with the strongest channel and value 0 for the rest. Using this weight vector, I can write the output of the diversity combiner as

$$v = \mathbf{w}^T \mathbf{y} \tag{5.27}$$

$$= s\frac{|G_n|^2}{\lambda_0 + \lambda_n} + \frac{G_n z_n}{\lambda_0 + \lambda_n} \tag{5.28}$$

$$= sG_m + Z_m \tag{5.29}$$

where index m indicates the index of the receiver with the strongest channel; i.e., $|G_m|^2 \geq |G_n|^2 \; \forall n = 1, 2, \ldots, N$. The outage probability can simply be written as

$$P_{\text{SC}}^{\text{out}}(\theta) \approx \pi E_s^{-\alpha} \sigma_I^\alpha \Gamma(1 - \alpha/2) \mathbb{E}\left[X^\alpha\right] \left(\sum_{n=0}^{N} \frac{\lambda_n + \lambda_0}{N}\right) \mathbb{E}\left[|G_m|^{-\alpha}\right] \theta^{\frac{\alpha}{2}} \tag{5.30}$$

$$= \pi \left(\frac{\sigma_I}{E_s \sigma_S}\right)^\alpha \Gamma(1 + \alpha/2) \Gamma(1 - \alpha/2) \mathbb{E}\left[X^\alpha\right] \left(\sum_{n=0}^{N} \frac{\lambda_n + \lambda_0}{N}\right) \times$$

$$\left(\sum_{m=0}^{N} (-1)^{m+1} \binom{N}{m} m^{\frac{\alpha}{2}}\right) \theta^{\frac{\alpha}{2}}. \tag{5.31}$$

5.6 Outage Performance of Non-Linear Receivers

In Section 5.5, I evaluated outage performance for receivers implementing a weighted combiner, as shown in Figure 5.2. In this section, I evaluate the
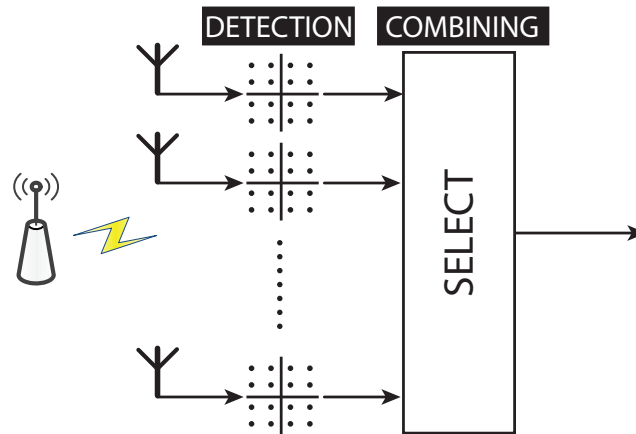
Figure 5.3: Block diagram of a receiver in which diversity combining is performed after symbol detection.

outage performance for a receiver that implements selection combining after performing detection. Such a receiver attempts to detect the transmitted signal individually at each antenna and then selects the output based on the post-detection SIR. The block diagram for this receiver is shown in Figure 5.3. This receiver has higher complexity since it implements a detection block for each antenna as opposed to the receiver in Figure 5.2 which implements only one detection block. I assume that the SIR estimate obtained at the receiver after detection at antenna n is the true SIR, in other words $\text{SIR}_n = \frac{|G_n|^2}{|z_n|^2}$, which provides us with a lower bound on the outage performance. Under these conditions, such a receiver would be in outage when the per-antenna SIR is below the detection threshold at every antenna. The probability of this event can be expressed as

$$P_{\text{PDC}}^{\text{out}} = \mathbb{P}\{\text{SIR}_1 < \theta, \text{SIR}_2 < \theta, \ldots, \text{SIR}_N < \theta\}$$

$$= \mathbb{E}\left[\mathbb{P}\left\{\frac{E_s |G_1|^2}{\left|\sum_{i_0 \in \mathcal{S}_0} B_{i_0}^0 D_{0,i_0}^{-\frac{\gamma}{2}} H_{1,i_0}^0 e^{j(\chi_{i_0}^0 + \Theta_{1,i_0}^0)} + \sum_{i \in \mathcal{S}_1} B_i^1 D_{1,i}^{-\frac{\gamma}{2}} H_i^1 e^{j(\chi_i^1 + \Theta_i^1)}\right|^2} < \theta, \right.\right.$$

$$\left.\left.\ldots, \frac{E_s |G_N|^2}{\left|\sum_{i_0 \in \mathcal{S}_0} B_{i_0}^0 D_{0,i_0}^{-\frac{\gamma}{2}} H_{n,i_0}^0 e^{j(\chi_{i_0}^0 + \Theta_{N,i_0}^0)} + \sum_{i \in \mathcal{S}_n} B_i^N D_{N,i}^{-\frac{\gamma}{2}} H_i^n e^{j(\chi_i^N + \Theta_i^N)}\right|^2} < \theta\right\}\right] \quad (5.32)$$

$$= \mathbb{E}\left[\mathbb{P}\left\{|G_1|^2 < \frac{\theta \left|\sum_{i_0 \in \mathcal{S}_0} B_{i_0}^0 D_{0,i_0}^{-\frac{\gamma}{2}} H_{n,i_0}^0 e^{j(\chi_{i_0}^0 + \Theta_{n,i_0}^0)} + \sum_{i \in \mathcal{S}_n} B_i^n D_{n,i}^{-\frac{\gamma}{2}} H_i^n e^{j(\chi_i^n + \Theta_i^n)}\right|^2}{E_s}, \right.\right.$$

$$\left.\left.\ldots, |G_N|^2 < \frac{\theta \left|\sum_{i_0 \in \mathcal{S}_0} B_{i_0}^0 D_{0,i_0}^{-\frac{\gamma}{2}} H_{n,i_0}^0 e^{j(\chi_{i_0}^0 + \Theta_{N,i_0}^0)} + \sum_{i \in \mathcal{S}_N} B_i^N D_{N,i}^{-\frac{\gamma}{2}} H_i^N e^{j(\chi_i^N + \Theta_i^N)}\right|^2}{E_s}\right\}\right]$$

$$(5.33)$$

$$= \mathbb{E}\left[\prod_{n=1}^N \left(1 - e^{\frac{\theta}{E_s}\left|\sum_{i_0 \in \mathcal{S}_0} B_{i_0}^0 D_{0,i_0}^{-\frac{\gamma}{2}} H_{n,i_0}^0 e^{j(\chi_{i_0}^0 + \Theta_{n,i_0}^0)} + \sum_{i \in \mathcal{S}_n} B_i^n D_{n,i}^{-\frac{\gamma}{2}} H_i^n e^{j(\chi_i^n + \Theta_i^n)}\right|^2}\right)\right] \quad (5.34)$$

$$\approx \mathbb{E}\left[\prod_{n=1}^N \left(1 - e^{\sum_{i_0 \in \mathcal{S}_0} (B_{i_0}^0)^2 D_{0,i_0}^{\gamma}\left|H_{n,i_0}^0\right|^2 + \sum_{i \in \mathcal{S}_n} (B_i^n)^2 D_{n,i}^{-\gamma}\left|H_i^n\right|^2}\right)\right]. \quad (5.35)$$

I proceed by setting the number of receive antennae, $N = 2$, in order to facilitate brevity and comprehension of this derivation. Later, I will provide the outage probability for any number of receive antennae. Assuming $N = 2$, I can

136

expand (5.34) as

$$
P_{\text{PDC}}^{\text{out}} = 1 - \mathbb{E}\left[e^{\frac{\theta}{E_s}\sum_{i_0\in\mathcal{S}_0}(B_{i_0}^0)^2 D_{0,i_0}^\gamma\left|H_{1,i_0}^0\right|^2+\sum_{i\in\mathcal{S}_1}(B_i^1)^2 D_{1,i}^{-\gamma}\left|H_i^1\right|^2}\right]
$$

$$
- \mathbb{E}\left[e^{\frac{\theta}{E_s}\sum_{i_0\in\mathcal{S}_0}(B_{i_0}^0)^2 D_{0,i_0}^\gamma\left|H_{2,i_0}^0\right|^2+\sum_{i\in\mathcal{S}_2}(B_i^2)^2 D_{2,i}^{-\gamma}\left|H_i^2\right|^2}\right]
$$

$$
+ \mathbb{E}\left[e^{\frac{\theta}{E_s}\sum_{i_0\in\mathcal{S}_0}(B_{i_0}^0)^2 D_{0,i_0}^\gamma\left(\left|H_{1,i_0}^0\right|^2+\left|H_{2,i_0}^0\right|^2\right)+\sum_{i\in\mathcal{S}_1}(B_i^1)^2 D_{1,i}^{-\gamma}\left|H_i^1\right|^2+\sum_{i\in\mathcal{S}_2}(B_i^2)^2 D_{2,i}^{-\gamma}\left|H_i^2\right|^2}\right].
$$

$$(5.36)$$

Taking expectation over H, I get

$$
P_{\text{PDC}}^{\text{out}} = 1 - \mathbb{E}\left[\frac{\theta}{E_s}\prod_{i_0\in\mathcal{S}_0}\left(1+\sigma_I^2\left|B_{0,i_0}\right|^2 D_{0,i_0}^{-\gamma}\right)^{-1}\prod_{i_1\in\mathcal{S}_n}\left(1+\sigma_I^2\left|B_{1,i_1}\right|^2 D_{1,i_1}^{-\gamma}\right)^{-1}\right]
$$

$$
- \mathbb{E}\left[\frac{\theta}{E_s}\prod_{i_0\in\mathcal{S}_0}\left(1+\sigma_I^2\left|B_{0,i_0}\right|^2 D_{0,i_0}^{-\gamma}\right)^{-1}\prod_{i_2\in\mathcal{S}_2}\left(1+\sigma_I^2\left|B_{2,i_2}\right|^2 D_{2,i_2}^{-\gamma}\right)^{-1}\right]
$$

$$
+ \mathbb{E}\left[\frac{\theta}{E_s}\prod_{i_0\in\mathcal{S}_0}\left(1+\sigma_I^2\left|B_{0,i_0}\right|^2 D_{0,i_0}^{-\gamma}\right)^{-2}\prod_{i_1\in\mathcal{S}_n}\left(1+\sigma_I^2\left|B_{1,i_1}\right|^2 D_{1,i_1}^{-\gamma}\right)^{-1}\times\right.
$$

$$
\left.\prod_{i_2\in\mathcal{S}_2}\left(1+\sigma_I^2\left|B_{2,i_2}\right|^2 D_{2,i_2}^{-\gamma}\right)^{-1}\right].
$$

$$(5.37)$$

Using the point generating functional property of Poisson point processes[61], I can write the outage probability $P_{\text{PDC}}^{\text{out}}$ as

$$
P_{\text{PDC}}^{\text{out}} = \mathbb{E}\left[1 - e^{(\lambda_0+\lambda_1)\int_{\mathbf{t}\in\mathbb{R}}1-\left(1+\frac{\theta X^2}{E_s}\|t\|^{-\gamma}\right)^{-1}d\mathbf{t}} - e^{(\lambda_0+\lambda_2)\int_{\mathbf{t}\in\mathbb{R}}1-\left(1+\frac{\theta X^2}{E_s}\|t\|^{-\gamma}\right)^{-1}d\mathbf{t}}\right.
$$

$$
\left.+ e^{\lambda_1\int_{\mathbf{t}\in\mathbb{R}}1-\left(1+\frac{\theta X^2}{E_s}\|t\|^{-\gamma}\right)^{-1}d\mathbf{t}}e^{\lambda_2\int_{\mathbf{t}\in\mathbb{R}}1-\left(1+\frac{\theta X^2}{E_s}\|t\|^{-\gamma}\right)^{-1}d\mathbf{t}}e^{\lambda_0\int_{\mathbf{t}\in\mathbb{R}}1-\left(1+\frac{\theta X^2}{E_s}\|t\|^{-\gamma}\right)^{-2}d\mathbf{t}}\right].
$$

$$(5.38)$$

After integration and subsequent simplification, and noting that in a low outage regime the operand in the exponential is close to 0, I get an approximation of the

137

outage probability as

$$P_{\text{PDC}}^{\text{out}} = \frac{(1-\alpha/2)\alpha\pi^2}{\sin(\alpha\pi)}\lambda_0\theta^{\alpha/2} + \left(\frac{\alpha\pi^2}{4\sin(\alpha\pi)}\right)^2(\lambda_0+\lambda_1)(\lambda_0+\lambda_2)\theta^\alpha \qquad (5.39)$$

(5.39) shows the contribution to the outage probability from the interferer set $\mathcal{S}_0$ and the interferer sets $\mathcal{S}_n$ for $n = 1,\ldots,N$. Extending this result to an N antenna receiver is simple but leads to a more involved outage probability expression. The outage probability expression is a summation of terms containing $\theta^{k\alpha/2}$ with $k = 1,\ldots,N$. The $\theta^{\alpha/2}$ term is the outage component purely due to interferers from $\mathcal{S}_0$, the $\theta^{N\alpha/2}$ term is purely due to interferers from $\mathcal{S}_n$ for $n = 1,\ldots,N$, and the $\theta^{k\alpha2}$ terms are due to interference from all the sets $\mathcal{S}_n$ for $n = 0,\ldots,N$. I approximate the outage probability by keeping only the $\theta^{\alpha/2}$ and $\theta^{N\alpha/2}$ terms and ignoring the rest. The justification is that when $\lambda_0 \neq 0$, the $\theta^{\alpha/2}$ term dominates the overall sum, and when $\lambda_0 = 0$, the outage probability reduces to contain only the $\theta^{N\alpha/2}$ term. Thus, by continuing the derivation from (5.34) for $N > 2$ and keeping only the two significant terms, I get the outage probability as

$$P_{\text{PDC}}^{\text{out}} = \sum_{m=1}^{N}\left(\binom{N}{m}\frac{(-1)^{m+1}(m-1+\alpha/2)!\alpha\pi^2}{4(m-1)!\sin(\alpha\pi)}\right)\lambda_0\theta^{\alpha/2} +$$
$$\left(\frac{\alpha\pi^2}{4\sin(\alpha\pi)}\right)^N\prod_{n=1}^{N}(\lambda_0+\lambda_n)\theta^{N\alpha/2} \qquad (5.40)$$

It is important to note that full diversity order is achieved if there are no common interferers, however, there is no diversity gain in PDC when interference is spherically isotropic.

138

Table 5.1: Parameter values used in simulations.

Parameter	Description	Value
λ_{tot}	Per-antenna total intensity of interferers	0.001
γ	Power path-loss exponent	3.5
$\overline{B}$	Mean amplitude of interferer emissions	1.0
σ_H	Variance of in-phase and quadrature components of the fading channel	1.0

5.7   Simulation Results

To validate my outage probability derivations, I numerically simulate a multi-antenna receiver located within a field of Poisson distributed interferers. I transmit a $16-$QAM signal and interference is simulated according to the system model described in Section 5.4. Incorrect symbol detection is considered an outage event and the outage probability is calculated accordingly. Based on the average signal energy and modulation index, the effective SIR threshold for correct detection can be calculated and plugged into the derived outage probability expressions to compare with simulated results. Table 5.1 lists the various parameter values used in simulations.

Figure 5.4 shows the impact of spatial dependence on outage probability of the various diversity combining receivers with channel state information. In Figure 5.4, the intensities of interferer sets observable by a single antenna $(\lambda_i, i = 1, \dots, N)$ are set to the same value, denoted by λ_e. Further, $\lambda_0 + \lambda_e$ is set to a fixed value 0.001, so that the total interference observed by each antenna has the same power. Varying λ_0 from 0.0 to 0.001 essentially changes the interference statistics from spatially independent to spherically isotropic. It is easy to see that

increasing spatial dependence in interference negatively impacts the communication performance of all receiver algorithms. In interference with low spatial dependence, PDC receiver has the best performance, while the other pre-detection receivers still show poor performance. This shows that exploiting channel diversity may not compensate for impulsive events. The proposed pre-detection diversity algorithm however shows much better outage performance compared to the typical pre-detection diversity algorithms. It thus provides a good trade-off between communication performance and computational complexity.

Figures 5.5, 5.6, and 5.7 show the impact of receive antennae on outage probability for receivers with channel state information, and Figures 5.8, 5.9, and 5.10 show the impact of receive antennae on outage probability for receivers without channel state information (and the MRC receiver added as a benchmark). In Figures 5.5 and 5.8, I simulate spatially independent interference by setting $\lambda_0 = 0$ and $\lambda_e = 0.001$. In Figures 5.6 and 5.9, I set $\lambda_e = 0$ and $\lambda_0 = 0.001$ to simulate spherically isotropic interference. It is interesting to see that the diversity gain is lost in all algorithms in the presence of spherically isotropic interference. In Figure 5.7 and 5.10 I simulate partial spatial dependence by setting $\lambda_0 = 5 \times 10^{-5}$ and $\lambda_e = 9.5 \times 10^{-4}$. Even a low amount of spatial dependence can severely reduce the diversity gain in interference. In all of these figures, I see that the theoretical expressions derived in Sections 5.5 and 5.6 match very well to the simulated receiver. The theoretical expressions are useful as they allow us to analyze the impact of parameters such as γ diversity performance of typical multi-antenna receivers.

140

Figure 5.4: Outage probability vs. λ_0 for equal gain combining (EGC), maximal ratio combining (MRC), selection combining (SC), and post-detection combining (PDC) in a 3−antenna receiver. The symbols indicate the theoretical outage probability ('Expr'), whereas the lines indicate the simulated outage probability ('Sim'). $\lambda_e = 10^{-3} - \lambda_0$.

Figure 5.5: Outage probability vs. number of receive antennae for for equal gain combining (EGC), maximal ratio combining (MRC), selection combining (SC), and post-detection combining (PDC) in presence of spatially independent interference. The symbols indicate the theoretical outage probability ('Expr'), whereas the lines indicate the simulated outage probability ('Sim'). Parameter values $\lambda_0 = 0, \lambda_e = 10^{-3}$ are used in simulations.

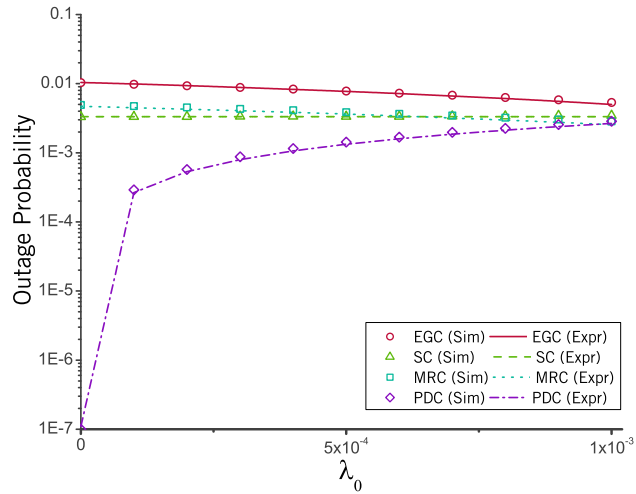Figure 5.6: Outage probability vs. number of receive antennae for for equal gain combining (EGC), maximal ratio combining (MRC), selection combining (SC), and post-detection combining (PDC) in presence of spherically isotropic interference. The symbols indicate the theoretical outage probability ('Expr'), whereas the lines indicate the simulated outage probability ('Sim'). Parameter values $\lambda_0 = 10^{-3}, \lambda_e = 0$ are used in simulations.
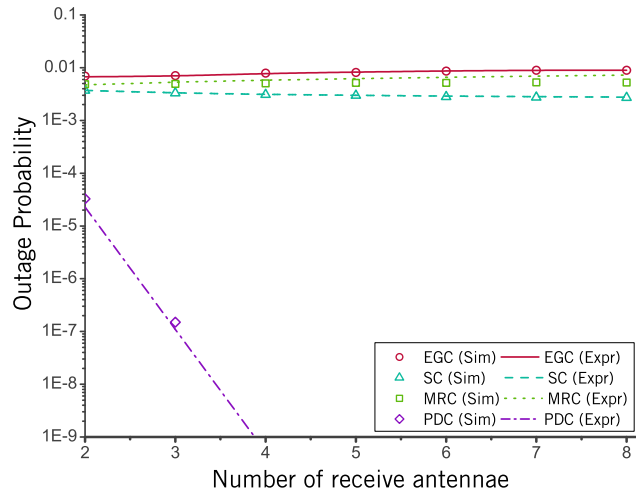
Figure 5.7: Outage probability vs. number of receive antennae for equal gain combining (EGC), maximal ratio combining (MRC), selection combining (SC), and post-detection combining (PDC) in presence of partially spatially dependent interference. The symbols indicate the theoretical outage probability ('Expr'), whereas the lines indicate the simulated outage probability ('Sim'). $\lambda_0 = 5 \times 10^{-5}, \lambda_e = 9.5 \times 10^{-4}$ are used in simulations.
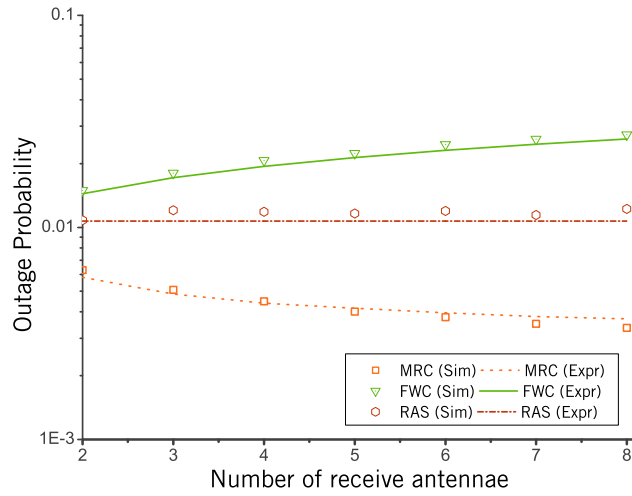
Figure 5.8: Outage probability vs. number of receive antennae for maximal ratio combining (MRC), fixed weight combining (FWC), and random antenna selection (RAS) in presence of spatially independent interference. The symbols indicate the theoretical outage probability ('Expr'), whereas the lines indicate the simulated outage probability ('Sim'). Parameter values $\lambda_0 = 0, \lambda_e = 10^{-3}$ are used in simulations.
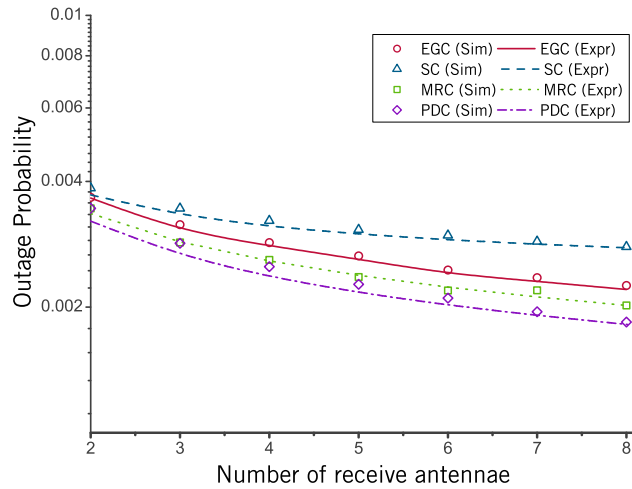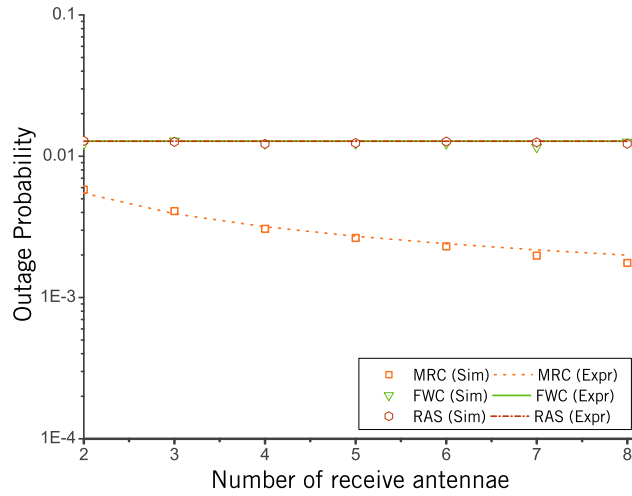
Figure 5.9: Outage probability vs. number of receive antennae for maximal ratio combining (MRC), fixed weight combining (FWC), and random antenna selection (RAS) in presence of spherically isotropic interference. The symbols indicate the theoretical outage probability ('Expr'), whereas the lines indicate the simulated outage probability ('Sim'). Parameter values $\lambda_0 = 10^{-3}, \lambda_e = 0$ are used in simulations.
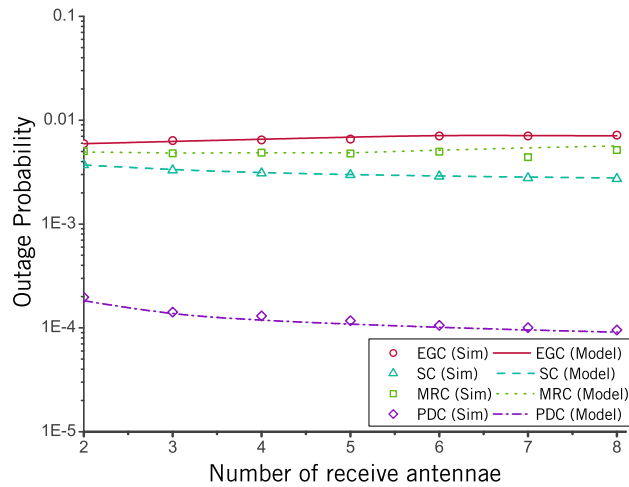
146
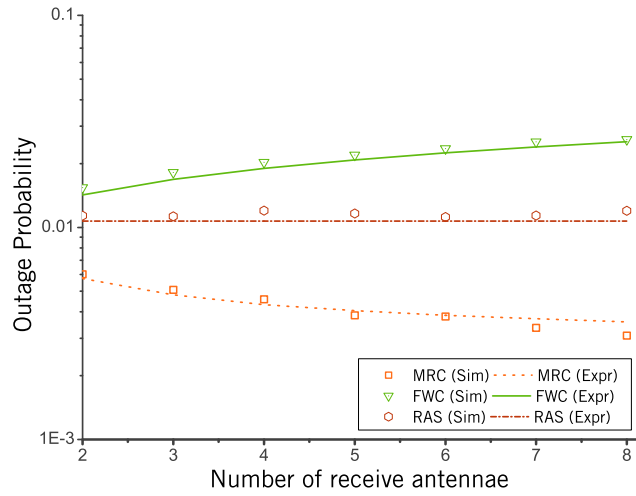
Figure 5.10: Outage probability vs. number of receive antennae for maximal ratio combining (MRC), fixed weight combining (FWC), and random antenna selection (RAS) in presence of partially spatially dependent interference. The symbols indicate the theoretical outage probability ('Expr'), whereas the lines indicate the simulated outage probability ('Sim'). $\lambda_0 = 5 \times 10^{-5}, \lambda_e = 9.5 \times 10^{-4}$ are used in simulations.

147

5.8 Conclusion

In this chapter, I derived outage probability expressions for different diversity combining algorithms in the presence of interference, such as equal gain combining, fixed weight combining, maximum ratio combining, selection combining, and post-detection combining. From Chapter 4, I used a framework to model spatially dependent wireless interference with joint statistics in a continuum from spatially independent interference to spherically isotropic interference. While this framework can be used to model interference in common scenarios which usually fall at either extreme of this continuum, it provides a key advantage when modeling scenarios which fall within the continuum.

The post-detection diversity combiner exhibits significantly better outage performance compared to the pre-detection diversity combining receivers. In spatially independent interference, the post-detection combiner achieves full diversity order in outage performance. This diversity order is quickly lost upon increasing spatial dependence in interference observed across receiver antennae. The post-detection combiner suffers from high computational complexity requirements as it requires a symbol decoding block for each receiver antenna, compared to the pre-detection combiner which requires one symbol decoding block regardless of the number of receiver antennae. My results can inform analysis of communication performance vs. computational complexity tradeoffs of multi-antennae receivers designed to operate in the presence of impulsive interference.

In the next chapter, I use the statistical framework of spatially depen-

dent interference, and develop two novel diversity combining algorithms which improve upon the outage performance of pre-detection diversity combining receivers, while using the same amount of computational complexity. In Chapter 4, I showed that this statistical framework also captures antenna separation in a Poisson field of interferers. In the next chapter, I use this framework to develop antenna selection strategies in distributed antenna receivers operating in interference-limited networks.

Chapter 6

Receiver Design in Interference-Limited Wireless Networks

6.1 Introduction

The recent increase in the density of users in wireless networks and increasing demand for high data rates motivates the design of multi-antenna wireless transceivers that are robust to interference. Wireless receivers have typically been designed and their performance analyzed under the assumption of Gaussian distributed additive noise[23]. While thermal noise at the receiver certainly exhibits Gaussian statistics[92, 126, 142], interference at the receiver from external sources is also assumed to exhibit Gaussian statistics due to the Central Limit Theorem[103].

In Chapters 3 and 4, I developed a statistical-physical model of interferer distribution, interference generation and propagation, in centralized and decentralized wireless networks, respectively. From this statistical-physical framework, I derived the joint and marginal statistics of interference observed by wireless receivers placed in a randomly distributed field of interferers. In particular, I showed that joint interference statistics across receiver antennae are either isotropic, independent, or lie in a continuum between the isotropic and

independent. Subsequently in Chapter 5, I analyzed the communication performance of conventional linear multi-antenna signal combining algorithms in the presence of non-Gaussian interference.

Using accurate statistical models of interference from Chapters 3 and 4, I develop novel algorithms for multi-antenna signal combining as well as cooperative antenna selection in the presence of interference. In this chapter, I propose new wireless receiver algorithms that offer significant improvement in communication performance in interference-limited channels.

6.2 Contributions, Organization, and Notation

In Section 6.3, I propose new non-linear diversity combiners and evaluate their performance in the presence of spatially dependent interference. In Section 6.3, I propose novel strategies for distributed antenna selection in the presence of interference. These two sections represent two different areas in wireless communication systems where accurate statistical models of interference can facilitate design of better receivers. Within each of these sections, I present a short survey of prior work on the subject, a detailed discussion on the novel receiver algorithm, and numerical simulations to demonstrate improved communication performance of the proposed algorithms in face of interference.

6.3 Receiver Design in Interference

In Chapter 5, I evaluated the performance of several multi-antenna combining algorithms in the presence of interference. The performance analysis results indicated that the post-detection combining receiver can outperform pre-detection diversity combining algorithms in the presence of impulsive interference, especially when interference exhibits low spatial dependence across receive antennae. However, the post-detection combiner is impractical to implement as it assumes perfect knowledge of SIR at the receiver, and practical versions of the algorithm require deploying multiple signal decoding blocks in the receiver hardware as shown in Figure 5.3. In this section, I propose alternative pre-detection diversity combining algorithms are designed with the knowledge that interference is impulsive in nature.

6.3.1 Background and Prior Work

The design of detection and estimation strategies in impulsive noise has been an active area of research[4]. Interference in many wireless networks has been well modeled to exhibit impulsive statistics, typically using the symmetric alpha stable distribution. Prior work has typically focused on single antenna receiver design in the presence of additive alpha stable distributed interference.

In the seminal work on signal detection in alpha stable noise[156, 158], the authors studied a multitude of linear and non-linear detectors in alpha stable noise for a single antenna receiver. This work was complemented by [155] with incoherent detection techniques in alpha stable noise, and [157] with parameter

estimation algorithms for alpha stable noise. Many suboptimal detectors have also been proposed for detection in alpha stable noise[100, 101, 106, 122].

In [22], the authors propose receivers with decision feedback equalizers to improve wireless communication performance in symmetric alpha stable distributed interference. As is usually the case in the presence of symmetric alpha stable noise, much of the receiver performance can be attributed to non-linear blanking, or clipping filters in the receive chain. In [123] and [124], the authors derive the BER optimal receivers for CDMA communication systems in the presence of alpha stable noise. These combiner algorithms assume statistically independent noise samples across the various combining paths.

Since the probability density function of the alpha stable distribution is not known for most values of the α parameter, optimal detectors are hard to find. If $\alpha = 1$, however, the probability density function has a known closed-form expression[140], consequently, the optimal detector is well known. The optimal detector, also known as the Cauchy detector, is practical to implement for binary signal schemes such as BPSK. While it is optimal only when $\alpha = 1$, it has been applied for different values of α[50].

The filter structures proposed in prior work are limited in applicability to multi-antenna wireless receivers due to lack of statistical-physical generation based interference models. In particular, there is little prior work that considers spatial dependence in interference across receive antennas, which is a key factor in multi-antenna interference. Analyzing the effect of such spatial dependence on typical receiver algorithms is relevant to improving the communication per-

153

formance of wireless receivers in frequency selective fading.

6.3.2   System Model

6.3.3   Linear Receivers Without Channel Information

Assuming that the receiver has knowledge of interference statistics, I can choose **w** to minimize the outage probability as

$$P_{\text{FWC}}^{\text{out}}(\theta) = \frac{4}{\sqrt{\pi}\cos(\frac{\pi\alpha}{4})} E_s^{-\alpha} \sigma_S^{-\alpha} \sigma_I^{\alpha} \Gamma(\frac{1+\alpha}{2}) \Gamma(1-\alpha/2) \mathbb{E}[X^{\alpha}] \theta^{\frac{\alpha}{2}} \times$$
$$\min_{\mathbf{w}\in\mathbb{R}^N} \left\{ \frac{\sum_{n=1}^{N} \lambda_n w_n^{\alpha} + \lambda_0 \|w\|_2^{\alpha}}{\|\mathbf{w}\|_2^{\alpha}} \right\}. \tag{6.1}$$

(6.1) attains its minimum value when the receiver selects the antenna with the minimum average interference power. Since interference power is directly proportional to the intensity, I can write (6.1) as

$$P_{\text{FWC}}^{\text{out}}(\theta) = \frac{4}{\sqrt{\pi}\cos(\frac{\pi\alpha}{4})} E_s^{-\alpha} \sigma_S^{-\alpha} \sigma_I^{\alpha} \Gamma(\frac{1+\alpha}{2}) \Gamma(1-\alpha/2) \mathbb{E}[X^{\alpha}] \theta^{\frac{\alpha}{2}} \min_{n=1,\dots,N} \{\lambda_n + \lambda_0\}. \tag{6.2}$$

6.3.4   Linear Receivers With Channel Information

In this section, I attempt to derive linear receivers which minimize outage probability. First, I analyze the two extreme scenarios of spatially independent and spatially isotropic interference. In spatially isotropic interference, $\lambda_n = 0 \ \forall$

$n > 0$, consequently, I can write the outage probability as

$$P_{\mathbf{w}}^{\text{out}}(\theta) \approx \frac{4\Gamma(1-\alpha/2)}{\cos(\frac{\pi\alpha}{4})} 2^{\frac{\alpha}{2}} \Gamma(\frac{1+\alpha}{2}) \mathbb{E}[X^\alpha] \left(\lambda_0 \|\mathbf{w}\|_2^\alpha \sigma_I^\alpha \right) \times$$
$$\mathbb{E}\left[\left(\frac{E_s \left| \sum_{n=1}^N w_n G_n \right|}{\sqrt{\theta}} \right)^{-\alpha} \right]. \tag{6.3}$$

The appropriate weight vector $\mathbf{w}_{\text{iso}}^{\text{opt}}$ that minimizes this outage probability is given as

$$\mathbf{w}_{\text{iso}}^{\text{opt}} = \arg\min_{\mathbb{R}^n} \frac{\|\mathbf{w}\|_2^\alpha}{\left| \sum_{n=1}^N w_n G_n \right|^\alpha} \tag{6.4}$$

$$= \arg\min_{\mathbb{R}^n} \frac{\|\mathbf{w}\|_2}{\left| \sum_{n=1}^N w_n G_n \right|} \tag{6.5}$$

Using the Cauchy-Schwarz inequality, the optimum value of $\mathbf{w}_{\text{iso}}^{\text{opt}}$ is the conjugate of the channel vector $\mathbf{G}^*$. Thus, the MRC weighting vector is the optimum linear combiner in isotropic interference.

If interference in spatially independent across receive antennae, the outage probability can be evaluated by setting $\lambda_0 = 0$ in (5.14), yielding

$$P_{\mathbf{w}}^{\text{out}}(\theta) \approx \frac{4\Gamma(1-\alpha/2)}{\cos(\frac{\pi\alpha}{4})} 2^{\frac{\alpha}{2}} \Gamma(\frac{1+\alpha}{2}) \mathbb{E}[X^\alpha] \left(\sum_{n=1}^N \lambda_n w_n^\alpha \sigma_I^\alpha \right) \times$$
$$\mathbb{E}\left[\left(\frac{E_s \left| \sum_{n=1}^N w_n G_n \right|}{\sqrt{\theta}} \right)^{-\alpha} \right]. \tag{6.6}$$

and consequently, the optimum weight vector is given by

$$\mathbf{w}_{\text{ind}}^{\text{opt}} = \arg\min_{\mathbb{R}^n} \frac{\|\mathbf{w}\|_\alpha^\alpha}{\left| \sum_{n=1}^N w_n G_n \right|^\alpha}. \tag{6.7}$$

155

Using Cauchy-Schwarz inequality and Holders inequality, I can write

$$\left| \sum_{n=1}^{N} w_n G_n \right| \leq \sum_{n=1}^{N} |w_n G_n| \tag{6.8}$$

$$\leq \|\mathbf{w}\|_\alpha \|\mathbf{G}\|_{\frac{\alpha}{\alpha-1}} \tag{6.9}$$

$$\tag{6.10}$$

which is equivalent to

$$\frac{\|\mathbf{w}\|_\alpha}{\left| \sum_{n=1}^{N} w_n G_n \right|} \geq \frac{1}{\|\mathbf{G}\|_{\frac{\alpha}{\alpha-1}}} \tag{6.11}$$

Note that Holders inequality can be applied only if $\alpha > 1$. Substituting $w_n = G_n^* |G_n|^{\frac{2-\alpha}{\alpha-1}}$ into (6.11), the left and the right sides of the equation become equal. Thus the optimal linear combiner weight vector can be derived for $\alpha > 1$.

Deriving the optimal weight vector for alpha stable interference with joint statistics in a continuum between isotropic and independent is not mathematically tractable. However, I can lower bound the optimal linear receiver outage probability as

$$P_{\text{OPT}}^{\text{out}}(\theta) \geq P_{\text{IND}}^{\text{out}}(\theta) + P_{\text{ISO}}^{\text{out}}(\theta) \tag{6.12}$$

where $P_{\text{IND}}^{\text{out}}(\theta)$ and $P_{\text{ISO}}^{\text{out}}(\theta)$ are the outage probability components from the independent and isotropic components of interference, respectively. Figure 6.1 shows the outage performance of the optimal linear combiner in the presence of spatially independent interference. The optimal combiner offers very little reduction in outage probability compared to the MRC combiner. Since the optimal combiner for spatially isotropic interference is the MRC combiner, the lower bound on the outage probability for spatially dependent interference should be

156
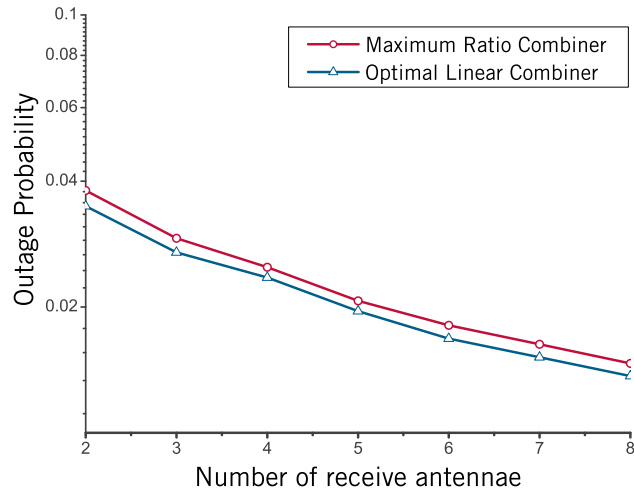
Figure 6.1: Outage probability vs. number of receiver antennae for optimal linear combiner in spatially independent interference. $\lambda_e = 0$, $\gamma = 3$, and $\lambda_0 = 0.001$.

very close to the outage probability of the MRC combiner. This indicates that there is little benefit to be obtained by developing a optimal linear combiner for symmetric alpha stable interference with joint statistics that are in a continuum between isotropic and spatially independent. Thus, in the next section, I study non linear receivers in the presence of interference.

6.3.5   Non-Linear Receivers

6.3.5.1   Hard-Limiting Combiner

Conventional pre-detection diversity combiners, discussed in Chapter 5, do not distinguish between an antenna suffering from an impulsive interference event and an antenna observing a non-impulsive interference event. Diversity combining only utilizes spatial independence of fast fading across the multiple receive antennae to mitigate the impact of deep channel fades on one of the an-

157

tennae.

I propose a multi-antenna combiner that first attempts to detect whether an antenna is observing an impulsive event, and if so, removes the signal from that antenna from the combining block. Thus the combiner decides a 'hard limit' within which an receive antenna's contribution must lie. The weight vector of this combiner is written as

$$w_n^{HL} = \begin{cases} h_n^* & \text{if} \quad \|y_n - \text{median}(\mathbf{y})\| \leq \tau \\ 0 & \text{if} \quad \|y_n - \text{median}(\mathbf{y})\| \geq \tau \end{cases}. \tag{6.13}$$

The receiver assumes that an impulsive interference event has occurred if the sample at an antenna is significantly deviated from the median of the all the receive antenna samples. In signal processing with impulsive noise, the median is often used as a metric to denote the typical value of a signal[118]. If the data sample is determined as non-impulsive, then the receiver uses the MRC algorithm for incorporating channel diversity into combining, otherwise the sample from that antenna does not contribute to the combiner output.

Note that the HL combiner uses a parameter τ to determine the range within which a receive antenna's signal can deviate from the median. If $\tau = 0$, the combiner essentially becomes a spatial median filter, whereas $\tau \rightarrow \infty$ would cause the receiver to act as a conventional MRC combiner. It is non-trivial to derive the best possible value of τ given the noise parameters. However, τ should depend on the parameters α, σ_0, and σ_n.

Consider the case where interference is independent across the receive antennae. It is well known that the MRC combiner is optimal in the presence

158

of Gaussian distributed noise, therefore for $\alpha = 2$, $\tau \to \infty$ is the best possible parameter setting. On the other hand, as $\alpha \to 0$, noise becomes extremely impulsive and the median filter ($\tau \to 0$) is the optimal filter[68].

6.3.5.2   Soft-Limiting Combiner

The hard-limiting combiner completely removes an antenna from the diversity combination process if it detects the presence of an interference impulse event. The soft-limiting combiner, on the other hand, gradually reduces the weighting of an antenna if it estimates an impulse event at the antenna. The soft-limiting weight vector is given as

$$w_n^{SL} = e^{-\eta \|y_n - \text{median}(\mathbf{y})\|} h_n^*. \tag{6.14}$$

Here the MRC combining algorithm is modified to reduce the weight of an antenna if its received signal deviates highly from the signals at other antennae. Unlike the hard-limiting combiner, this algorithm gradually reduces the signal weight as the signal becomes more impulsive. If $\eta = 0$, this combiner reduces to the MRC algorithm, while $\eta \to \infty$ converts it into a median antenna selector.

Both diversity combiners are suboptimal modifications to the MRC receiver. These combiners are non-linear in nature and derivation of their outage probability expressions is mathematically intractable. Subsequently, evaluating the optimal value of parameters τ and η is also difficult and would make for an interesting subject of future work. Practical implementations of these receivers is also a interesting problem as it would require tracking τ and η based on im-

159

Table 6.1: Parameter values used in simulations.

Parameter	Description	Value
λ_{tot}	Per-antenna total intensity of interferers	0.001
γ	Power path-loss exponent	3
$\overline{B}$	Mean amplitude of interferer emissions	1.0
σ_H	Variance of in-phase and quadrature components of the fading channel	1.0

pulsive noise parameter estimation[132].

6.3.6   Numerical Simulations

Using the parameters from Table 6.1, I show the outage performance of my proposed algorithms in Figure 6.2 and 6.3. I can observe that at low spatial dependence in interference my proposed algorithms outperform the other pre-detection diversity combining receivers. Consequently, these algorithms may be used as an alternative to the computationally intensive post-detection combining receiver.

6.4   Cooperative Antenna Selection in Interference-Limited Networks

In this section, I apply interference modeling to improve communication performance of relay assisted wireless networks. As discussed in Chapter 1, the introduction of relays in wireless networks can yield improvements in communication performance, and lower costs such as power usage[129, 160]. Relays, however, are not immune to the impairments of wireless communications such as the fading channel[160], and interference. In the following subsections,

Figure 6.2: Outage probability vs. λ_0 for maximal ratio combining (MRC), post-detection combining (PDC), and the novel hard-limiting (HL) and soft-limiting (SL) combiners in a 3−antenna receiver. $\lambda_e = 10^{-3} - \lambda_0$, $\tau = 1$, and $\eta = 1$.

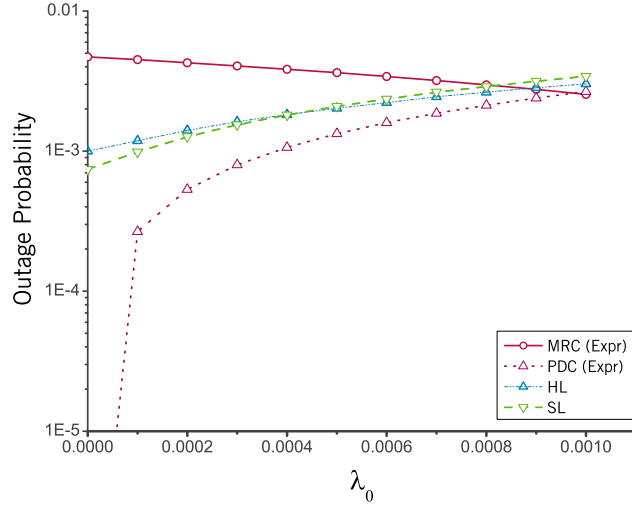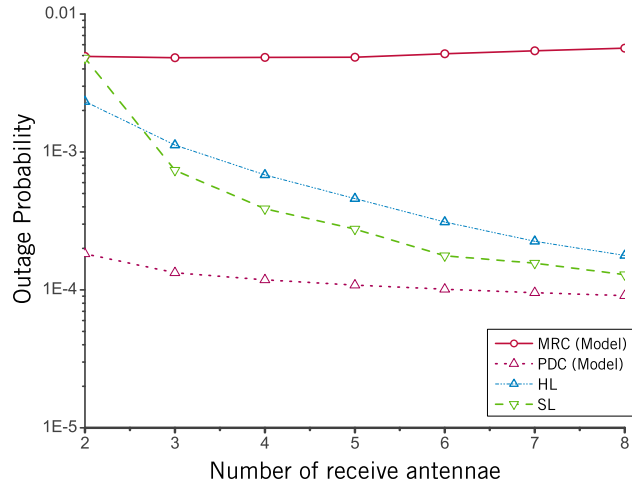Figure 6.3: Outage probability vs. number of receive antennae for maximal ratio combining (MRC), post-detection combining (PDC), and the novel hard-limiting (HL) and soft-limiting (SL) combiners in presence of partially spatially dependent interference. $\lambda_0 = 5 \times 10^{-5}, \lambda_e = 9.5 \times 10^{-4}$, $\tau = 1$, and $\eta = 1$ are used in simulations.

161

I derive joint interference statistics across a wireless receiver and its assisting relay. Subsequently, the joint interference statistics are used in deriving the outage probability of relay-assisted reception, and I derive a relay-selection strategy to minimize power usage of the assisting relay.

6.4.1 Background

Typical relay assisted communication systems assume that relays are situated between the source and the destination, consequently, the destination is expected to receive more reliable information from the relays than from the source.

Prior work in cooperative reception focuses primarily on improve transmission capacity by mitigating the impact of deep channel fades between the source and the destination. For example, in [117] the authors analyze tradeoffs between various relay-forwarding strategies, such as AF, DF and hybrid DF strategy that forwards the relay signal only when relay decoding is reliable. Other research focuses on using relays to improve channel diversity[160], or suppress interference[63, 117, 151, 160] via receive side cancellation[20], or transmit side alignment[151]. Interference is usually assumed to be Gaussian distributed.

In [35], the authors consider a symmetric alpha stable model of interference in a two-hop amplify and forward cooperative reception scheme. Interference at the relay and the destination nodes is individually modeled as a symmetric alpha stable random variable, while the joint statistics of interference are ignored.

6.4.2 System model and List of Assumptions

In this section, I describe a interference-limited distributed antenna wireless communication system via the following assumptions:

Assumption 6.1. *A base-station $\mathcal{W}_S$ intends to communicate information to a receiver $\mathcal{W}_D$.*

Assumption 6.2. *The location of $\mathcal{W}_D$ is fixed at origin.*

Assumption 6.3. *As the wireless signal traverses through the environment, its energy decays according to the power-law path-loss model [65] with a coefficient of γ.*

Assumption 6.4. *The fast-fading channel between the transmitting source and the receiver as well as other interfering sources and the receiver is modeled using the Rayleigh distribution[65].*

Assumption 6.5. *Additive thermal noise is ignored at the receiver.*

Assumption 6.6. *Interferers are distributed in the two-dimensional plane around the receiver.*

The set $\mathcal{S}_I$ contains all *interfering* users distributed randomly in space. At each sampling time instant, the locations of the active interferers in $\mathcal{S}_I$ are distributed according to a homogeneous spatial Poisson Point Process in the two dimensional plane around the receiver. The intensity of set $\mathcal{S}_I$ is denoted by λ_I.

Assumption 6.7. *Cooperating antennae are distributed in the two-dimensional plane around the receiver.*

The set $\mathcal{S}_R$ contains all *non-transmitting* users also distributed randomly in space as a two dimensional Poisson point process with intensity λ_R. The intensity of set $\mathcal{S}_R$ is denoted by λ_R.

Assumption 6.8. *The destination receiver $\mathcal{W}_D$ can employ any other cooperating antenna from $\mathcal{S}_R$ to help it decode the signal. This assisting node, or relay, is denoted by $\mathcal{W}_R$.*

Assumption 6.9. *$\mathcal{W}_D$ and $\mathcal{W}_R$ can estimate the state of the fading channel between themselves and the transmitter.*

However, $\mathcal{W}_D$ does not know the channel state of $\mathcal{W}_R$. On the other hand, $\mathcal{W}_D$ has knowledge of the distances between it and cooperating antennae in $\mathcal{S}_R$.

Assumption 6.10. *The overhead associated with selecting another user to cooperatively receive the transmitted signal is neglected.*

Assumption 6.11. *Atleast one of the receiver node or relay node must decode the signal correctly for successful transmission.*

If both the nodes receive the signal incorrectly, a retransmission request is sent to the transmitter. The signal is transmitted again, until either the relay or destination node are able to decode it correctly. The receiver or the relay can correctly decode the signal if the SIR is greater than a fixed threshold.

Assumption 6.12. *There is a cost associated with every re-transmission between the $\mathcal{W}_R$ and $\mathcal{W}_D$.*
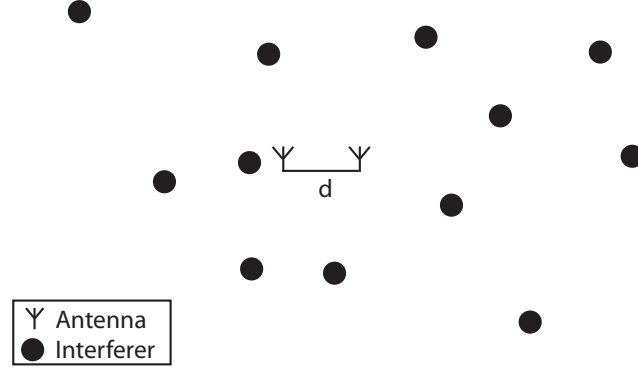
Figure 6.4: System model of two distributed antennae in a Poisson field of interferers.

This cost is denoted using the function $\mathcal{C}(d)$, where d is the distance between $\mathcal{W}_R$ and $\mathcal{W}_D$. A simple example of this cost function is power usage at the relay. Due to power-law pathloss through the medium, the relay to destination transmission uses power proportional d^γ; i.e., $\mathcal{C}(d) = C_P d^\gamma$, where C_P is a constant. In wireless systems, typically this cost function $\mathcal{C}(d)$ increases as the distance d increases. Figure 6.4 shows a realization of this system model.

6.4.3   Antenna Selection to Minimize Relay Power Consumption

The receiver $\mathcal{W}_R$ observes interference from all interfering users in $\mathcal{S}_I$. The sum interference at $\mathcal{W}_R$ can be expressed as

$$Z_{\mathcal{W}_R} = \sum_{i \in \mathcal{S}_I} B_i e^{j\chi_i} \|\mathbf{R}_i\|^{-\frac{\gamma}{2}} H_i e^{j\Theta_i}. \tag{6.15}$$

$Z_{\mathcal{W}_R}$ is the sum of interfering signals $B_i e^{j\chi_i}(D_i)^{-\frac{\gamma}{2}} H_i e^{j\Theta_i}$ emitted by each interferer $i \in \mathcal{S}_I$ located at $\mathbf{R}_i$. $B_i e^{j\chi_i}$ denotes emissions from interfering user i where B_i is the emission signal envelope and χ_i is the phase of the emission. γ is the

165

power pathloss coefficient ($\gamma > 2$), consequently, $\|\mathbf{R}_i\|^{-\frac{\gamma}{2}}$ indicates the energy loss during propagation through the wireless medium. $H_i e^{j\Theta_i}$ denotes the complex fast-fading channel between the interferer and destination. For the fast fading channel model, I assume that the channel amplitude H_i follows the Rayleigh distribution, and that the channel phase Θ_i is uniformly distributed on $[0, 2\pi]$. H_i, Θ_i, B_i, and χ_i are assumed to be *i.i.d.* across all interfering sources $i \in \mathcal{S}_T$.

The receiver $\mathcal{W}_D$ employs one non-transmitting node from $\mathcal{S}_R$, known as the relay node $\mathcal{W}_R$ in order to aid in signal reception. Consequently, the sum interference from the transmitters surrounding the relay node $\mathcal{W}_R$ can be written as

$$Z_{\mathcal{W}_R} = \sum_{i \in \mathcal{S}_I} B_i e^{j\chi_i} \|\mathbf{R}_i - \mathbf{R}_{\mathcal{W}_R}\|^{-\frac{\gamma}{2}} H_i' e^{j\Theta_i'}. \tag{6.16}$$

Here, $\mathbf{R}_{\mathcal{W}_R}$ denotes the location of the relay node. H' and Θ' are the fast fading channels between the relay node and the transmitter node, which are independent to fast fading channel between the transmitter and the destination node. The joint characteristic function of interference across $\mathcal{W}_D$ and $\mathcal{W}_R$ can be written as

$$\Phi_{\mathcal{W}_D, \mathcal{W}_R}(\omega_D, \omega_R) = \mathbb{E}\left\{ e^{\omega_{D,I} Z_{\mathcal{W}_D,I} + \omega_{D,Q} Z_{\mathcal{W}_D,Q} + \omega_{R,I} Z_{\mathcal{W}_R,I} + \omega_{R,Q} Z_{\mathcal{W}_R,Q}} \right\} \tag{6.17}$$

where $Z_{\mathcal{W}_D,I}$ and $Z_{\mathcal{W}_D,Q}$ represent the in-phase and quadrature components of $Z_{\mathcal{W}_D}$, respectively. $Z_{\mathcal{W}_R,I}$ and $Z_{\mathcal{W}_R,Q}$ represent the in-phase and quadrature components of $Z_{\mathcal{W}_D}$, respectively. ω_D and ω_R are the frequency parameters of the joint characteristic function $\Phi_{\mathcal{W}_D, \mathcal{W}_R}(\omega_D, \omega_R)$. $\omega_{D,I}$ and $\omega_{D,Q}$ are the real and imag-

166

inary components of ω_D, respectively. $\omega_{R,I}$ and $\omega_{R,Q}$ are the real and imaginary components of ω_R, respectively.

In Chapter 4, I derived the joint interference statistics across two distributed antennae. Using the results from (4.54), the joint characteristic function of interference across $\mathcal{W}_D$ and $\mathcal{W}_R$ can be expressed as

$$\Phi_{\mathcal{W}_D, \mathcal{W}_R}(\omega_D, \omega_R) = e^{-\sigma_0(1 - e^{-a(\gamma)\|\mathbf{R}_{\mathcal{W}_R}\|^{b(\gamma)}})(|\omega_D|^{4/\gamma} + |\omega_R|^{4/\gamma}) - \sigma_0(e^{-a(\gamma)\|\mathbf{R}_{\mathcal{W}_R}\|^{b(\gamma)}})(|\omega_D|^2 + |\omega_R|^2)^{2/\gamma}}$$

(6.18)

The parameter values for $a(\gamma)$ and $b(\gamma)$ are shown in Section 4.6. In the wireless system model described in Section 6.4.2, an outage occurs when both the relay and destination node are unable to correctly detect the signal. Assuming a SIR threshold requirement to correctly decode the transmitted signal, the outage probability in this system is given as

$$P^{\text{out}} = \mathbb{P}\{\text{SIR}_D < \theta, \text{SIR}_D < \theta\}$$

(6.19)

where SIR_D denotes the signal-to-interference ratio at the destination receiver $\mathcal{W}_D$, SIR_R denotes the signal-to-interference ratio at the assisting relay $\mathcal{W}_R$, and θ denotes the threshold for correct signal detection. From (5.39) this outage probability is given as

$$\begin{aligned}
P^{\text{out}} &= \mathbb{P}\{\text{SIR}_D < \theta, \text{SIR}_D < \theta\} \\
&= \frac{(1 - \alpha/2)\alpha\pi^2}{\sin(\alpha\pi)} \sigma_0 (e^{-a(\gamma)\|\mathbf{R}_{\mathcal{W}_R}\|^{b(\gamma)}}) \theta^{\alpha/2} + \left(\frac{\alpha\pi^2}{4\sin(\alpha\pi)}\right)^2 \sigma_0^2 \theta^\alpha
\end{aligned}$$

(6.20)

The cost of using the relay can be expressed as the number of re-transmissions that are needed in order for the receiver to correctly decode the transmitted signal, times the per transmission cost. This is given as

$$N_{TX} = \mathcal{C}(d)(1 - P^{\text{out}}) + 2\mathcal{C}(d)(P^{\text{out}})(1 - P^{\text{out}}) + 3\mathcal{C}(d)(P^{\text{out}})^2(1 - P^{\text{out}}) + \dots \quad (6.21)$$

$$= \mathcal{C}(d)\frac{1}{(1 - P^{\text{out}})^2} \quad (6.22)$$

Using relay transmit power as an example, the cost function can be defined as $\mathcal{C}(d) = P_0 + P_d d^{gamma}$. Applying the cost function definition in (6.22), the excess power usage at the relay can be expressed as

$$P_{\mathcal{W}_D} = \mathcal{C}(d)\frac{1}{(1 - P^{\text{out}})} \quad (6.23)$$

$$= \mathcal{C}(d)\frac{1}{1 - \frac{(1 - \alpha/2)\alpha\pi^2}{\sin(\alpha\pi)}\sigma_0(e^{-a(\gamma)\|\mathbf{R}_{\mathcal{W}_R}\|^{b(\gamma)}})\theta^{\alpha/2} + \left(\frac{\alpha\pi^2}{4\sin(\alpha\pi)}\right)^2\sigma_0\theta^{\alpha}} \quad (6.24)$$

$$= P_0 d^{\gamma}\frac{1}{1 - \frac{(1 - \alpha/2)\alpha\pi^2}{\sin(\alpha\pi)}\sigma_0(e^{-a(\gamma)\|\mathbf{R}_{\mathcal{W}_R}\|^{b(\gamma)}})\theta^{\alpha/2} + \left(\frac{\alpha\pi^2}{4\sin(\alpha\pi)}\right)^2\sigma_0\theta^{\alpha}} \quad (6.25)$$

using the power law model for relay transmission power. Clearly, there exists an optimum distance at which the relay should be located in order to minimize this excess power. In the network model described in Section 6.4.2, the relay nodes are also distributed randomly as a spatial Poisson point process. Therefore, the destination node must select a cooperative relay which is expected to be closest to the optimum location. Given that the relays are distributed as a Poisson point process with intensity λ_R, the distance d between the receiver and the kth nearest relay follows the distribution

$$f(d; k) = e^{-\lambda_0\pi d^2}\left(2\lambda_0\pi d\sum_{i=0}^{k-1}\frac{(\lambda_0\pi d^2)^k}{k!} - \sum_{i=1}^{k-1}\frac{2(\lambda_0\pi)^k d^{2k-1}}{(k-1)!}\right) \quad (6.26)$$

168
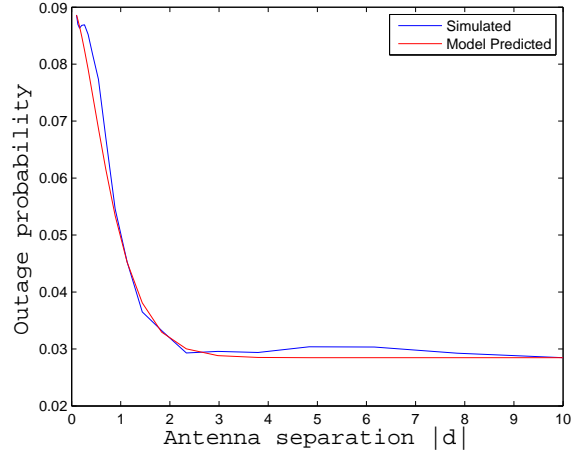
Figure 6.5: Outage probability vs. distance between two physically separate antennae. The intensity of signal emitting interferers $\lambda_T = 0.1$.

Thus, the expected power usage of choosing the kth nearest neighbor as the cooperating node is given as

$$P_k = \int_0^\infty P_{\mathcal{W}_D, \|\mathbf{R}_{\mathcal{W}_R}\| = d} f(d; k) \mathrm{d}d \qquad (6.27)$$

and the proposed selection algorithm selects the k^* nearest neighbor, such that

$$k^* = \arg\min_{k \in \mathbb{N}^+} P_k. \qquad (6.28)$$

6.5 Conclusions

This chapter demonstrates the advantages of incorporating interference statistics into receiver design for wireless systems in interference-limited networks. In the first example, multi-antenna receivers are improved by adding a filtering component to the receiver that removes, or reduces the strength of sig-

169

nals that are determined to be corrupted by impulsive component of interference. Interference statistics are also applied in designing cooperative reception strategies. Using accurate joint statistics of interference, I showed that antenna selection strategies can reduce power usage in cooperative communications.

Chapter 7

Conclusions

Interference in wireless communications has become a significant impairment, limiting network throughput and user density in wireless networks. In the face of exponentially increasing demand for wireless Internet data accessible by mobile users, interference mitigation has become a very active area of research. In this dissertation, I focus on the problem of interference mitigation in wireless networks and propose the following thesis statement:

Accurate statistical modeling of interference observed by multi-antenna wireless receivers facilitates design of multi-antenna wireless systems with significant improvement in communication performance in interference-limited networks.

My contributions towards defending this thesis statement are listed in the following section.

7.1   Summary

In this dissertation, I derive closed-form interference statistics to analyze and improve the communication performance of multi-antenna wireless receivers in interference-limited networks. There is extensive literature on statis-

171

tical models of interference observed by a single antenna in a variety of wireless networks. Prior work on statistics of multi-antenna interference has been limited to using multi-dimensional extensions of the single antenna statistical models.

The specific contributions of this dissertation towards improving communication performance of wireless networks are as follows:

In Chapter 3, I propose a statistical-physical framework for interference generation and propagation to a multi-antenna wireless receiver located within a field of randomly distributed interferers. I assume that the wireless receiver is part of a centralized network, such that a coordinating central authority limits the interferers to be located outside of a interferer-free *guard zone* around the receiver. I also allow interferers to be observed by either one antenna, or all antennae in the wireless receiver. I show that my proposed framework results in joint statistics of interference that are distributed as either isotropic Middleton Class A, independent Middleton Class A, or a mixture of the two.

In Chapter 4, I start with the statistical-physical network model proposed in Chapter 3, and remove the assumption of a interferer-free guard zone around the receiver. This network model is well applicable to decentralized, or *ad hoc* networks, where communicating devices are free to transmit data without regard to the interference caused to their neighbors. Such a framework is also useful in modeling interference from non-communicating devices such as computational platforms. I show that my proposed framework results in joint statistics of interference that are distributed as either isotropic symmetric alpha stable, independent symmetric alpha stable, or a mixture of the two. Furthermore, I

172

derive the statistics of interference in a wireless receiver with two antennae that are distributed in space. I show that the joint interference statistics are isotropic symmetric alpha stable, independent symmetric alpha stable, or a mixture of the two when the receiver antennae are colocated, infinitely far apart, or finitely separated, respectively. Thus, I have proposed a single generalized framework that can model interference in colocated as well as distributed antennae receivers.

In Chapter 5, I derive closed form expressions for communication performance of typical multi-antenna receivers in interference-limited network environments. I use the statistical-physical framework of interference generation in order to link network parameters to interference statistics. Accurate communication performance analysis can provide insight into the robustness of different multi-antenna receiver algorithms to interference.

In Chapter 6, I use interference statistics to improve the performance of multi-antenna wireless receivers. First, I add a non-linear spatial filtering block to conventional diversity combining receivers in order to increase their robustness against impulsive interference. Next, I analyze the communication performance and power cost of cooperative reception in the presence of interference. Using accurate statistics of interference in distributed antennae, I am able to derive the optimal distance between cooperating antennae. These results inform improved antenna selection strategies for mesh networks employing cooperating receiver nodes.

7.2   Future Work

In this section, I enumerate possible avenues of future research.

- *Interference statistics in a non-Poisson distributed field of interferers* The assumption of homogeneous Poisson distributed interferer locations is typically made for two reasons; (1) it provides analytical tractability in derivations, and (2) it has the highest entropy of a spatial Point Process and therefore yields very robust results. However, in realistic wireless networks, MAC protocols may break the homogeneity of interferer distribution, and the distribution of users may not be well modeled by Poisson Point Processes simply due to user clustering. There exists prior literature on deriving closed form statistics of interference using non-Poisson Point Process models of interferer distribution. It should be interesting to extend these models to deriving statistics of multi-antenna interference, which should intuitively follow the same isotropic and independent mixture model as proposed in this dissertation.

- *Interference statistics with more realistic pathloss function*

  In this dissertation, I assumed the power law pathloss model for interference propagation. While the power law pathloss model is very realistic at relatively large propagation distances, it may not be very accurate for interferers arising close to the wireless receiver. Incorporating realistic pathloss models into deriving interference statistics is a interesting avenue for future research. Another possible change to the pathloss model can be the

174

use of a random pathloss exponent. In many communication scenarios, especially indoor communications, pathloss can be modeled well using power law decay with random coefficients.

- *Interference statistics across two distributed antennae in centralized wireless networks*

  In this dissertation, I derived approximate statistics of interference in two physically separate wireless antennae in decentralized networks. A very useful extension of this work would be to derive joint interference statistics in centralized wireless networks; i.e., wireless networks with interferer-free guard zones around the receiver. A key aspect to deriving interference statistics would be to first define what a guard zone is in a distributed antenna system. One could develop three possible models: (1) the guard zone is a circular region with the two antennae located symmetrically about the center of the circle, (2) the guard zone is a circular region with one antenna located at the center, and the other antenna located within the circle, and (3) the guard zone is a circular region with both antennae located within this circle. Figures 7.1, 7.2, and 7.3 describe the guard zone models 1, 2, and 3, respectively.

- *Interference statistics across more than two distributed antennae in decentralized wireless network*

  In this dissertation, I derive joint statistics of interference for only two distributed antennae. A natural extension to this work would be extending

175

Figure 7.1: System model 1 of a receiver with 2 distributed antennae in a field of randomly distributed interferers in a centralized wireless network.

Figure 7.2: System model 2 of a receiver with 2 distributed antennae in a field of randomly distributed interferers in a centralized wireless network.
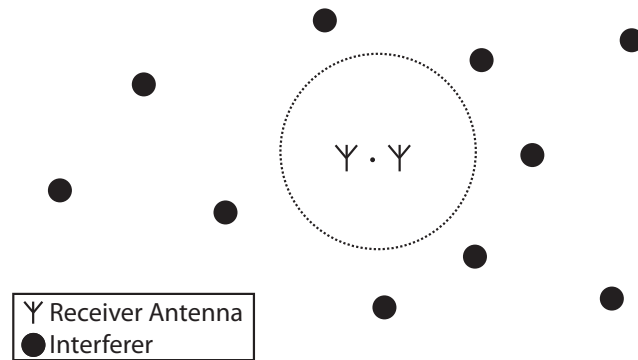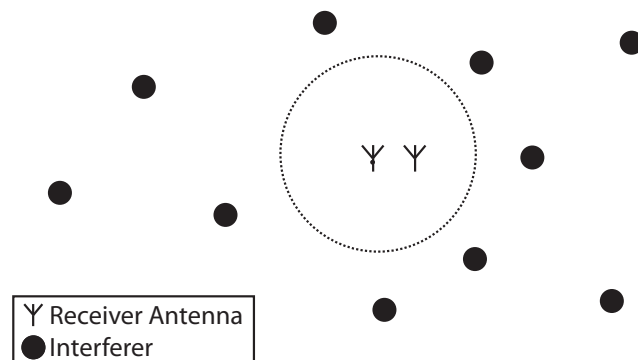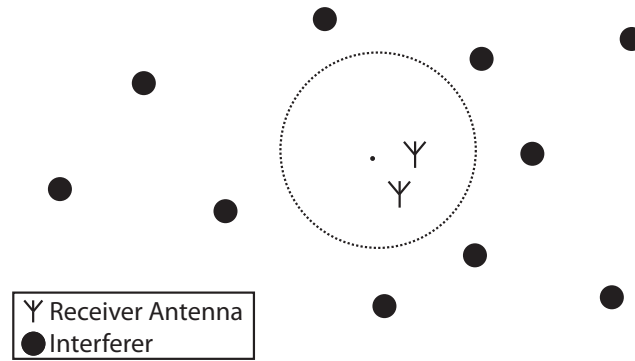
Figure 7.3: System model 3 of a receiver with 2 distributed antennae in a field of randomly distributed interferers in a centralized wireless network.

these results to N distributed antennae. The basic equations for such an extension are laid out in Section 4.6. However, instead of allowing antennae to be distributed in any manner, one could start with some potentially simpler antenna geometries. For example, Figures 7.4 and 7.5, show the antennae distributed as a uniform linear array and a uniform circular array, respectively. Intuitively, one can see that interference between a subset of antennae would exhibit a mixture of isotropic and independent statistics. The maximum separation between two antennae in each subset of antennae should impact the isotropy of joint interference statistics within that particular subset.

- *Joint spatio-temporal statistics of interference*

Multi-dimensional statistical models of interference arise when interference is observed from different points in space, or time. In this dissertation, I study multi-dimensional statistics of interference in a multiple spa-
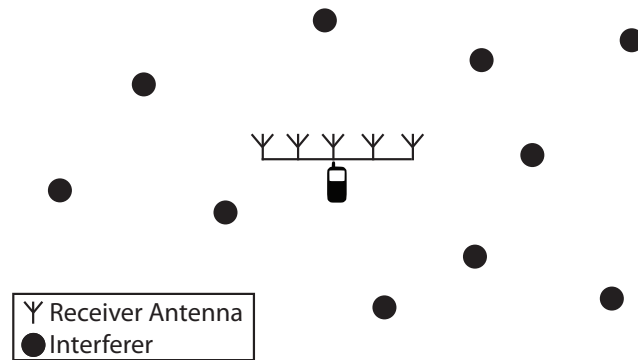
177

Figure 7.4: System model of a 5−antenna linear array receiver located in a field of randomly distributed interferers.
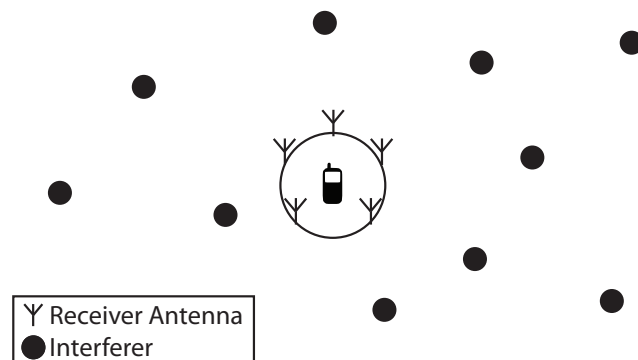

Figure 7.5: System model of a 5−antenna circular array receiver located in a field of randomly distributed interferers.

tial observation framework. These results can be extended to modeling temporal statistics of interference, and finally integrating the spatial and temporal statistics into a unified model. Such results would be very useful in modeling a network with mobile receivers and mobile interferers.

- *Outage performance analysis of non-linear multi-antennae receivers in presence of interference*

  In this dissertation, I analyze the outage performance of linear receivers in the presence of interference. However, non-linear receivers are shown to better mitigate non-Gaussian interference and closed-form communication performance analysis including bounds on performance of such receivers would yield incredible insights into receiver design to mitigate interference.

- *Estimation of key parameters from time-domain interference data*

  In this dissertation, I derived statistical models of interference based on network models. The parameters of interference are consequently a function of the parameters of the underlying wireless network model. A typical receiver deployed within this network would usually not have network parameter information. In such scenarios, receivers capture interference data and extract key parameters of interference statistics from these captured samples. Thus, fast receiver algorithms to analyze time domain interference samples, and fit these samples to the derived interference distributions would be essential to receivers operating in networks dominated by

179

interference[132]. Such algorithms would also require low computational complexity, fixed-point analysis for implementation in modern embedded wireless platforms.

Appendices

Appendix A

Poisson Point Processes

Let $\mathbb{S}$ be the set of all sequences of points in $\mathbb{R}^d$, such that any sequence $\mathcal{X} \in \mathbb{S}$

- is finite, i.e.,has only a finite number of points in any bounded subset of $\mathbb{R}^d$

- is simple, i.e., $a \neq b$ for any $a, b \in \mathcal{X}$.

Let $\mathcal{X}(B)$, for $\mathcal{X} \in \mathbb{S}$ and $B \in \mathbb{R}^d$, denote the number of points of the sequence $\mathcal{X}$ that lie in the set B.

A stationary Poisson point process (PPP) of intensity λ is characterized by the following two properties:

- The number of points in any set $B \in \mathbb{R}^d$ is a Poisson random variable with mean $\lambda |B|$, or in other words

$$P(\mathcal{X}(B) = k) = \frac{e^{-\lambda|B|}(\lambda|B|)^k}{k!} \tag{A.1}$$

- The number of points in disjoint sets are independent random variables.

Definition A.1. *PPP thinning:* The thinning of a PPP is defined as selecting a point of the process with probability p independently of the other points and

182

discarding it with probability $1p$. Thinning results in two independent PPPâĂŹs of intensities $p\lambda$ and $(1p)\lambda$.

Definition A.2. *Inhomogeneous PPP:* An inhomogeneous PPP of intensity measure Λ is defined in a similar manner as the stationary PPP, except that the number of points in a set B is a Poisson random variable with mean $\Lambda(B) = \int_B \Lambda(x)dx$. A stationary PPP is a special case of the inhomogeneous PPP with $\Lambda(B) = \lambda|B|$.

Theorem A.1. *Campbell's Theorem: Let $f(x) : \mathbb{R}^d \rightarrow [0, \infty)$ be a measurable function. Then*

$$\mathbb{E}\left[\sum_\Phi f(x)\right] = \int_{\mathbb{R}^d} f(x)\Lambda(dx) \tag{A.2}$$

When Φ is stationary with intensity λ the right side is equal to $\lambda \int_{\mathbb{R}^d} f(x)dx$.

Definition A.3. *Probability generating functional (PGFL):* Let $(x) : \mathbb{R}^d \rightarrow [0, \infty)$ be measurable. The PGFL of the point process $\mathcal{X}$ is defined as

$$\mathcal{G}(v) = \prod_{x \in \Phi} v(x) \tag{A.3}$$

Observe that the PGFL is a functional, i.e., acts on a function and when the function is a multivariate, a dot '·' is used to represent the variable that the PGFL acts on. The probability generating functional of a PPP it is equal to

$$\mathcal{G}(v) = e^{-\int_{\mathbb{R}}^d (1-v(x))\Lambda(x)dx} \tag{A.4}$$

183

Bibliography

[1] Cisco visual networking index: Global mobile data traffic forecast update, 2010 - 2015. Technical report, Feb. 2011.

[2] 3rd Generation Partnership Project (3GPP). *Technical Specification Group Radio Access Network; Physical layer aspects for evolved Universal Terrestrial Radio Access (E-UTRA)*, 3GPP TS 36.201, v10.0.0 edition, March 2011.

[3] M. Abramowitz and I. A. Stegun. *Handbook of mathematical functions with formulas, graphs, and mathematical tables*, volume 55. Courier Dover Publications, 1964.

[4] R.J. Adler, R.E. Feldman, and M.S. Taqqu. *A practical guide to heavy tails: Statistical techniques and applications.* Birkenhauser, 1998.

[5] S. Ahmed, T. Ratnarajah, M. Sellathurai, and C. Cowan. Iterative receivers for MIMO-OFDM and their convergence behavior. *IEEE Transactions on Vehicular Technology*, 58(1):461–468, 2009.

[6] S. Akoum and R. W. Heath. Limited feedback for temporally correlated MIMO channels with other cell interference. *IEEE Transactions on Signal Processing*, 58(10):5219–5232, 2010.

[7] O. B. S. Ali, C. Cardinal, and F. Gagnon. Performance of optimum combining in a Poisson field of interferers and Rayleigh fading channels. *IEEE Transactions on Wireless Communications*, 9(8):2461–2467, 2010.

[8] M.S. Alouini and A. J. Goldsmith. Area spectral efficiency of cellular mobile radio systems. *IEEE Transactions on Vehicular Technology*, 48(4):1047–1065, July 1999.

[9] D. L. Alspach and H. W. Sorenson. Nonlinear Bayesian estimation using Gaussian sum approximation. *IEEE Transactions on Automatic Control*, 17(4):439–448, Apr. 1972.

[10] A. Altieri, L.R. Vega, C. G. Galarza, and P. Piantanida. Cooperative strategies for interference-limited wireless networks. In *Proc. IEEE International Symposium on Information Theory*, pages 1623–1627, 2011.

[11] S. Ambike, J. Ilow, and D. Hatzinakos. Detection for binary transmission in a mixture of Gaussian noise and impulsive noise modeled as an alpha-stable process. *IEEE Signal Processing Letters*, 1(3):55–57, Mar. 1994.

[12] J. G. Andrews. Interference cancellation for cellular systems: A contemporary overview. *IEEE Wireless Communications Magazine*, 12(2):19–29, Apr. 2005.

[13] J. G. Andrews. A tractable framework for coverage and outage in heterogeneous cellular networks, Feb. 2011.

[14] J. G. Andrews, W. Choi, and R. W. Heath. Overcoming interference in spatial multiplexing MIMO cellular networks. *IEEE Wireless Communications Magazine*, 14(6):95–104, 2007.

[15] G. R. Arce. *Nonlinear Signal Processing: A Statistical Approach.* John Wiley & Sons, 2005.

[16] F. Baccelli and B. Błaszczyszyn. Stochastic geometry and wireless networks, volume 1 — theory. In *Foundations and Trends in Networking*, volume 3, pages 249–449. Now Publishers Inc., March 2009.

[17] F. Baccelli and B. Błaszczyszyn. Stochastic geometry and wireless networks, volume 2— applications. In *Foundations and Trends in Networking*, volume 4, pages 1–312. Now Publishers Inc., March 2009.

[18] F. Baccelli, B. Błaszczyszyn, and P. Muhlethaler. An ALOHA protocol for multihop mobile wireless networks. *IEEE Transaction on Information Theory*, 52(2):412–436, Sep. 2006.

[19] F. Baccelli, M. Klein, M. Lebourges, and S. Zuyev. Stochastic geometry and architecture of communication networks. *Journal of Telecommunication Systems*, 7:209–227, Jun. 1997.

[20] D. Benevides da Costa, H. Ding, and J. Ge. Interference-limited relaying transmissions in dual-hop cooperative networks over Nakagami-m fading. *IEEE Communications Letters*, 15(5):503–505, 2011.

[21] R. Bhagavatula and R. W. Heath. Predictive limited feedback for cooperative transmission. In *Proc. Asilomar Conference on Signals, Systems, and Computers*, pages 1237–1241, 2010.

[22] V. Bhatia, B. Mulgrew, and A. Th. Georgiadis. Minimum BER DFE equalizer in alpha stable noise. In *Proc. European Signal Processing Conference*, volume 12, pages 1829–1832, Sep. 2004.

[23] E. Biglieri, R. Calderbank, A. Constantinides, A. Goldsmith, A. Paulraj, and H. V. Poor. *MIMO Wireless Communications*. 2007.

[24] Bluetooth SIG. *Core Specification of the Bluetooth System*, v2.1 + edr edition, Jul. 2007.

[25] R. S. Blum, R. J. Kozick, and B.M. Sadler. An adaptive spatial diversity receiver for non-Gaussian interference and noise. *IEEE Transactions on Signal Processing*, 47(8):2100–2111, Aug. 1999.

[26] R. S. Blum, J. H. Winters, and N. R. Sollenberger. On the capacity of cellular systems with MIMO. *IEEE Communications Letters*, 6(6):242–244, 2002.

[27] C. L. Brown and A. M. Zoubir. A nonparametric approach to signal detection in impulsive interference. *IEEE Transactions on Signal Processing*, 48(9):2665–2669, 2000.

[28] V. R. Cadambe and S. A. Jafar. Interference alignment and spatial degrees of freedom for the K user interference channel. In *Proc. IEEE International Conference on Communications*, pages 971–975, May 2008.

187

[29] S. Catreux, P. F. Driessen, and L. J. Greenstein. Simulation results for an interference-limited multiple-input multiple-output cellular system. *IEEE Communications Letters*, 4(11):334–336, 2000.

[30] S. Catreux, P. F. Driessen, and L. J. Greenstein. Attainable throughput of an interference-limited multiple-input multiple-output (MIMO) cellular system. *IEEE Transactions on Communications*, 49(8):1307–1311, 2001.

[31] C. Chan-Byoung, K. Sang-hyun, and R. W. Heath. Linear network coordinated beamforming for cell-boundary users. In *Proc. IEEE Workshop on Signal Processing Advances in Wireless Communications*, pages 534–538, Jun. 2009.

[32] V. Chandrasekhar and J. Andrews. Spectrum allocation in two-tier networks. *IEEE Transactions on Wireless Communication*, 57(10):3059–3068, Oct. 2009.

[33] V. Chandrasekhar and J. G. Andrews. Uplink capacity and interference avoidance for two-tier femtocell networks. *IEEE Transactions on Wireless Communications*, 8(7):3498–3509, Jul. 2009.

[34] B. Chen and M. J. Gans. Mimo communications in ad hoc networks. *IEEE Transactions on Signal Processing*, 54(7):2773–2783, 2006.

[35] J. Chen, L. Clavier, Y. Xi, A. Burr, N. Rolland, and P.-A. Rolland. Alpha stable interference modelling and relay selection for regenerative cooperative IR-

UWB systems. In *Proc. European Wireless Technology Conference*, pages 81–84, 2010.

[36] S. Chen, W. Wang, and X. Zhang. Performance analysis of multiuser diversity in cooperative multi-relay networks under Rayleigh-fading channels. *IEEE Transactions on Wireless Communications*, 8(7):3415–3419, 2009.

[37] Y. Chen and R. S. Blum. Efficient algorithms for sequence detection in non-Gaussian noise with intersymbol interference. *IEEE Transactions on Communications*, 48(8):1249–1252, Aug. 2000.

[38] C. F. Chiasserini and R. R. Rao. Coexistence mechanisms for interference mitigation between IEEE 802.11 WLANs and Bluetooth. In *Proc. IEEE International Conference on Computer Communications*, volume 2, pages 590–598, Nov. 2002.

[39] W. Choi and J. G. Andrews. Downlink performance and capacity of distributed antenna systems in a multicell environment. *IEEE Transactions on Wireless Communications*, 6(1):69–73, 2007.

[40] W. Choi, J. G. Andrews, and C. Yi. The capacity of multicellular distributed antenna networks. In *Proc. IEEE International Conference on Wireless Networks, Communications and Mobile Computing*, volume 2, pages 1337–1342, 2005.

[41] A. Chopra, K. Gulati, B. L. Evans, K. R. Tinsley, and C. Sreerama. Performance bounds of MIMO receivers in the presence of radio frequency in-

terference. In *Proc. IEEE International Conference on Acoustics, Speech, and Signal Processing*, Taipei, Taiwan, Apr. 19–24 2009.

[42] L. Cohen. The history of noise. *IEEE Signal Processing Magazine*, 22(6):20–45, Nov. 2005.

[43] T. M. Cover and J. A. Thomas. *Elements of Information Theory*. Wiley & Sons, New York, second edition, 2006.

[44] D. Cox. Cochannel interference considerations in frequency reuse small-coverage-area radio systems. *IEEE Transactions on Communications*, 30(1):135–142, Jan 1982.

[45] M. J. Crisp, Sheng Li, A. Watts, R. V. Penty, and I. H. White. Uplink and downlink coverage improvements of 802.11g signals using a distributed antenna network. *IEEE/OSA Journal of Lightwave Technology*, 25(11):3388–3395, 2007.

[46] H. Dai, A. F. Molisch, and H. V. Poor. Downlink capacity of interference-limited MIMO systems with joint detection. *IEEE Transactions on Wireless Communications*, 3(2):442–453, 2004.

[47] P. A. Delaney. Signal detection in multivariate Class-A interference. *IEEE Transactions on Communications*, 43(4), Feb. 1995.

[48] M. J. Dumbrill and I. J. Rees. Sectorized cellular radio base station antenna, 1998.

[49] O. El Ayach, S. Peters, and R. W. Heath. The feasibility of interference alignment over measured MIMO-OFDM channels. *IEEE Transactions on Vehicular Technology*, 59(9):4309–4321, Nov. 2010.

[50] H. El Ghannudi, L. Clavier, N. Azzaoui, F. Septier, and P.-a. Rolland. Alpha-stable interference modeling and cauchy receiver for an IR-UWB *ad hoc* network. *IEEE Transactions on Communications*, 58(6):1748–1757, 2010.

[51] Y.C. Eldar and A. Yeredor. Finite-memory denoising in impulsive noise using Gaussian mixture models. *IEEE Transactions on Circuits and Systems II: Analog and Digital Signal Processing*, 48(11):1069–1077, Nov. 2001.

[52] R. Fantacci. Proposal of an interference cancellation receiver with low complexity for DS/CDMA mobile communication systems. *IEEE Transactions on Vehicular Technology*, 48(4):1039–1046, 1999.

[53] Federal Communications Commission. *Code of Federal Regulations - Part 15 : Radio Frequency Device*, 47 edition, Oct 2009.

[54] N. S. Ferdinand and N. Rajatheva. Unified performance analysis of two-hop amplify-and-forward relay systems with antenna correlation. *IEEE Transactions on Wireless Communications*, 10(9):3002–3011, 2011.

[55] D. Fertonani and G. Colavolpe. A robust metric for soft-output detection in the presence of class-A noise. *IEEE Transactions on Communications*, 57(1):36–40, Jan. 2009.

[56] M. Franceschetti, O. Dousse, D. Tse, and P. Thiran. Closing the gap in the capacity of wireless networks via percolation theory. *IEEE Transactions on Information Theory*, 53(3):1009–1018, Mar. 2007.

[57] M. Franceschetti, M. D. Migliore, and P. Minero. The capacity of wireless networks: Information-theoretic and physical limits. *IEEE Transactions on Information Theory*, 55(8):3413–3424, Aug. 2009.

[58] W. Freitas, R. Cavalcanti, and A. de Almeida. Interference cancellation receiver for multiple-access space-time block-coded systems over frequency selective channels. In *Proc. IEEE International Telecommunications Symposium*, pages 555 – 559, Sept. 2006.

[59] Y. Fu, L. Yang, and W. Zhu. A nearly optimal amplify-and-forward relaying scheme for two-hop MIMO multi-relay networks. *IEEE Communications Letters*, 14(3):229–231, 2010.

[60] R. K. Ganti and J. G. Andrews. A new method for computing the transmission capacity of non-Poisson wireless networks. In *Proc. IEEE International Symposium on Information Theory*, pages 1693–1697, Austin, TX, Jun. 13–18 2010.

[61] R.K. Ganti and M. Haenggi. Interference and outage in clustered wireless *ad hoc* networks. *IEEE Transactions on Information Theory*, 55(9):4067–4086, Sep. 2009.

192

[62] P. Gao and C. Tepedelenlioglu. Space-time coding over fading channels with impulsive noise. *IEEE Transactions on Wireless Communications*, 6(1):220–229, Jan. 2007.

[63] D. Gesbert, S. Hanly, H. Huang, S. Shamai Shitz, O. Simeone, and W. Yu. Multi-cell MIMO cooperative networks: A new look at interference. *IEEE Journal on Selected Areas in Communications*, 28(9):1380–1408, 2010.

[64] D. Günduz, M. A. Khojastepour, A. Goldsmith, and H. V. Poor. Multi-hop MIMO relay networks: Diversity-multiplexing trade-off analysis. *IEEE Transactions on Wireless Communications*, 9(5):1738–1747, 2010.

[65] A. Goldsmith. *Wireless Communications*. Cambridge University Press, 2005.

[66] J. Gonzalez, D. Griffith, and G. Arce. Matched myriad filtering for robust communications. In *Proc. Conference on Information Sciences and Systems*, 1996.

[67] J. G. Gonzalez. *Robust techniques for wireless communications in Non-Gaussian environments*. PhD thesis, University of Delaware, Newark, 1997.

[68] J. G. Gonzalez and G.R. Arce. Optimality of the myriad filter in practical impulsive-noise environments. *IEEE Transactions on Signal Processing*, 49(2):438–441, Feb. 2001.

[69] K. Gulati, A. Chopra, R. W. Heath, B. L. Evans, K. R. Tinsley, and X. E. Lin. MIMO receiver design in the presence of radio frequency interference. In *Proc. IEEE Global Telecommunications Conference*, pages 1–5, Dec. 2008.

[70] K. Gulati, B. L. Evans, and K. R. Tinsley. Statistical modeling of co-channel interference in a field of Poisson distributed interferers. In *Proc. IEEE International Conference on Acoustics, Speech, and Signal Processing*, pages 3490–3493, Dallas, TX, Mar. 14–19 2010.

[71] K. Gulati, B.L. Evans, J.G. Andrews, and K.R. Tinsley. Statistics of co-channel interference in a field of Poisson and Poisson-Poisson clustered interferers. *IEEE Transactions on Signal Processing*, 58, Dec. 2010.

[72] P. Gupta and P. R. Kumar. The capacity of wireless networks. *IEEE Transactions on Information Theory*, 46(2):388–404, Mar. 2000.

[73] M. Haenggi. Outage, local throughput, and capacity of random wireless networks. *IEEE Transactions on Wireless Communications*, 8(8):4350–4359, Aug. 2009.

[74] M. Haenggi and R. K. Ganti. Interference in large wireless networks. In *Foundations and Trends in Networking*, volume 3, pages 127–248. Now Publishers Inc., Dec. 2008.

[75] U. Hammes and A. M. Zoubir. A semi-parametric approach for robust multiuser detection. In *Proc. IEEE Int. Conf. Acoustics, Speech and Signal Processing*, pages 3401–3404, 2008.

[76] J. Han, E. Oh, S. Ahn, and D. Hong. A simple technique to enhance diversity order in wireless fading relay channels. *IEEE Communications Letters*, 12(3):194–196, 2008.

[77] J. Haring and A. J. H. Vinck. Performance bounds for optimum and sub-optimum reception under class-A impulsive noise. *IEEE Transactions on Communications*, 50(7):1130– 1136, Jul. 2002.

[78] A. Hasan and J. G. Andrews. Scheduling using near-optimal guard zones for CDMA *ad hoc* networks. In *Proc. IEEE International Conference on Communications*, volume 9, pages 4002–4007, Jun. 2006.

[79] A. Hasan and J. G. Andrews. The guard zone in wireless *ad hoc* networks. *IEEE Transactions on Wireless Communications*, 4(3):897–906, Mar. 2007.

[80] K. Huang, J. G. Andrews, R. W. Heath Jr., D. Guo, and R. Berry. Spatial interference cancellation for multi-antenna mobile *ad hoc* networks. *IEEE Transactions on Information Theory*, Jul. 2008. submitted.

[81] K. Huang, R. W. Heath, and J. G. Andrews. Limited feedback beamforming over temporally-correlated channels. *IEEE Transactions on Signal Processing*, 57(5):1959–1975, 2009.

[82] P. J. Huber. *Robust Statistics.* John Wiley & Sons, 1981.

[83] A. M. Hunter, J. G. Andrews, and S. P. Weber. Transmission capacity of *ad hoc* networks with spatial diversity. *IEEE Transactions on Wireless Communications*, 7(12):5058–5071, Dec. 2008.

195

[84] A. M. Hunter, R. K. Ganti, and J. G. Andrews. Transmission capacity of multi-antenna ad hoc networks with CSMA. In *Proc. Asilomar Conference on Signals, Systems and Computers*, pages 1577–1581, 2010.

[85] IEEE ComSoc LAN MAN Standards Committee. *Wireless LAN Medium Access Control (MAC) and Physical Layer (PHY) Specifications: IEEE Standard 802.11*. The Institute of Electrical and Electronics Engineers, 1997.

[86] J. Ilow and D. Hatzinakos. Analytic alpha-stable noise modeling in a Poisson field of interferers or scatterers. *IEEE Transactions on Signal Processing*, 46(6):1601–1611, Jun. 1998.

[87] T. Inoue and R. W. Heath. Grassmannian predictive coding for delayed limited feedback MIMO systems. In *Proc. Allerton Conference on Communication, Control, and Computing*, pages 783–788, 2009.

[88] L. Izzo and M. Tanda. Diversity reception of fading signals in spherically invariant noise. *Proc. IEE Communications*, 145(4):272–276, 1998.

[89] P. S. Jha. Frequency reuse scheme with reduced co-channel interference for fixed cellular systems. In *IEEE Electronic Letters*, volume 34, pages 237–238, Feb 1998.

[90] Y. Jiang, X. Hu, W. Li, and S. Zhang. Estimation of two-dimensional class A noise model parameters by Markov chain Monte Carlo. In *Proc. IEEE International Workshop on Computational Advances in Multi-Sensor Adaptive Processing*, pages 249–252, Apr. 2007.

[91] N. Jindal, J. G. Andrews, and S. Weber. Multi-antenna communication in *ad hoc* networks: Achieving MIMO gains with SIMO transmission. *IEEE Transactions on Communications*, 59(2):529–540, 2011.

[92] J. B. Johnson. Thermal agitation of electricity in conductors. *Physical Review*, 32:97–109, Jul 1928.

[93] M. Ju and I. Kim. Joint relay selection and opportunistic source selection in bidirectional cooperative diversity networks. *IEEE Transactions on Vehicular Technology*, 59(6):2885–2897, 2010.

[94] A. Kamerman and N. Erkocevic. Microwave oven interference on wireless LANs operating in the 2.4 GHz ISM band. In *Proc. IEEE International Symposium on Personal, Indoor and Mobile Radio Communications*, volume 3, pages 1221–1227, Helsinki , Finland, Sep. 1–4 1997.

[95] M. Kang and M.-S. Alouini. Quadratic forms in complex Gaussian matrices and performance analysis of MIMO systems with cochannel interference. *IEEE Transactions on Wireless Communications*, 3(2):418–431, 2004.

[96] M. Kang, Lin Yang, and M.-S. Alouini. Capacity of MIMO Rician channels with multiple correlated Rayleigh co-channel interferers. In *Proc. IEEE Global Telecommunications Conference*, volume 2, pages 1119–1123, 2003.

[97] M. Kaynia, G. E. Oien, and N. Jindal. Joint transmitter and receiver sensing capability of CSMA in MANETs. In *Proc. IEEE International Conference*

on Wireless Communications and Signal Processing, Nanjing, China, Nov. 2009.

[98] A. Kortun and A. Hocanin. Performance of DS-CDMA in fading channels with impulsive noise. In *Proc. IEEE Conference on Signal Processing and Communications Applications*, pages 720–723, Apr. 2004.

[99] R. T. Krishnamachari and M. K. Varanasi. Interference alignment under limited feedback for MIMO interference channels. In *Proc. IEEE International Symposium on Information Theory*, pages 619–623, Jun. 13–18 2010.

[100] E. Kuruoglu. *Signal processing in alpha-stable environments: A least lp-norm approach.* PhD thesis, 1998.

[101] E. E. Kuruoglu, W. J. Fitzgerald, and P. J. W. Rayner. Near optimal detection of signals in impulsive noise modeled with a symmetric alpha-stable distribution. *IEEE Communications Letters*, 2(10):282–284, 1998.

[102] A. Kyung Seung and R. W. Heath. Performance analysis of maximum ratio combining with imperfect channel estimation in the presence of cochannel interferences. *IEEE Transactions on Wireless Communications*, 8(3):1080–1085, Mar. 2009.

[103] L. Le Cam. The central limit theorem around 1935. *Statistical Science*, 1(1):78–91, 1986.

[104] J. Lee, D. Toumpakaris, and W. Yu. Interference mitigation via joint detection. *IEEE Journal on Selected Areas in Communications*, 29(6):1172–1184, 2011.

[105] T. S. Lee and Z. S. Lee. A sectorized beamspace adaptive diversity combiner for multipath environments. *IEEE Transactions on Vehicular Technology*, 48(5):1503–1510, 1999.

[106] A. Li, Y. Wang, W. Xu, and Z. Zhou. The minimum error entropy based robust receiver design of MIMO systems in alpha stable noise. In *Proc. IEEE Conference on Vehicular Technology*, volume 2, pages 851–855, 2005.

[107] X. J. Li and P. H. J. Chong. A medium access control scheme for TDD-CDMA cellular networks with two-hop relay architecture. *IEEE Transactions on Wireless Communications*, 8(5):2280–2285, 2009.

[108] D. N. Liu and M. P. Fitz. Low complexity affine MMSE detector for iterative detection-decoding MIMO OFDM systems. *IEEE Transactions on Communications*, 56(1):150–158, 2008.

[109] D. Lopez-Perez, A. Juttner, and J. Zhang. Dynamic frequency planning versus frequency reuse schemes in OFDMA networks. In *IEEE Vehicular Technology Conference*, pages 1 –5, Apr. 2009.

[110] M. F. Madkour, S. C. Gupta, and Y.-P. E. Wang. Successive interference cancellation algorithms for downlink W-CDMA communications. *IEEE Transactions on Wireless Communications*, 1(1):169–177, 2002.

199

[111] R. Martinez-Rodriguez-Osorio, L. de Haro-Ariet, M. Calvo-Ramon, and M. G. Sanchez. Performance evaluation of W-CDMA in actual impulsive noise scenarios using adaptive antennas. *Proc. IEE Communications*, 151(6):589–594, Dec. 2004.

[112] K. F. McDonald and R. S. Blum. A physically-based impulsive noise model for array observations. In *Proc. IEEE Asilomar Conference on Signals, Systems and Computers*, volume 1, pages 448–452, 2-5 Nov. 1997.

[113] K. F. McDonald and R. S. Blum. A statistical and physical mechanisms-based interference and noise model for array observations. *IEEE Transactions on Signal Processing*, 48:2044–2056, July 2000.

[114] D. Middleton. Statistical–physical models of man–made and natural radio noise part II: First order probability models of the envelope and phase. Technical report, U.S. Department of Commerce, Office of Telecommunications, Apr. 1976.

[115] D. Middleton. Non-Gaussian noise models in signal processing for telecommunications: New methods and results for class A and class B noise models. *IEEE Transactions on Information Theory*, 45(4):1129–1149, May 1999.

[116] J. H. Miller and J. B. Thomas. Detectors for discrete-time signals in non-Gaussian noise. *IEEE Transactions on Information Theory*, 18:241–250, Mar. 1972.

[117] A. Nasri, R. Schober, and I. F. Blake. Performance and optimization of amplify-and-forward cooperative diversity systems in generic noise and interference. *IEEE Transactions on Wireless Communications*, 10(4):1132–1143, 2011.

[118] M. Nassar, K. Gulati, A. K. Sujeeth, N. Aghasadeghi, B. L. Evans, and K. R. Tinsley. Mitigating near-field interference in laptop embedded wireless transceivers. In *Proc. IEEE International Conference on Acoustics, Speech and Signal Processing*, pages 1405–1408, May 2008.

[119] R. Negi and A. Rajeswaran. Capacity of power constrained *ad hoc* networks. In *Proc. IEEE Conference on Computer Communications*, pages 443–453, Hong Kong, May 2004.

[120] Technical Specification Group Radio Access Network. 3GPP TR 25.814 v7.0 physical layer aspects for evolved universal terrestrial radio access (UTRA).

[121] U. Niesen. Interference alignment in dense wireless networks. In *Proc. IEEE Information Theory Workshop*, pages 1–5, Cairo, Jan. 6–8 2010.

[122] C.L. Nikias and M. Shao. *Signal Processing with Alpha-Stable Distributions and Applications*. John Wiley & Sons, 1995.

[123] S. Niranjayan and N. C. Beaulieu. The BER optimal linear RAKE receiver for signal detection in symmetric alpha-stable noise. *IEEE Transactions on Communications*, 57(12):3585–3588, 2009.

[124] S. Niranjayan and N. C. Beaulieu. BER optimal linear combiner for signal detection in symmetric alpha-stable noise: Small values of alpha. *IEEE Transactions on Wireless Communications*, 9(3):886–890, 2010.

[125] J. P. Nolan. Multivariate stable densities and distribution functions: General and elliptical case. In *Deutsche Bundesbank's Annual Fall Conference*, 2005.

[126] H. Nyquist. Thermal agitation of electric charge in conductors. *Phys. Rev.*, 32:110–113, Jul 1928.

[127] H. Ong and A.M. Zoubir. Estimation and detection in a mixture of symmetric alpha stable and Gaussian interference. In *Proc. IEEE Signal Processing Workshop on High-Order Statistics*, Madison, Wisconsin, Jun. 14–16 1999.

[128] J. Park, E. Song, and W. Sung. Capacity analysis for distributed antenna systems using cooperative transmission schemes in fading channels. *IEEE Transactions on Wireless Communications*, 8(2):586–592, 2009.

[129] S. W. Peters and R. W. Heath. Cooperative algorithms for MIMO interference channels. *IEEE Transactions on Vehicular Technology*, 60(1):206–218, 2011.

[130] R. Prasad and A. Kegel. Improved assessment of interference limits in cellular radio performance. *IEEE Transactions on Vehicular Technology*, 40:412–419, May 1991.

[131] A. Rabbachin, T. Q. S. Quek, H. Shin, and M. Z. Win. Cognitive network interference. *IEEE Transactions on Selected Areas in Communications*, 29(2):480–493, Feb. 2011.

[132] S. Rachev and S. Mittnik. *Stable Paretian models in finance.* Wiley, 2000.

[133] M. I. Rahman, E. de Carvalho, and R. Prasad. Mitigation of MIMO co-channel interference using robust interference cancellation receiver. pages 531 – 535, 2007.

[134] A. Rajan and C. Tepedelenlioglu. Diversity combining over Rayleigh fading channels with symmetric alpha-stable noise. *IEEE Transactions on Wireless Communications*, 9(9):2968–2976, 2010.

[135] R. Ramanathan, J. Redi, C. Santivanez, D. Wiggins, and S. Polit. Ad hoc networking with directional antennas: a complete system solution. 23(3):496–506, 2005.

[136] S. S. Rappaport and L. Kurz. An optimal nonlinear detector for digital data transmission through non-Gaussian channels. *IEEE Transactions on Communications Technology*, 14(3):266–274, Jun. 1966.

[137] J. L. Rodgers and W. A. Nicewander. Thirteen ways to look at the correlation coefficient. *The American Statistician*, 42(1), Feb. 1988.

[138] Fa Rui, B. S. Sharif, and C. C. Tsimenidis. Performance analysis for MC-CDMA system in impulsive noise. In *Proc. IEEE Wireless Communications and Networking Conference*, pages 1–5, Apr. 2009.

[139] E. Salbaroli and A. Zanella. Interference analysis in a Poisson field of nodes of finite area. *IEEE Transactions on Vehicular Technology*, 58(4):1776–1783, May 2009.

[140] G. Samorodnitsky and M. S. Taqqu. *Stable Non-Gaussian Random Processes: Stochastic Models with Infinite Variance*. Chapman and Hall, New York, 1994.

[141] M. G. Sanchez, M. A. Acuna, and I. Cuinas. Cochannel and adjacent channel interference in actual terrestrial TV scenarios - part i: Field measurements. *EEE Transactions on Broadcasting*, 48(2):111–115, Jun. 2002.

[142] W. Schottky. Uber spontane stromschwankungen in verschiedenen elektrizitatsleitern. *Annalen der Physik*, 362(23):541–567, 1918.

[143] L. Schumacher, K.I. Pedersen, and P.E. Mogensen. From antenna spacings to theoretical capacities - guidelines for simulating MIMO systems. In *IEEE International Symposium on Personal, Indoor and Mobile Radio Communications*, volume 2, pages 587 – 592, Sept. 2002.

[144] D. Senaratne and C. Tellambura. Unified exact performance analysis of two-hop amplify-and-forward relaying in Nakagami fading. *IEEE Transactions on Vehicular Technology*, 59(3):1529–1534, 2010.

[145] S. Senthuran, A. Anpalagan, and O. Das. Cooperative subcarrier and power allocation for a two-hop decode-and-forward OFCMD based relay net-

work. *IEEE Transactions on Wireless Communications*, 8(9):4797–4805, 2009.

[146] M. K. Simon and M.-S. Alouini. *Digital Communications Over Fading Channels.* 2nd edition.

[147] K. Slattery and H. Skinner. *Platform Interference in Wireless Systems: Models, Measurement, and Mitigation.* Newnes (Elsevier) Publishing, 2008.

[148] H. W. Sorenson and D. L. Alspach. Recursive Bayesian estimation using Gaussian sums. *Automatica*, 7:465–479, 1971.

[149] E. S. Sousa. Performance of a spread spectrum packet radio network link in a Poisson field of interferers. *IEEE Transactions on Information Theory*, 38(6):1743–1754, Nov. 1992.

[150] C. Suh and D. Tse. Interference alignment for cellular networks. In *Proc. Allerton Conference on Communication, Control, and Computing*, pages 1037–1044, Sep. 23–26 2008.

[151] C. K. Sung and I. B. Collings. Multiuser cooperative multiplexing with interference suppression in wireless relay networks. *IEEE Transactions on Wireless Communications*, 9(8):2528–2538, 2010.

[152] C. Tepedelenlioglu and P. Gao. On diversity reception over fading channels with impulsive noise. *IEEE Transactions on Vehicular Technology*, 54(6):2037–2047, Nov. 2005.

[153] R. Tresch and M. Guillaud. Performance of interference alignment in clustered wireless *ad hoc* networks. In *Proc. IEEE International Symposium on Information Theory*, pages 1703–1707, Jun. 13–18 2010.

[154] R. Tresch, M. Guillaud, and E. Riegler. On the achievability of interference alignment in the K-user constant MIMO interference channel. In *Proc. IEEE Workshop on Statistical Signal Processing*, pages 277–280, Aug. 31 – Sep. 3 2009.

[155] G. A. Tsihrintzis and C. L. Nikias. Incoherent receivers in alpha-stable impulsive noise. In *Proc. IEEE Military Communications Conf.*, volume 1, pages 130–134, 1995.

[156] G. A. Tsihrintzis and C. L. Nikias. Performance of optimum and suboptimum receivers in the presence of impulsive noise modeled as an alpha-stable process. *IEEE Transactions on Communications*, 43(234):904–914, 1995.

[157] G. A. Tsihrintzis and C. L. Nikias. Fast estimation of the parameters of alpha-stable impulsive interference. *IEEE Transactions on Signal Processing*, 44(6):1492–1503, June 1996.

[158] G.A. Tsihrintzis and C.L. Nikias. Detection and classification of signals in impulsive noise modeled as an alpha-stable process. *Proc. Asilomar Conference on Signals, Systems and Computers*, pages 707–710, Nov. 1993.

[159] A. H. Ulusoy and A. Rizaner. Adaptive path selective fuzzy decorrelating detector under impulsive noise for multipath fading CDMA systems. *IEEE Communications Letters*, 12(4):228–230, Apr. 2008.

[160] S. Vakil and B. Liang. Cooperative diversity in interference limited wireless networks. *IEEE Transactions on Wireless Communications*, 7(8):3185–3195, 2008.

[161] R. Vaze and R. W. Heath. End-to-end antenna selection strategies for multi-hop relay channels. In *Proc. Asilomar Conference on Signals, Systems and Computers*, pages 1506–1510, 2008.

[162] R. Vaze and R. W. Heath. Optimal amplify and forward strategy for two-way relay channel with multiple relays. In *Proc. IEEE Information Theory Workshop*, pages 181–185, 2009.

[163] R. Vaze and R. W. Heath. On the capacity and diversity-multiplexing trade-off of the two-way relay channel. *IEEE Transactions on Information Theory*, 57(7):4219–4234, 2011.

[164] R. Vaze and Jr. R. W. Heath. Transmission capacity of multiple antenna *ad hoc* networks without channel state information at the transmitter and interference cancelation at the receiver. In *Proc. Asilomar Conference on Signals, Systems, and Computers*, Pacific Grove, CA, Nov. 1–4 2009.

[165] R. Vaze, K. T. Truong, S. Weber, and R. W. Heath. Two-way transmission

capacity of wireless *ad hoc* networks. *IEEE Transactions on Wireless Communications*, 10(6):1966–1975, 2011.

[166] S. Verdú. *Multiuser Detection*. Cambridge University Press, 1998.

[167] H. Vikalo, B. Hassibi, and T. Kailath. On robust multiuser detection. In *Proc. Asilomar Conference on Signals, Systems and Computers*, number Nov., pages 1168 –1172, 29 Oct .–1 Nov. 2000.

[168] Q. Wang, S. R. Kulkarni, and S. Verdú. Divergence estimation of continuous distributions based on data-dependent partitions. *IEEE Transactions on Information Theory*, 51(9), Sep. 2005.

[169] W. Wang and R. Wu. Capacity maximization for OFDM two-hop relay system with separate power constraints. *IEEE Transactions on Vehicular Technology*, 58(9):4943–4954, 2009.

[170] X. Wang and H. V. Poor. Blind adaptive interference suppression in DS-CDMA communications with impulsive noise. In *Proc. IEEE International Conference on Acoustics, Speech and Signal Processing*, volume 6, pages 3169–3172 vol.6, May 1998.

[171] X. Wang and C. Rong. Adaptive Bayesian multiuser detection for synchronous CDMA with Gaussian and impulsive noise. *IEEE Transactions on Signal Processing*, 48(7):2013–2028, Jul. 2000.

[172] S. Weber, J. G. Andrews, and N. Jindal. An overview of the transmission capacity of wireless networks. *IEEE Transactions on Communications*, 58(12):3593–3604, Dec. 2010.

[173] S. Weber, J. G. Andrews, X. Yang, and G. de Veciana. Transmission capacity of wireless *ad hoc* networks with successive interference cancellation. *IEEE Transactions on Information Theory*, 53(8):2799–2814, Aug. 2007.

[174] S. Weber, X. Yang, J. G. Andrews, and G. de Veciana. Transmission capacity of wireless *ad hoc* networks with outage constraints. *IEEE Transactions on Information Theory*, 51(12):4091–4102, Dec. 2005.

[175] M. Z. Win, P. C. Pinto, and L. A. Shepp. A mathematical theory of network interference and its applications. *Proceedings of the IEEE*, 97(2):205–230, Feb. 2009.

[176] I. C. Wong. *A Unified Framework for Optimal Resource Allocation in Multiuser Multicarrier Wireless Systems*. PhD thesis, The University of Texas at Austin, May 2007.

[177] P. Xu, Z. Wu, and M. Ji. An efficient STBC detection algorithm under interference-limited environment. In *Proc. International Conference on Wireless Communications, Networking and Mobile Computing*, pages 1332–1335, 2007.

[178] X. Yang and A.P. Petropulu. Co-channel interference modeling and analysis in a Poisson field of interferers in wireless communications. *IEEE*

Transactions on Signal Processing, 51, Jan. 2003.

[179] S. M. Zabin and H. V. Poor. Efficient estimation of class A noise parameters via the EM algorithm. *IEEE Transactions on Information Theory*, 37(1):60–72, Jan 1991.

[180] J. Zhang and J. Andrews. Distributed antenna systems with randomness. *IEEE Transactions on Wireless Communications*, 7(9):3636–3646, 2008.

[181] J. Zhang, J. G. Andrews, and R. W. Heath. Block diagonalization in the MIMO broadcast channel with delayed CSIT. In *Proc. IEEE Global Telecommunications Conference*, pages 1–6, 2009.

[182] J. Zhang, M. Kountouris, J. G. Andrews, and R. W. Heath. Multi-mode transmission for the MIMO broadcast channel with imperfect channel state information. *IEEE Transactions on Communications*, 59(3):803–814, 2011.

[183] H. Zhou and T. Ratnarajah. A novel interference draining scheme for cognitive radio based on interference alignment. In *Proc. IEEE Symposium on New Frontiers in Dynamic Spectrum*, pages 1–6, Apr. 6–9 2010.

[184] J. Zhu and H. Yin. Enabling collocated coexistence in IEEE 802.16 networks via perceived concurrency. *IEEE Communications Magazine*, 47(6):108–114, Jun. 2009.

[185] ZigBee Alliance. *Zigbee Specification Document 053474, Rev. 14*, Nov. 2006.

Index

Vita

Aditya Chopra received the Bachelor of Technology in Electronics and Communications Engineering at the Indian Institute of Technology, Delhi, India in May 2006 and the Masters of Science in Electrical Engineering at The University of Texas at Austin, Texas in May 2008. He has held internship positions at in Corporate Research and Development (Systems) at Qualcomm, and National Instruments. At Qualcomm, he has developed interference cancellation algorithms for broadcast OFDM, resource negotiation and allocation algorithms for macro-pico and femto-cell wireless environments and enhanced receiver algorithms for WCDMA. He also worked as an intern at Agder University, Grimstad, Norway where he worked on statistical-geometrical models of MIMO wireless channels. His research interests include statistical signal processing and receiver design for high-speed wireless communications.

Permanent address: 40/173 Chittaranjan Park
New Delhi, India 110019

This dissertation was typeset with LaTeX† by the author.

---

†LaTeX is a document preparation system developed by Leslie Lamport as a special version of Donald Knuth's TEX Program.